THE UNIVERSITY OF HULL

The Effects of Natural Convection During Solidification. Granular Flow.

being a Thesis submitted for the Degree of

Doctor of Philosophy

in the University of Hull

by

Richard Alfred Guenigault, B.Sc.

August 1984

Acknowledgements

I wish to express my appreciation to Professor Graham Poots for his encouragement and inspiration leading up to, and during, the past three years. My thanks also go to Dr. John Howarth.

I am grateful to the Science and Engineering Research Council for providing me with the financial support necessary for the pursuit of this study.

Miss Gillian Lenton, B.Sc. has my sincere gratitude for the time and effort which she has expended in typing the final manuscript.

Last, but not least, I thank my parents for their support and encouragement. It is to them that I dedicate this thesis.

Abstract

It is a purpose of this thesis to present numerical results on the inward solidification of spheres and (horizontal) cylinders filled with liquid which is initially at a temperature above the fusion temperature. The changes in density within the liquid, due to temperature variations, induce a liquid motion by natural convection. There is a non-uniform heat transfer from the liquid to the solid phase producing a non-symmetrical inward moving solidification interface in the shape of a limacon of Pascal. The degree of distortion in the front is dependent on the size of the (initial) Rayleigh number of the natural convective flow. Small time perturbation expansions are employed to calculate the thermal fields in both the liquid and solid phases, to obtain the stream function for the convective motion and to locate the non-uniform solidification front. Numerical results are presented graphically for both the sphere and the cylinder.

Another purpose of this thesis is to investigate the flow profiles of a granular material in a hopper. A simplified approximate analysis is presented for the transient flow. The equations governing the motion of the material in a two-dimensional hopper are solved and the results obtained are compared with those for the steady state flow. The use of this transient model in conjunction with experimental observation will be of use in practical applications.

Contents

Nomenclature

For the Solidification Problem:

a	radius of sphere or cylinder
A, B	constants of integration
C_p	specific heat
$C(\underline{r},t) = 0$	equation of the interface
D_r^2, H_r^n, L_r	operators
E	interface variable defined by (2.2.19)
$\underline{F}$	body force per unit mass
$\underline{g}$	gravitational vector
k	thermal diffusivity
K	thermal conductivity
L	latent heat of fusion
p	pressure
P_n	particular integral
Pr	Prandtl number defined by (2.2.10)
q	variable for numerical computation
r	radial position
R	dimensionless radial position
Ra	Rayleigh number defined by (2.2.10)
t	time
T	temperature distribution
$\underline{v}$	velocity of the liquid
$\underline{V}$	dimensionless velocity of the liquid
$vol(\tau)$	volume of liquid as a function of time
x	independent variable
y	dependent variable

Greek Letters

α	coefficient of cubical expansion
β	Stefan number defined on page 7
γ	thermal head defined on page 27
θ	polar angle
Θ	dimensionless temperature distribution
λ	ratio of diffusivities
μ	$\mu = \cos\theta$
ξ	dimensionless variable defined by (2.2.17)
ρ	density
τ	dimensionless time
φ, Φ	forms of the interface equation
ψ	stream function
Ψ	dimensionless stream function

Superscripts

*	liquid property
$-$	single bar system
$=$	double bar system

Subscripts

1	initial condition
o	surface condition at r = a
f	fusion.
n	n^{th} order perturbation function
c	complete solidification

For the Granular Flow Problem:

g	gavitational constant
h	height of the material at any time
k	constant defined by (5.2.3)
M	constant defined by (6.2.15)
r	radial position
r_1	radial distance of orifice from 0
r_2	radial distance of initial height from 0
t	time
u	velocity of material (radial)
u_T	terminal velocity

Greek Letters

α, β, γ	constants
γ_ω	constant defined by (5.2.5)
δ	angle of friction between wall and material
ε	perturbation parameter
θ	polar angle
σ	stress
θ_ω	angle of inclination of sloping wall
φ	angle of internal friction

Superscript

$-$	dimensional property

Chapter 1

Moving Interface Problems With Change of Phase

1.1 General Introduction

Moving interface or moving boundary problems are encountered in many scientific, industrial and engineering problems. The general formulation of the moving boundary problem can be considered as follows. Two substances are separated by a surface and diffusion from one substance to the other takes place. This diffusion process may cause changes which create the formulation or dematerialization of matter at the interface in one, or both of the substances. The interface is thus seen to move relative to one, or both of these substances. This problem is commonly referred to as a Stefan problem of which there are at least two categories; those involving the diffusion of a substance and those involving the transfer of heat in the substance. Within the first category there falls, for example, the diffusion of oxygen into muscle when the oxygen combines with lactic acid. The absorption or diffusion of certain dyes into material fabric is of interest to the textile industry, whilst the effect of the diffusion of carbon during the melting of iron interests the steel industry. Other moving boundary problems which are concerned with diffusion involve the back-diffusion of a chemical solution into the remaining solution when evaporation occurs at the free surface. The rate at which a layer of soil or clay consolidates and increases in thickness is of interest to geologists, and in chemistry there arises the problem which is concerned with the diffusion-controlled growth of a new phase such as a crystal in solution.

It is, however, with the second category of heat transfer problems that there can arise the additional problem of change of phase. A fundamental feature of a phase-change problem is the moving interface which exists between the two phases of the substance. These phases,

which have different thermophysical properties, are separated by the transient interface across which latent heat is either liberated or absorbed. It is this transfer of thermal energy which introduces a non-linear phase-change process at the interface. As a consequence, the number of exact solutions known to the problem is restricted.

In 1860 Franz Neumann found the first and probably the only exact solution. He considered a substance of constant temperature which occupied the half-space $x > 0$ and was subjected to a predescribed temperature at the boundary $x=0$. The solution which Neumann obtained was characterized by a similarity variable $x/\sqrt{t}$. Nevertheless, it was not until 1891 that this type of problem was called a 'Stefan' problem, due to Stefan's classical investigation into the thickness of polar ice. The results Stefan obtained, or the method by which he achieved them, could be applied to a wide range of other phenomena in earth science. In particular, investigations have been made into the freezing and thawing of expanses of water, the solidification of lava streams and the ablation of glaciers.

Phase-change or Stefan problems are still of great practical importance in the present day, although this interest originates from a more commercial aspect. For instance, studies have been made for the steel industry into the solidification of steel ingots. The position of the solid-liquid interface was investigated since its profile during solidification can be of great interest in relation to the quality of the end product. Changing the shape of the ingot moulds can make considerable changes to this solidification process and this too has been studied.

Another area of interest created by phase-change problems is the latent heat of fusion storage devices. In this type of problem the

need to know the position of the interface is again important, as are the heat transfer characteristics of the phase-change material. This subject has received much recent attention and there have been several papers published on both theoretical and experimental studies.

Indeed, the Stefan problem has been the subject of a great deal of theoretical investigations. Of course constructing a mathematical model for such a problem can be extremely complicated and hence many things may be over-simplified. In particular, the consideration of the density changes in the material and the formation of dendrites is complex. Such complications will be discussed in a later section.

There have been many solutions presented, each using a method of differing complexity. These methods can be classified under the following headings: exact analytical, semi-analytical, integral, perturbation, numerical and other methods.

It is, perhaps at this point, worth presenting Neumann's one dimensional model and solution as generalised by Carslaw and Jaeger [1]. The semi-infinite region $x > 0$ contains a liquid at a temperature T_1 which is above the fusion temperature T_F. At time $t=0$ the temperature at the boundary $x=0$ is instantaneously reduced to below the fusion temperature. This results in the liquid immediately adjacent to the boundary solidifying and hence, a solid-liquid interface moves into the liquid. The temperature is assumed to be the only independent variable and the solid and liquid regions are considered separately. The position of the interface at any time is given by $x = E(t)$. And so, the heat conduction equation for the solid is,

$$\frac{\partial^2 T}{\partial x^2} = \frac{1}{k}\frac{\partial T}{\partial t} \quad , \quad 0 < t \leq t_c \qquad (1.1.1)$$

and for the liquid,

$$\frac{\partial^2 T^*}{\partial x^2} = \frac{1}{k^*} \frac{\partial T^*}{\partial t} , \quad 0 < t \leq t_c \tag{1.1.2}$$

The boundary conditions to be imposed are,

$$T = T_0 \ (< T_F) , \ x = 0 , \ t > 0 \tag{1.1.3}$$

$$T^* = T_F \ \text{as} \ x \to \infty , \ t > 0 \tag{1.1.4}$$

and the initial conditions are,

$$T = T_0 = T^* \ \text{at} \ t = 0 \ \text{with} \ E(0) = 0 \tag{1.1.5}$$

The latent heat condition is,

$$K \frac{\partial T}{\partial x} - K^* \frac{\partial T^*}{\partial x} = \rho h \frac{dE}{dt} \ ; \ \text{on} \ x = E(t) \tag{1.1.6}$$

and also at the interface,

$$T = T^* = 0 \quad \text{on} \quad x = E(t) , \ t > 0 \tag{1.1.7}$$

The exact solutions are found to be,

$$E(t) = 2\lambda \sqrt{Kt} \tag{1.1.8}$$

$$T = T_0 \left\{ 1 - \frac{\operatorname{erf}\left[\frac{x}{2(kt)^{\frac{1}{2}}}\right]}{\operatorname{erf}\lambda} \right\} \qquad (1.1.9)$$

and

$$T^* = T_F \left\{ 1 - \frac{\operatorname{erfc}\left[\frac{x}{2(k^*t)^{\frac{1}{2}}}\right]}{\operatorname{erfc}\left[\lambda\sqrt{\frac{k}{k^*}}\right]} \right\} \qquad (1.1.10)$$

where λ is a root of the transcendental equation,

$$\frac{e^{-\lambda^2}}{\operatorname{erf}\lambda} + \frac{K^*}{K}\frac{T_F}{T_0}\sqrt{\frac{k}{k^*}}\,\frac{e^{-\lambda^2 k/k^*}}{\operatorname{erfc}\left(\lambda\sqrt{\frac{k}{k^*}}\right)} + \frac{\lambda L\sqrt{\pi}}{C_p T_0} = 0 \qquad (1.1.11)$$

In the above a * denotes a liquid property, k the thermal diffusivity, K the thermal conductivity, L the latent heat and C_p the specific heat. The time taken until solidification is complete is t_c.

1.2 A Review of Literature on Solidification Problems with Free Convection Ignored.

An aim of this thesis is to investigate the inward solidification of a liquid, not necessarily at fusion temperature, which is contained in a sphere or a cylinder. This study was motivated by problems on ingot solidification emanating from the British Steel Corporation.

Before this investigation proceeds, however, it is worthwhile making a survey of the literature already available on and connected with this subject. The majority of these papers make the following assumptions:

(1) the initial temperature of the liquid is the fusion temperature;

(2) there exists a definite fusion temperature at which

solidification occurs and hence there exists a demarcation line or interface;

(3) all the thermal and transport properties of the system are independent of the temperature;

(4) the density changes at the change of phase and elsewhere in the solidification process are ignored.

Poots [2] investigated the solidification of a liquid at fusion temperature in several different shaped containers using heat balance techniques. Assumptions were made as to the temperature distribution and the shape of the interface. Then employing the Kármán-Pohlhausen technique, he was able to find small time solutions.

Goodman [3] also presented the solutions to several problems using a heat balance integral. He found that these results compared favourably with Neumann's exact solution for large values of the Stefan number

$$\beta = \frac{L}{c_p(T_F - T_0)}$$

- the ratio of the latent heat to the sensible heat of the substance. It should be noted that for $\beta = 0.25$ (steel) the error in Goodman's method is approximately 30%.

In 1967 Tao [4] published his generalized numerical solutions for the freezing of a liquid in a cylinder or sphere. Assuming the convective heat transfer coefficients to be constant, as is the heat capacity of the solid phase, Tao used differences to solve the set of coupled differential equations. The solution was then obtained using an iterative procedure.

Pedroso and Domoto [5] used a perturbation expansion for large Stefan number for the solidification of the sphere. They showed that the total time for solidification, that is as $E \rightarrow 1$, is given by

$$t_c = \frac{1}{6}\left(1 + \frac{1}{\beta}\right) \qquad (1.2.1)$$

which was obtained for two terms only. However, it was found that near to total solidification the regular perturbation series diverged. And so, an Euler Transformation together with an overall energy balance was employed to modify the series solution. Huang and Shih [6] applied Landau's Transformation to immobilize the moving boundary and, replacing the time variable by the normalized position of the moving interface, they too introduced a perturbation expansion to solve the solidification problem for the sphere and the cylinder.

Riley, Smith and Poots [7] investigated the sphere and the cylinder using the method of matched asymptotic expansions for large β. They used a two layer analysis. Using Pedroso and Domoto's solution as their outer region, they found that an inner layer $O(\beta^{-\frac{1}{2}})$ was required. The results obtained for small E - the depth of solidification - were found to compare well with the small time solutions of Poots. The total time for solidification of the sphere was found to be,

$$t_c = \frac{1}{6} + \frac{1}{6\beta} - \frac{1}{3(2\pi)^{\frac{1}{2}}\beta^{\frac{3}{2}}} + O\left(\frac{1}{\beta^2}\right) \qquad (1.2.2)$$

and for the cylinder,

$$t_c = \frac{1}{4} + \frac{1}{4\beta} + O\left(\frac{1}{\beta^2}\right) \qquad (1.2.3)$$

Nevertheless, Stewartson and Waechter [8] showed that even this second region analysis breaks down just before the centre solidifies, that is, at time

$$t_c - t = O\left(\frac{e^{-\beta^2}}{\beta}\right) \qquad (1.2.4)$$

Whilst studying the problem for the sphere, they introduced yet another region and thus employed a triple-region procedure. Although the resulting analysis was very complex, Stewartson and Waechter were able to obtain the temperature profile in the neighbourhood of the region near to the time of total solidification. This was a major contribution to this field of study. More recently (1980), Soward [9] developed a simpler method and was able to solve this problem for the cylinder as well as the sphere. Essentially Soward's method ameliorates the procedures used by Riley et al. and, although the results had been previously obtained, clarified the nature of the solution in various domains.

Hill and Kucera [10], using a semi-analytical procedure, considered the freezing of a liquid inside a sphere. In their analysis they included the effect of radiation at the surface and, by use of an integral formulation, they were able to show that the time for complete solidification lay between the bounds,

$$\frac{(1+2\alpha)}{6}\beta \leqslant t_c \leqslant (1+2\alpha)\frac{(1+\beta)}{6} \qquad (1.2.5)$$

where α is defined by $\alpha = \frac{k}{ha}$. If the radiation at the surface is ignored, that is $\alpha = 0$, it can be seen that the upper bound agrees well with the solution obtained by Pedroso and Domoto.

Furzeland [11] has made a comprehensive and excellent survey of numerical techniques which have been used to solve one dimensional moving boundary or Stefan problems. In this paper, Furzeland compared several viable methods and examined each one for efficiency and accuracy

and, in particular, the ease with which the method could be generalized to more than one dimension. More recently Schulze et al. [12] developed analytical and numerical solutions to two-dimensional moving interface problems. Although these solutions were applicable to the solidification of steel ingots in the steel industry, the studies made on small time expansions are of interest in the analysis of this thesis.

1.3 A Review of Literature on Solidification Problems with Free Convection

Until now, all the papers considered have approached the phase-change problem classically. That is, the effects of natural convection within the liquid fluid have been ignored and the problem has been treated as one of pure conduction. This means that the interface can be treated as axisymmetrical. One of the reasons for this neglect is that the analysis determining the position of the interface and the heat transfer would be greatly complicated by the inclusion of the convection. But in reality assumption (1) is rarely achieved and the initial temperature of the liquid is usually greater than its fusion temperature. Although initially solidification will occur solely in a conduction mode, appreciable temperature gradients will exist in the liquid adjacent to the interface and these temperature differences will produce density variations. It is these variations which result in the introduction of buoyancy forces which then induce conductive motion in the liquid. This will lead to the non-uniform convection of the liquid sensible heat across the interface which, as a consequence, becomes non-symmetrical in shape.

There have been many studies made to see how important this convection is during solidification and melting. As with the earlier pure conduction models, the solutions to these studies can be divided into three groups: analytical, experimental and numerical. However, it seems that there

have not been many analytical solutions obtained and this is probably due to the previously described complication.

In an early investigation Sparrow et al. [13] discussed the effects of natural convection on the rate of melting and heat transfer. They studied a melted region around a vertically heated cylinder embedded in a solid which was at its fusion temperature. Using an implicit finite-difference scheme to find the position of the interface as time progressed, these authors concluded that the addition of convection does indeed have a noticeable effect. In this investigation, as in many others, it was assumed that the Stefan number β was large so that the melting front moved slowly. This assumption permitted a quasi-steady approximation to be made for the convective motion.

Sparrow et al. [14] investigated experimentally the effects of natural convection on the outward freezing from a cooled vertical cylinder. A theoretical model based on empirical heat transfer coefficients at the interface gave good agreement with experiment. A numerical study of the transient effects of solidification accompanied by natural convection in a rectangular enclosure has been considered by Ramachandran et al. [15]. The quasi-steady approximations of Sparrow et al. [13] were again invoked and results were presented for large Stefan number and moderate Rayleigh number of order 10^3.

Yao and Chen [16] used a regular perturbation solution to show that, although conduction was initially the dominant heat transfer mode, the natural convection had an increasing effect during the melting process.

Gartling [17] used a finite element scheme to effect a method which could be used in a two-dimensional region of arbitrary shape. And in a later paper, Morgan [18], retaining the generality of this work, employed an explicit finite element technique to solve the same equations.

Morgan used this method to investigate the effects of convection during the process of melting and solidification in a cylindrical cavity. The results obtained for a solidifying substance were shown to agree qualitatively with experimental observations.

Problems of latent heat thermal energy storage in a horizontal cylindrical capsule involving large Rayleigh number - large diameters - were studied by Saitoh and Hirose [19]. Using a Landau transformation and an explicit finite difference scheme, these authors also concluded that the effect of natural convection played an important role.

Recently Gadgil and Gobin [20] and Ho and Viskanta [21] have explored the effects of natural convection on the thermal storage of phase-change material in a rectangular enclosure. Heat transfer during the inward melting in a horizontal tube has also been investigated theoretically and experimentally by Ho and Viskanta [22]. They found good agreement between the results obtained from these two methods. In Viskanta and Gau [23], experimental and theoretical work has established that for the inward solidification of a superheated liquid in a horizontal circular tube, the effect of natural convection is important for large Stefan number. The theoretical work was based on the quasi-steady approximation and on the assumption of an empirical heat transfer coefficient at the solid-liquid interface as proposed by Sparrow et al., see [13] and [14] respectively.

Further complications which arise in both the melting and solidification problem with, or without, convection originate from assumption (2), the existance of a definite fusion temperature. Unfortunately, not all substances, particularly in engineering practice, have this definite fusion temperature at which solidification occurs and which gives rise to a distinct demarcation line, or solid-

liquid interface, between the two phases. Instead solidification occurs over a temperature range and, of course, there is no discernable interface. Such amorphous substances - glass, wax and plastics being examples - change from a solid state to a liquid state by a continual absorption of heat and pass through decreasingly viscous stages. Similarly to an amorphous substance, alloys often have an ill-defined interface between the two phases and during the change of phase, the solidification or melting process is determined by the combination of its constituents. Generally fusion, which in this case is a vague concept anyway, is a gradual process.

Another problem which complicates the determination of the interface is that of dendritic freezing. It might be thought that an eutectic substance - a substance composed of a mixture of constituents so as to solidify at a single temperature - would produce a well defined interface. But, in practice (such as the steel industry), this is not so. For example, when steel solidifies, and particularly if the rate of solidification is slow, an instability is created at the interface. This can lead to the formation of dendrites, branching crystalline structures, from the solidus into the liquidus. From these primary dendrites, secondary dendrites evolve and, in turn, tertiary but smaller dendrites are formed. It is the 'mushy' region which is formed by these dendrites between the solid and liquid regions which creates a complex heat transfer structure.

Another consequence of these dendrites during, for example, the solidification of steel is the build up of impurities. These are caused by the more rapid solidification of the purer metal constituents which allow the impure constituents to form into a dense layer in the liquid region. This action is known as segregation and can alter the quantity of steel produced. (see Schulze [24])

The last assumption made - the neglection of changes in density at the change of phase - is also open to discussion. Volume increases or decreases which occur at the change of phase affect the magnitude of the heat transfer regions. Density changes at the interface together with the variations in the physical properties with the temperature, affect the propagation of heat in the liquid and solid phases.

Carslaw and Jaeger considered the effect of the change of density on solidification and presented an analytical solution. The heat conduction equation for the liquid region now becomes,

$$\frac{\partial^2 T^*}{\partial x^2} = \frac{1}{k^*}\left\{\frac{\partial T^*}{\partial t} + u^* \frac{\partial T^*}{\partial x}\right\} \qquad (1.3.1)$$

where the velocity of the liquid along the x-axis is given by,

$$u^* = -\left\{\frac{\rho}{\rho^*} - 1\right\}\frac{d\xi}{dt} \qquad (1.3.2)$$

The solution for the solid region is,

$$T = T_0\left\{1 - \frac{\operatorname{erf}\left[\frac{x}{2(kt)^{\frac{1}{2}}}\right]}{\operatorname{erf}\lambda}\right\} \qquad (1.3.3)$$

which is the same as equation (1.1.9). However the solution for the liquid region is now,

$$T^* = T_F\left\{1 - \frac{\operatorname{erfc}\left[\frac{x}{2(k^*t)^{\frac{1}{2}}} + \frac{\lambda(\rho-\rho^*)k}{\rho^* k^*}\right]}{\operatorname{erfc}\left[\frac{\lambda\rho}{\rho^*}\left(\frac{k}{k^*}\right)^{\frac{1}{2}}\right]}\right\} \qquad (1.3.4)$$

and, in this case, λ is a root of the transcendental equation,

$$\frac{e^{-\lambda^2}}{\operatorname{erf}\lambda} + \frac{K^*}{K}\frac{T_F}{T_0}\left(\frac{k}{k^*}\right)^{\frac{1}{2}} \frac{e^{-\lambda^2 \frac{\rho^2 k}{\rho^{*2} k^*}}}{\operatorname{erfc}\left[\lambda \frac{\rho}{\rho^*}\sqrt{\frac{k}{k^*}}\right]} + \frac{L\sqrt{\pi}\lambda}{T_0 c_p} = 0 \qquad (1.3.5)$$

Obviously if the densities of the two phases are the same, then $\rho = \rho^*$ and these solutions reduce to (1.1.10) and (1.1.11).

Tao [25] also considered the problem of solidification which included the density jump at the transient interface. But by employing an appropriate transformation of variables in time and space as well as material constants, he was able to convert the problem to one which had equal densities in both phases. This reduced problem, which is now a classical free-boundary problem, was designated as the associated problem.

A description of the physical situation which is created by the effects of natural convection during solidification in a liquid sphere or a liquid cylinder is now given. The changes in the densities, due to the temperature variations inducing motion in the liquid, mean that the rate of heat transfer across the interface will be greater at the north pole of the container than it will be at the south pole. Since the rate of increase in the solidification is dependent on the difference in the heat flux between the two phases at the interface, the solidification front would be expected to move towards the centre at a faster rate at the south pole than at the north. Consequently the front will initially move inwards symmetrically, but will soon evolve into the shape of a limacon of Pascal, and thus it would become non-symmetrical about the centre.

In Chapter 2 the effects of the natural convection during solidification in a sphere is investigated. The equations governing the thermal fields in the two phases, the equation governing the liquid motion and the latent

heat condition at the interface together with their boundary conditions are derived. Small time expansions of the coupled partial differential equations are then developed. These perturbation expansions, which represent the temperature distributions and the interfacial position, proceed in powers of $\tau^{1/2}$ and the first six terms up to (and including) $\tau^{5/2}$ are obtained. The resulting system of ordinary (linear) differential equations and the interface condition are solved numerically in Chapter 4. These results are then used to locate the position of the interface, calculate the temperature distributions in both phases, the velocity distributions, the streamlines and the Nusselt numbers. Solutions for different parameters, the thermal head (which is proportional to the difference between the initial temperature of the liquid and its fusion temperature), the Stefan, Rayleigh and Prandtl numbers are then computed and displayed graphically.

In Chapter 3 the equations which describe the effects that the natural convection has during the inward solidification of a cylinder are derived.

Such results may be useful in helping to complete our understanding of the effects of natural convection during the solidification or melting of metal and alloy systems, see Chiesa and Guthrie [26] and Schulze [24]. They are also relevant to the study of heat transfer in latent heat of fusion energy storage systems.

Chapter 2

The Effects of Natural Convection During Solidification in a Liquid Sphere

2.1 The Derivation of the Governing Equations

In the derivation of the equations governing the heat and mass transfer in a liquid undergoing the process of change of phase, certain assumptions from previous theoretical works are to be retained. These are:

(1) there exists a definite fusion temperature at which solidification occurs and thus a sharp demarcation line between the two phases;

(2) all thermal and transport properties are independent of the temperature;

(3) the density changes at the change of phase and elsewhere in the solidification process are ignored except in the calculation of the gravitational buoyancy force in the liquid phase.

The above form the starting point in the construction of mathematical models for solidification and melting, see [20] to [23]. Essentially it is assumed that there is no volume change on change of phase. Moreover, it is implied that the liquid velocity along the normal to the interface, which is induced by the change of density at change of phase, is also negligible. These assumptions have been substantiated experimentally by Sparrow et al. [29]. However, for any specified material it is a simple matter to compare, for example, the size of the velocities induced by the density jump at the moving boundary with that representative of the natural convective flow, and so establish the validity of the approximations which have been made, see Tao [25].

The physical situation to be examined is illustrated in figure 1.

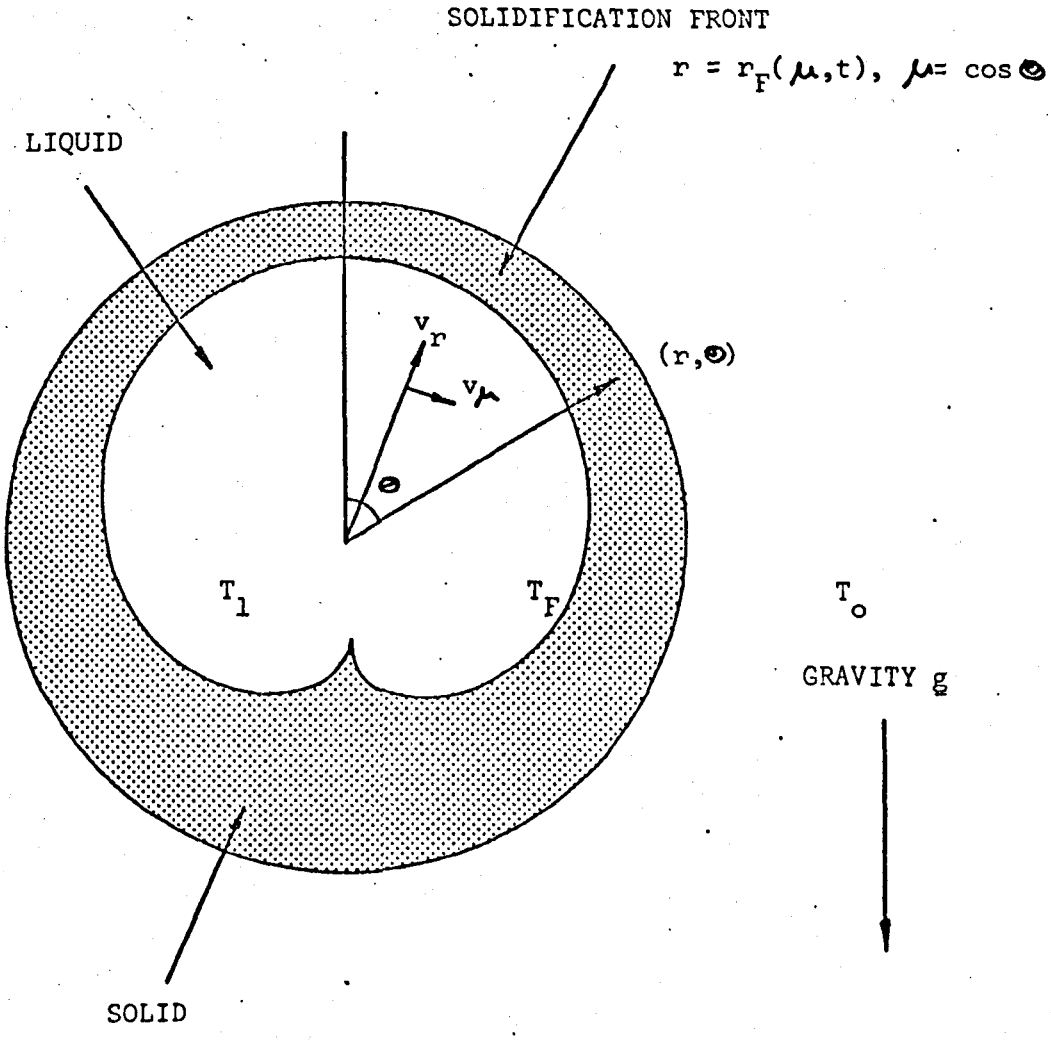

Figure 1

Initially a sphere of radius a is filled with a liquid at a constant temperature T_l, which is above its fusion temperature T_F. At time t = 0 the temperature at the surface r = a is instantaneously reduced to a temperature T_o which is below the fusion temperature. This causes the liquid adjacent to the surface to emit latent heat and solidify. The surface temperature T_o is maintained and, as time progresses, the solid-liquid interface moves towards the centre. The interface will be symmetrical about the azimuthal angle and its radial position is represented by

$$C(r,t) = r - r_F(\mu,t) \quad , \quad \mu = \cos\theta \tag{2.1.1}$$

The transient governing equations for the solid and liquid, subject to the previous assumptions, together with their corresponding boundary and initial conditions are as follows.

In the solid region the equation of heat conduction is,

$$k\left\{\frac{1}{r^2}\frac{\partial}{\partial r}\left(r^2\frac{\partial T}{\partial r}\right) + \frac{1}{r^2}\frac{\partial}{\partial \mu}\left[(1-\mu^2)\frac{\partial T}{\partial \mu}\right]\right\} = \frac{\partial T}{\partial t} \tag{2.1.2}$$

where the temperature distribution is described by $T(r,\mu,t)$ and k is the thermal diffusivity in the solid. This equation is subject to the boundary conditions,

$$T(a,\mu,t) = T_o$$

and (2.1.3)

$$T(r_F(\mu,t),\mu,t) = T_F$$

In the liquid region the Boussinesq approximation is now invoked on the equations of motion and heat. This approximation is based on the assumption that the properties of the molecules in the liquid may be considered constant and that the variations in the density field are important only in the calculation of the buoyancy force term in the equation of motion. Under these conditions, and assuming that the temperature and velocity distributions in the liquid are given by $T^*(r,\mu,t)$ and $\underline{v}(v_r,v_\mu)$ respectively (where $\mu = \cos\theta$), the equations of energy, continuity and momentum can be written as:

the thermal energy equation,

$$k^*\left\{\frac{1}{r^2}\frac{\partial}{\partial r}\left(r^2\frac{\partial T^*}{\partial r}\right) + \frac{1}{r^2}\frac{\partial}{\partial \mu}\left[(1-\mu^2)\frac{\partial T^*}{\partial \mu}\right]\right\} = \frac{\partial T^*}{\partial t} + v_r\frac{\partial T^*}{\partial r} - \frac{(1-\mu^2)^{\frac{1}{2}}}{r}\frac{\partial T^*}{\partial \mu}\cdot v_\mu \qquad (2.1.4)$$

where k^* is the thermal diffusivity in the liquid.

The equation of continuity is,

$$\frac{1}{r^2}\frac{\partial}{\partial r}\left(r^2 v_r\right) - \frac{1}{r}\frac{\partial}{\partial \mu}\left[(1-\mu^2)^{\frac{1}{2}} v_\mu\right] = 0 \qquad (2.1.5)$$

and the momentum or Navier-Stokes equation is,

$$\rho_F^*\left[\frac{\partial \underline{v}}{\partial t} - \underline{v}\times(\nabla\times\underline{v})\right] - \rho^*\underline{F} = -\nabla\left(p + \frac{1}{2}\rho_F^*\underline{v}^2\right) - \nu^*\rho_F^*\left[\nabla\times\nabla\times\underline{v}\right] \qquad (2.1.6)$$

where p is the pressure, ν^* the kinematic viscosity and ρ^* the density of the fluid. The temperature distribution $T^*(r,\mu,t)$ and the velocity $\underline{v}$ are determined by the coupled non-linear partial differential equations. The vector $\underline{F}$ in equation (2.1.6) is the external force due to gravity and is given by

$$\underline{F} = (-g\mu,\ g(1-\mu^2)^{\frac{1}{2}},\ 0) \qquad (2.1.7)$$

The equation of state is,

$$\rho^* = \rho_F^*\left[1 - \alpha(T - T_F)\right] \qquad (2.1.8)$$

where ρ_F^* is the density of the liquid at fusion temperature and α

is the coefficient of cubical expansion. Substitution of the equations (2.1.7) and (2.1.8) into (2.1.6) and then taking the curl of this equation gives,

$$\nabla \times \frac{\partial \underline{v}}{\partial t} - \nabla \times \left[\underline{v} \times (\nabla \times \underline{v}) \right] = -\nu^* \nabla \times \nabla \times \underline{v} + \nabla \times \left\{ \left[1 - \alpha (T - T_F) \right] \underline{F} \right\} \tag{2.1.9}$$

The pressure term has now been eliminated.

Examination of equation (2.1.5) reveals that the stream function $\psi (r, \mu, t)$ can be introduced such that,

$$v_r = -\frac{1}{r^2} \frac{\partial \psi}{\partial \mu} \quad \text{and} \quad v_\mu = \frac{-1}{r(1-\mu^2)^{\frac{1}{2}}} \frac{\partial \psi}{\partial r} \tag{2.1.10}$$

On substituting (2.1.10) into (2.1.9), and after some further analysis has been performed, the vector equation in $\underline{v}$ is reduced to a scalar equation in ψ. That is,

$$\nu^* D_r^4 \psi = \frac{\partial}{\partial t} (D_r^2 \psi) + g \alpha r (1-\mu^2) \left\{ \frac{\mu}{r} \frac{\partial T^*}{\partial \mu} - \frac{\partial T^*}{\partial r} \right\} + \frac{1}{r^2} \left\{ \frac{\partial (\psi, D_r^2 \psi)}{\partial (r, \mu)} + 2 D_r^2 \psi . L_r \psi \right\} \tag{2.1.11}$$

The operators $D_r^2 \cdot$ and $L_r \cdot$ are defined as,

$$D_r^2 \cdot = \frac{\partial^2 \cdot}{\partial r^2} + \frac{(1-\mu^2)^{\frac{1}{2}}}{r^2} \frac{\partial^2 \cdot}{\partial \mu^2} \tag{2.1.12}$$

and

$$L_r \cdot = \frac{\mu}{(1-\mu^2)} \frac{\partial \cdot}{\partial r} + \frac{1}{r} \frac{\partial \cdot}{\partial \mu} \tag{2.1.13}$$

The Jacobian is defined by

$$\frac{\partial(P,Q)}{\partial(x,y)} = \frac{\partial P}{\partial x}\cdot\frac{\partial Q}{\partial y} - \frac{\partial P}{\partial y}\cdot\frac{\partial Q}{\partial x} \qquad (2.1.14)$$

These equations are subject to the following boundary conditions:

(i) initially,

$$\left.\begin{aligned} T^* &= T_I \\ \underline{r} &= 0 \end{aligned}\right\} \text{ at } t=0,\ 0 \leqslant r \leqslant a \qquad (2.1.15)$$

(ii) at the interface,

$$\left.\begin{aligned} T^* &= T_F \\ \psi = \frac{\partial \psi}{\partial r} &= 0 \end{aligned}\right\} \text{ at } r = r_F(\mu,t),\ t>0 \qquad (2.1.16)$$

The second condition in (2.1.16) is the no-slip condition.

The equations for the heat transfer in the two quite separate and distinct solid and liquid regions have now been established. However, the boundary condition at the solid-liquid interface has yet to be derived. This condition, concerned with the absorption and liberation of heat across the interface, is non-linear and controls the motion of the interface. The generalised derivation of this boundary condition is given in appendix A. The condition can be written as

$$K(\nabla T.\nabla C) - K^*(\nabla T^*.\nabla C) = -\rho L\frac{\partial C}{\partial t} \qquad (2.1.17)$$

For this particular problem, using spherical coordinates, the Stefan condition along the interface $C(r,\mu,t)$, which is given by (2.1.1), is

$$K\left(\frac{\partial T}{\partial r} - \frac{(1-\mu^2)}{r^2}\frac{\partial T}{\partial \mu}\cdot\frac{\partial r_F}{\partial \mu}\right) -$$

$$-k^*\left(\frac{\partial T^*}{\partial r} - \frac{(1-\mu^2)}{r^2}\frac{\partial T^*}{\partial \mu}\cdot\frac{\partial r_F}{\partial \mu}\right) = \rho L \frac{\partial r_F}{\partial t} \qquad (2.1.18)$$

2.2 Dimensionless and Neumann Variables

In order to simplify the established equations and their corresponding boundary conditions, the following dimensionless variables are introduced: for the solid region,

$$R = \frac{r}{a} \quad ; \quad R_F = \frac{r_F}{a}$$

$$\tau' = \frac{kt}{a^2} \quad ; \quad \Theta(R,\mu,\tau') = \frac{(T-T_0)}{(T_F-T_0)} \qquad (2.2.1)$$

and for the liquid region,

$$R = \frac{r}{a} \quad ; \quad R_F = \frac{r_F}{a}$$

$$\tau^{*\prime} = \frac{k^*t}{a^2} \quad ; \quad \Theta^*(R,\mu,\tau^{*\prime}) = \frac{(T^*-T_F)}{(T_1-T_F)} \qquad (2.2.2)$$

It is worth noting that $\frac{kt}{a^2}$ is the Fourier number F_o and that the dimensionless parameter λ is defined as $\lambda = \frac{k^*}{k}$.

For the stream function the dimensionless variable

$$\Psi = \frac{\psi}{ak^*} \qquad (2.2.3)$$

is introduced. Inspection of (2.1.10) will reveal that the dimensionless velocity vector can be written as,

$$\underline{V} = \frac{a}{k^*}\underline{v} \qquad (2.2.4)$$

Substituting these variables into the derived equations and simplifying gives the following equations:

for the solid region the heat conduction equation is,

$$\frac{1}{R^2}\frac{\partial}{\partial R}\left(R^2\frac{\partial \Theta}{\partial R}\right) - \frac{1}{R^2}\frac{\partial}{\partial \mu}\left[(1-\mu^2)\frac{\partial \Theta}{\partial \mu}\right] = \frac{\partial \Theta}{\partial \tau'}, \qquad (2.2.5)$$

which is subject to the boundary conditions,

$$\Theta(1, \mu, \tau') = 0$$

and

$$\Theta(R_F(\mu,\tau'), \mu, \tau') = 1 \qquad (2.2.6)$$

for the liquid region the heat conduction and convection equation is,

$$\frac{1}{R^2}\frac{\partial}{\partial R}\left(R^2\frac{\partial \Theta^*}{\partial R}\right) - \frac{1}{R^2}\frac{\partial}{\partial \mu}\left[(1-\mu^2)\frac{\partial \Theta^*}{\partial \mu}\right] - \frac{1}{R^2}\frac{\partial(\Psi, \Theta^*)}{\partial(R,\mu)} = \frac{\partial \Theta^*}{\partial \tau^{*'}}, \qquad (2.2.7)$$

which is subject to the conditions,

$$\Theta^*(R, \mu, 0) = 1$$

and

$$\Theta^*(R_F, \mu, \tau^{*'}) = 0 \qquad (2.2.8)$$

The convective motion in the liquid is governed by the stream function Ψ which satisfies the equation,

$$D_R^4\Psi = \frac{1}{P_r}\left\{\frac{\partial D_R^2\Psi}{\partial \tau^{*'}} + \frac{1}{R^2}\left[\frac{\partial(\Psi, D_R^2\Psi)}{\partial(R,\mu)} + 2D_R^2\Psi . L_R\Psi\right]\right\} + Ra(1-\mu^2)R\left\{\frac{\mu}{R}\frac{\partial \Theta^*}{\partial \mu} - \frac{\partial \Theta^*}{\partial R}\right\} \qquad (2.2.9)$$

This equation introduces the dimensionless Prandtl number - the ratio of the molecular diffusivity of momentum to that of heat - and also the Rayleigh number - the ratio of the buoyancy to viscous forces - which can be written as

$$P_r = \frac{\nu^*}{k^*} \quad \text{and} \quad Ra = \frac{g\alpha a^3 (T_i - T_F)}{\nu^* k^*} \tag{2.2.10}$$

respectively.

The operators D_R^2 and L_R are now defined as

$$D_R^2 \cdot = \frac{\partial^2 \cdot}{\partial R^2} + \frac{(1-\mu^2)}{R^2} \frac{\partial^2 \cdot}{\partial \mu^2} \tag{2.2.11}$$

and

$$L_R \cdot = \frac{\mu}{(1-\mu^2)} \frac{\partial \cdot}{\partial R} + \frac{1}{R} \frac{\partial \cdot}{\partial \mu} \tag{2.2.12}$$

The stream function satisfies the boundary conditions at the interface,

$$\underline{\Psi} = \frac{\partial \Phi}{\partial R} = \frac{\partial \Phi}{\partial \mu} = 0 \quad \text{at} \quad R = R_F \tag{2.2.13}$$

and the initial condition

$$\frac{\partial \Phi}{\partial R}(R, \mu, 0) = 0 \tag{2.2.14}$$

Finally substitution of the dimensionless variables into the Stefan condition at the interface yields

$$\left[\frac{\partial \Theta}{\partial R} - \frac{(1-\mu^2)}{R^2} \frac{\partial \Theta}{\partial \mu} \cdot \frac{\partial R_F}{\partial \mu} \right] -$$

$$-\gamma\left[\frac{\partial \Theta^*}{\partial R} - (1-\mu^2)\frac{\partial \Theta^*}{\partial \mu}\cdot\frac{\partial R_F}{\partial \mu}\right] = \beta\frac{\partial R_F}{\partial \tau'} \qquad (2.2.15)$$

where β is the dimensionless Stefan number defined as $\beta = \frac{L}{C_p(T_1 - T_0)}$ and the dimensionless parameter γ is defined as $\gamma = \frac{R^*}{R}\frac{(T_1 - T_F)}{(T_F - T_0)}$ The solidification process commences at $\tau = 0$, at which time the location of the solidification front is at the surface of the sphere. That is,

$$R_F = 1 \quad \text{at} \quad \tau' = 0 \qquad (2.2.16)$$

Introduction of the Neumann Variables

Clearly for small time the local structure of the solidification process at every point on the surface of the sphere will be that for a semi-infinite region of liquid initially at a temperature above the fusion temperature. Consequently, the following Neumann variables (see Carslaw and Jaeger) are introduced. For the solidified region these are,

$$\xi = \frac{(1-R)}{2(\tau')^{1/2}}, \quad \mu = \cos\theta, \quad \tau = \tau' \qquad (2.2.17)$$

and for the liquid region,

$$\xi^* = \frac{(1-R)}{2(\tau^{*\prime})^{1/2}}, \quad \mu = \cos\theta, \quad \tau^* = \tau^{*\prime} \qquad (2.2.18)$$

and it is found convenient to introduce a new interface variable,

$$E(\mu,\tau) = \frac{(1-R_F)}{2\tau^{1/2}} \qquad (2.2.19)$$

In terms of these Neumann variables the interface is located in the solid region at $\xi = E$ and in the liquid region at $\xi^* = E/\lambda^{1/2}$.

Note that from (2.2.17)

$$\frac{\partial \cdot}{\partial R} = -\frac{1}{2\tau^{1/2}} \frac{\partial \cdot}{\partial \xi} \quad \text{and} \quad \frac{\partial \cdot}{\partial \tau'} = \frac{\partial \cdot}{\partial \tau} - \frac{\xi}{2\tau} \frac{\partial \cdot}{\partial \xi} \tag{2.2.20}$$

with similar results for $\frac{\partial \cdot}{\partial R}$, $\frac{\partial \cdot}{\partial \tau^{*\prime}}$ obtained from (2.2.18). And so, on employing these Neumann variables, the heat conduction equation (2.2.5) for the solid region becomes,

$$\frac{\partial}{\partial \xi}\left[(1-2\tau^{1/2}\xi)^2 \frac{\partial \Theta}{\partial \xi}\right] - 4\tau \frac{\partial}{\partial \mu}\left[(1-\mu^2)\frac{\partial \Theta}{\partial \mu}\right] = (1-2\tau^{1/2}\xi)^2\left[4\tau \frac{\partial \Theta}{\partial \tau} - 2\xi \frac{\partial \Theta}{\partial \xi}\right] \tag{2.2.21}$$

and the boundary conditions are

$$\Theta(0,\mu,\tau) = 0$$

and $$\Theta(E,\mu,\tau) = 1 \tag{2.2.22}$$

For the liquid region the heat conduction and convection equation (2.2.7) becomes,

$$\frac{\partial}{\partial \xi^*}\left[(1-2\tau^{*1/2}\xi^*)^2 \frac{\partial \Theta^*}{\partial \xi^*}\right] - 4\tau^* \frac{\partial}{\partial \mu}\left[(1-\mu^2)\frac{\partial \Theta^*}{\partial \mu}\right] + 2\tau^{1/2} \frac{\partial(\bar{\Psi}, \Theta^*)}{\partial(\xi^*, \mu)} = (1-2\tau^{*1/2}\xi^*)^2\left\{4\tau^* \frac{\partial \Theta^*}{\partial \tau^*} - 2\xi^* \frac{\partial \Theta^*}{\partial \xi^*}\right\} \tag{2.2.23}$$

which is subject to the conditions,

$$\Theta^*(\infty, \mu, 0) = 1$$

and (2.2.24)

$$\Theta^*\left(\frac{E}{\lambda^{1/2}}, \mu, \tau^*\right) = 0$$

and in addition,

$$\frac{\partial \Theta^*}{\partial \xi^*}(\infty, \mu, 0) = \frac{\partial \Theta^*}{\partial \mu}(\infty, \mu, 0) = 0 \qquad (2.2.25)$$

The flow field is governed by the equation,

$$D^4_{\xi^*}\Psi = \frac{1}{P_r}\left\{\left(\frac{\partial}{\partial \tau^*} - \frac{\xi^*}{2\tau^*}\frac{\partial}{\partial \xi^*}\right) D^2_{\xi^*}\Psi + \right.$$

$$\left. + \frac{1}{(1-2\tau^{*1/2}\xi^*)^2}\left[-\frac{1}{2\tau^{*1/2}}\frac{\partial(\Psi, D^2_{\xi^*}\Psi)}{\partial(\xi^*, \mu)} + 2D^2_{\xi^*}\Psi . L_{\xi^*}\Psi\right]\right\} +$$

$$+ Ra(1-\mu^2)(1-2\xi^*\tau^{*1/2})\left[\frac{\mu}{(1-2\tau^{*1/2}\xi^*)}\frac{\partial \Theta^*}{\partial \mu} + \frac{1}{2\tau^{*1/2}}\frac{\partial \Theta^*}{\partial \xi^*}\right] \qquad (2.2.26)$$

which is subject to the boundary conditions

$$\Psi = \frac{\partial \Psi}{\partial \xi^*} = \frac{\partial \Psi}{\partial \mu} = 0 \quad \text{at} \quad \xi^* = \frac{E}{\lambda^{1/2}}$$

and (2.2.27)

$$\frac{\partial \Psi}{\partial \xi^*}(\infty, \mu, 0) = 0$$

The operators $D^2_{\xi^*}$ and L_{ξ^*} are now defined by

$$D^2_{\xi^*}(\cdot) = \frac{1}{4\tau^*}\frac{\partial^2(\cdot)}{\partial \xi^{*2}} + \frac{(1-\mu^2)}{(1-2\xi^*\tau^{*1/2})^2}\frac{\partial^2(\cdot)}{\partial \mu^2} \qquad (2.2.28)$$

and

$$L_{\xi^*}(\cdot) = \frac{\mu}{2\tau^{*1/2}(1-\mu^2)}\frac{\partial(\cdot)}{\partial \xi^*} + \frac{1}{(1-2\tau^{*1/2}\xi^*)}\frac{\partial(\cdot)}{\partial \mu} \qquad (2.2.29)$$

The Jacobian is transformed to become,

$$\frac{\partial(\Psi,\Theta^*)}{\partial(R,\mu)} = -\frac{1}{2\tau^{*\frac{1}{2}}}\frac{\partial(\Psi,\Theta^*)}{\partial(\xi^*,\mu)} \tag{2.2.30}$$

To complete the transformations of the equations, the latent heat condition at the interface is,

$$\left[\frac{1}{2\tau^{\frac{1}{2}}}\frac{\partial\Theta}{\partial\xi} - \frac{2\tau^{\frac{1}{2}}(1-\mu^2)^{\frac{1}{2}}}{(1-2\tau^{\frac{1}{2}}\xi)^2}\cdot\frac{\partial\Theta}{\partial\mu}\cdot\frac{\partial E}{\partial\mu}\right]_{\xi=\varepsilon_0}$$
$$-\gamma\left[\frac{1}{2\tau^{*\frac{1}{2}}}\frac{\partial\Theta^*}{\partial\xi^*} - \frac{2\tau^{*\frac{1}{2}}(1-\mu^2)^{\frac{1}{2}}}{(1-2\tau^{*\frac{1}{2}}\xi^*)^2}\cdot\frac{\partial\Theta^*}{\partial\mu}\cdot\frac{\partial E}{\partial\mu}\right]_{\xi^*=\frac{\varepsilon_0}{\lambda^2}}$$
$$= 2\beta\frac{\partial}{\partial\tau}(E\tau^{\frac{1}{2}}) \tag{2.2.31}$$

and the initial condition on E is,

$$E(\mu,0) = 0 \tag{2.2.32}$$

2.3 The Perturbation Procedure

The non-linear system of partial differential equations derived in the previous section can be solved by assuming, for small time, the following regular perturbation expansions:

$$\Theta(\xi,\mu,\tau) = \sum_{n=0}^{\infty}\Theta_n(\xi,\mu)\tau^{\frac{n}{2}} \tag{2.3.1}$$

$$\Theta^*(\xi^*,\mu,\tau^*) = \sum_{n=0}^{\infty}\Theta_n^*(\xi^*,\mu)\tau^{*\frac{n}{2}} \tag{2.3.2}$$

$$E(\mu,\tau) = \sum_{n=0}^{\infty}E_n(\mu)\tau^{\frac{n}{2}} \tag{2.3.3}$$

and

$$E(\mu,\tau^*) = \sum_{n=0}^{\infty} E_n(\mu)\left(\frac{\tau^*}{\lambda}\right)^{\frac{n}{2}} \tag{2.3.4}$$

However, the perturbation expansion for the stream function $\Psi(\xi^*,\mu,\tau^*)$ is more complicated and has yet to be determined. Suppose that this function can be written in the form,

$$\Psi(\xi^*,\mu,\tau^*) = \Psi_n(\xi^*,\mu)\tau^{*\frac{n}{2}} \tag{2.3.5}$$

Then, on substituting (2.3.5) into the flow field governing equation (2.2.26) and expanding for small time, the following equation is obtained:

$$\frac{1}{16\tau^{*2}}\frac{\partial^4(\Psi_n\tau^{*n})}{\partial\xi^{*4}} - \frac{1}{Pr}\left\{-\frac{1}{4\tau^{*2}}\frac{\partial^2(\Psi_n\tau^{*n})}{\partial\xi^{*2}} + \frac{n}{4\tau^*}\frac{\partial^2}{\partial\xi^{*2}}(\Psi_n\tau^{*n-1}) - \frac{\xi^*}{8\tau^{*2}}\frac{\partial^3}{\partial\xi^{*3}}(\Psi_n\tau^{*n})\right\} + O(\tau^{*n-1})$$

$$= (1-2\tau^{*\frac{1}{2}}\xi^*)\frac{Ra(1-\mu^2)}{2\tau^{*\frac{1}{2}}}\frac{\partial\Theta^*}{\partial\xi^*} + O(1) \tag{2.3.6}$$

Comparing both sides of this equation, it can be seen that n must take the value of 3/2 and hence

$$\Psi(\xi^*,\mu,\tau^*) = \sum_{n=3}^{\infty}\Psi_n(\xi^*,\mu)\,\tau^{*\frac{n}{2}} \tag{2.3.7}$$

or equivalently,

$$\Psi(\xi^*,\mu,\tau^*) = \sum_{n=0}^{\infty}\Psi_{n+3}(\xi^*,\mu)\tau^{*\frac{n+3}{2}} \tag{2.3.8}$$

Substitution of these perturbation expansions into the derived governing

equations (and the corresponding boundary conditions) yields, on equating coefficients of like powers of τ (or τ^*) in the usual method, a system of ordinary linear differential equations. Thus the difficulty due to the complication of the non-linearity at the interface is removed. The perturbation functions Θ_n, Θ_n^*, ε_n and Ψ_n are then determined from the resulting equations.

Investigation of the coupled partial differential equations with the perturbation expansions will reveal that the first perturbation functions to have a dependency on μ are Θ_4, Θ_4^* and E_4. Hence, the expansions can be written as:

$$\Theta(\xi,\mu,\tau) = \Theta_0(\xi) + \Theta_1(\xi)\tau^{1/2} + \Theta_2(\xi)\tau + \Theta_3(\xi)\tau^{3/2} + \Theta_4(\xi,\mu)\tau^2 + \Theta_5(\xi,\mu)\tau^{5/2} + \ldots . \tag{2.3.9}$$

$$\Theta^*(\xi^*,\mu,\tau^*) = \Theta_0^*(\xi^*) + \Theta_1^*(\xi^*)\tau^{*1/2} + \Theta_2^*(\xi^*)\tau^* + \Theta_3^*(\xi^*)\tau^{*3/2} + \Theta_4^*(\xi^*,\mu)\tau^{*2} + \Theta_5^*(\xi^*,\mu)\tau^{*5/2} + \ldots . \tag{2.3.10}$$

$$E(\mu,\tau) = E_0 + E_1\tau^{1/2} + E_2\tau + E_3\tau^{3/2} + E_4(\mu)\tau^2 + E_5(\mu)\tau^{5/2} + \ldots . \tag{2.3.11}$$

and finally,

$$\Psi(\xi^*,\mu,\tau^*) = \Psi_3(\xi^*,\mu)\tau^{*3/2} + \Psi_4(\xi^*,\mu)\tau^{*2} + \ldots \tag{2.3.12}$$

Unfortunately the boundary condition at the interface introduces a complexity into the normal perturbation procedure. To illustrate this problem we consider the boundary condition at the interface in the solid region. Direct substitution of the perturbation expansion (2.3.9) into the boundary condition

$$\Theta(E_0 + \tau^{1/2}E_1 + \tau E_2 + \dots, \mu, \tau) = 1 \tag{2.3.13}$$

results in,

$$\Theta_0(E_0 + \tau^{1/2}E_1 + \cdots) + \tau^{1/2}\Theta_1(E_0 + \tau^{1/2}E_1 + \cdots) + \cdots = 1 \tag{2.3.14}$$

Obviously, the terms of $O(\tau^{\frac{n}{2}})$ cannot be immediately equated since τ appears both implicitly and explicitly. This then necessitates releasing τ from the arguments of the perturbation functions. Utilizing the method of Van Dyke [27], the perturbation function is expanded as a Taylor series about $\xi = E_0$. So, expanding $\Theta(\xi, \mu, \tau)$ about $\xi = E_0$, it is found that at $\xi = E$,

$$\begin{aligned}\Theta(E, \mu, \tau) = {} & \Theta(E_0, \mu, \tau) + \\ & + (\tau^{1/2}E_1 + \tau E_2 + \cdots)\Theta'(E_0, \mu, \tau) + \\ & + \frac{1}{2!}(\tau^{1/2}E_1 + \tau E_2 + \cdots)^2\Theta''(E_0, \mu, \tau) + \cdots\end{aligned} \tag{2.3.15}$$

where $'$ denotes differentiation with respect to ξ. Now, substitution of the perturbation series (2.3.9) for $\Theta(E_0, \mu, \tau)$ in the above equation, gives an equation in which τ appears only explicitly. Thus,

$$\begin{aligned}&\left[\Theta_0(E_0) + \tau^{1/2}\Theta_1(E_0) + \cdots + \tau^{s/2}\Theta_s(E_0, \mu) + \cdots\right] + \\ &+ (\tau^{1/2}E_1 + \tau E_2 + \cdots)\left[\Theta_0'(E_0) + \tau^{1/2}\Theta_1'(E_0) + \cdots\right] + \\ &+ \frac{(\tau^{1/2}E_1 + \tau E_2 + \cdots)^2}{2!}\left[\Theta_0''(E_0) + \tau^{1/2}\Theta_1''(E_0) + \cdots\right] + \\ &+ \cdots = 1\end{aligned} \tag{2.3.16}$$

Similarly the boundary conditions which include the terms $\frac{\partial \Theta}{\partial \xi}$, Θ^*, $\frac{\partial \Theta^*}{\partial \xi^*}$, Ψ, $\frac{\partial \Psi}{\partial \xi^*}$ and $\frac{\partial \Psi}{\partial \mu}$ at the interface have τ released from their arguments and, in this way, terms of order τ^2 may be collected since τ now appears, as required only explicitly.

Because of the spacial derivatives occurring in the latent heat condition (2.2.31), the perturbation equations and their boundary conditions become more and more complex with increasing exponent of τ. It is noteworthy that these complications (and others) would be removed if the further approximations proposed by Sparrow et al. in [13] and [14] were invoked.

2.4 Determination of Perturbation Functions

Applying the perturbation procedure described in the last section to the governing equations and their corresponding boundary conditions, the perturbation functions can now be determined. Accordingly, the systems of ordinary linear differential equations can be written as follows:

Zeroth Order

Collecting terms of order τ^0, that is O(1), the zeroth order perturbation functions Θ_0, Θ_0^* and E_0 are governed by the equations which are now given.

For the solid region $0 \leq \xi \leq E_0$, Θ_0 satisfies

$$\frac{d^2\Theta_0}{d\xi^2} + 2\xi \frac{d\Theta_0}{d\xi} = 0 \qquad (2.4.1)$$

which is subject to the boundary conditions,

$$\Theta_0(0) = 0$$

and

$$\Theta_0(E_0) = 1 \qquad (2.4.2)$$

For the liquid region $\frac{E_0}{\lambda^{1/2}} \leq \xi^* < \infty$, Θ_0^* satisfies

$$\frac{d^2\Theta_0^*}{d\xi^{*2}} + 2\xi^* \frac{d\Theta_0^*}{d\xi^*} = 0 \qquad (2.4.3)$$

which is subject to the boundary conditions,

$$\Theta_0^*\left(\frac{E_0}{\lambda^{1/2}}\right) = 0$$

and (2.4.4)

$$\Theta_0^*(\infty) = 1$$

The perturbation function E_0 is given by the interface equation,

$$2\beta E_0 = \left[\frac{d\Theta_0}{d\xi}\right]_{\xi=E_0} - \frac{\gamma}{\lambda^{1/2}}\left[\frac{d\Theta_0^*}{d\xi^*}\right]_{\xi^*=\frac{E_0}{\lambda^{1/2}}} \qquad (2.4.5)$$

First Order

Collecting terms of order $\tau^{1/2}$, the perturbation functions Θ_1, Θ_1^* and E_1 are determined by the equations:

For the solid region, Θ_1 satisfies

$$\frac{d^2\Theta_1}{d\xi^2} + 2\xi\frac{d\Theta_1}{d\xi} - 2\Theta_1 = 4\frac{d\Theta_0}{d\xi} \qquad (2.4.6)$$

subject to,

$$\Theta_1(0) = 0$$

and (2.4.7)

$$\left[\Theta_1 + E_1\frac{d\Theta_0}{d\xi}\right]_{\xi=E_0} = 0$$

For the liquid region, Θ_1^* satisfies

$$\frac{d^2\Theta_1^*}{d\xi^{*2}} + 2\xi^*\frac{d\Theta_1^*}{d\xi^*} - 2\Theta_1^* = 4\frac{d\Theta_0^*}{d\xi^*} \qquad (2.4.8)$$

subject to the conditions

$$\left[\Theta_1^* + \frac{E_1}{\lambda} \frac{d\Theta_0^*}{d\xi^*} \right]_{\xi^* = \frac{\epsilon_0}{\lambda^{1/2}}} = 0$$

and

$$\Theta_1^*(\infty) = 0 \qquad (2.4.9)$$

The perturbation function E_1 is determined by

$$4\beta E_1 = \left[\frac{d\Theta_1}{d\xi} - 2E_0 E_1 \frac{d\Theta_0}{d\xi} \right]_{\xi = \epsilon_0}$$

$$- \gamma \left[\frac{d\Theta_1^*}{d\xi^*} - \frac{2E_0 E_1}{\lambda^{3/2}} \frac{d\Theta_0^*}{d\xi^*} \right]_{\xi^* = \frac{\epsilon_0}{\lambda^{1/2}}} \qquad (2.4.10)$$

Second Order

Terms of order τ give the following set of equations:

For the solid region, Θ_2 satisfies

$$\frac{d^2\Theta_2}{d\xi^2} + 2\xi \frac{d\Theta_2}{d\xi} - 4\Theta_2 = 8\xi \frac{d\Theta_0}{d\xi} + 4 \frac{d\Theta_1}{d\xi} \qquad (2.4.11)$$

subject to the boundary conditions,

$$\Theta_2(0) = 0$$

and

$$\left[\Theta_2 + E_1 \frac{d\Theta_1}{d\xi} + (E_2 - E_0 E_1^2) \frac{d\Theta_0}{d\xi} \right]_{\xi = \epsilon_0} = 0 \qquad (2.4.12)$$

For the liquid region, Θ_2^* satisfies

$$\frac{d^2\Theta_2^*}{d\xi^{*2}} + 2\xi^* \frac{d\Theta_2^*}{d\xi^*} - 4\Theta_2^* = 8\xi^* \frac{d\Theta_0^*}{d\xi^*} + 4\frac{d\Theta_1^*}{d\xi^*} \tag{2.4.13}$$

subject to the boundary conditions,

$$\left[\Theta_2^* + \frac{E_1}{\lambda}\frac{d\Theta_1^*}{d\xi^*} + \left(\frac{E_2}{\lambda^{3/2}} - \frac{E_0E_1^2}{\lambda^{5/2}}\right)\frac{d\Theta_0^*}{d\xi^*}\right]_{\xi^* = \frac{\epsilon_0}{\lambda^{1/2}}} = 0$$

and (2.4.14)

$$\Theta_2^*(\infty) = 0$$

The interface equation determines E_2.

$$6\beta E_2 = \left[\frac{d\Theta_2}{d\xi} - 2E_0E_1\frac{d\Theta_1}{d\xi} + (4E_1 - 3E_1^2 + 2E_0^2E_1^2 - 2E_0E_2)\frac{d\Theta_0}{d\xi}\right]_{\xi=\epsilon_0} - \lambda^{1/2}\gamma\left[\frac{d\Theta_2^*}{d\xi^*} - \frac{2E_0E_1}{\lambda^{3/2}}\frac{d\Theta_1^*}{d\xi^*} + \left(\frac{4E_1}{\lambda} - \frac{3E_1^2}{\lambda^2} + \frac{2E_0^2E_1^2}{\lambda^3} - \frac{2E_0E_2}{\lambda^2}\right)\frac{d\Theta_0^*}{d\xi^*}\right]_{\xi^* = \frac{\epsilon_0}{\lambda^{1/2}}} \tag{2.4.15}$$

Third Order

On collecting terms of order $\tau^{\frac{3}{2}}$ (or equivalently $\tau^{*\frac{3}{2}}$), the perturbation function Ψ_3 is introduced from the flow field governing equation. Firstly, however, the third order perturbation functions for the thermal fields are given.

For the solid region, Θ_3 satisfies the equation,

$$\frac{d^2\Theta_3}{d\xi^2} + 2\xi\frac{d\Theta_3}{d\xi} - 6\Theta_3 = 16\xi^2\frac{d\Theta_0}{d\xi} + 8\xi\frac{d\Theta_1}{d\xi} + 4\frac{d\Theta_2}{d\xi}$$

(2.4.16)

which is subject to the conditions

$$\Theta_3(0) = 0$$

and (2.4.17)

$$\left[\Theta_3 + \epsilon_1 \frac{d\Theta_2}{d\xi} + (\epsilon_2 - \epsilon_0\epsilon_1^2) \frac{d\Theta_1}{d\xi} + \right.$$

$$\left. + \left(\epsilon_3 + 2\epsilon_1^2 - 2\epsilon_0\epsilon_1\epsilon_2 + \frac{2}{3}\epsilon_0^2\epsilon_1^3 - \frac{4}{3}\epsilon_1^3\right) \frac{d\Theta_0}{d\xi} \right]_{\xi=\epsilon_0} = 0$$

For the liquid region, Θ_3^* satisfies the equation

$$\frac{d^2\Theta_3^*}{d\xi^{*2}} + 2\xi^* \frac{d\Theta_3^*}{d\xi^*} - 6\Theta_3^* =$$

$$16\xi^{*2} \frac{d\Theta_0^*}{d\xi^*} + 8\xi^* \frac{d\Theta_1^*}{d\xi^*} + 4 \frac{d\Theta_2^*}{d\xi^*} \qquad (2.4.18)$$

which is subject to,

$$\left[\Theta_3^* + \frac{\epsilon_1}{\lambda} \frac{d\Theta_2^*}{d\xi^*} + \left(\frac{\epsilon_2}{\lambda^2} - \frac{\epsilon_0\epsilon_1^2}{\lambda^3} \right) \frac{d\Theta_1^*}{d\xi^*} + \right.$$

$$\left. + \left(\frac{\epsilon_3}{\lambda^2} + \frac{2\epsilon_1^2}{\lambda^2} - \frac{2\epsilon_0\epsilon_1\epsilon_2}{\lambda^3} + \frac{2}{3}\frac{\epsilon_0^2\epsilon_1^3}{\lambda^4} - \frac{4}{3}\frac{\epsilon_1^3}{\lambda^3} \right) \frac{d\Theta_0^*}{d\xi^*} \right]_{\xi^* = \frac{\epsilon_0}{\lambda^2}}$$

$$= 0$$

and (2.4.19)

$$\Theta_3^*(\infty) = 0$$

E_3 can be determined from the interface equation

$$8\beta E_3 = \left[\frac{d\Theta_3}{d\zeta} - 2E_0E_1 \frac{d\Theta_2}{d\zeta} + \left(4E_1 - 4E_1^2 - 2E_0E_2 + 2E_0^2E_1^2\right) \frac{d\Theta_1}{d\zeta} + \left(8E_0E_1 + 8E_0E_1^3 - 8E_1E_2 + 4E_2 - 2E_0E_3 - 8E_0E_1^2 + 4E_0^2E_1E_2 - \frac{4}{3}E_0^3E_1^3\right) \frac{d\Theta_0}{d\zeta} \right]_{\zeta=E_0}$$

$$- \lambda\gamma \left[\frac{d\Theta_3^*}{d\zeta^*} - \frac{2E_0E_1}{\lambda^{3/2}} \frac{d\Theta_2^*}{d\zeta^*} + \left(\frac{4E_1}{\lambda} - \frac{4E_1^2}{\lambda^2} - \frac{2E_0E_2}{\lambda^2} + \frac{2E_0^2E_1^2}{\lambda^3}\right) \frac{d\Theta_1^*}{d\zeta^*} + \left(\frac{8E_0E_1}{\lambda^{3/2}} + \frac{8E_0E_1^3}{\lambda^{7/2}} - \frac{8E_1E_2}{\lambda^{5/2}} + \frac{4E_2}{\lambda^{3/2}} - \frac{2E_0E_3}{\lambda^{5/2}} - \frac{8E_0E_1^2}{\lambda^{5/2}} + \frac{4E_0^2E_1E_2}{\lambda^{7/2}} - \frac{4}{3}\frac{E_0^3E_1^3}{\lambda^{9/2}}\right) \frac{d\Theta_0^*}{d\zeta^*} \right]_{\zeta^* = \frac{E_0}{\lambda^{1/2}}}$$

(2.4.20)

Finally, the flow function for Ψ_3 is given by the partial differential equation,

$$\frac{\partial^4\Psi_3}{\partial\zeta^{*4}} + \frac{2\zeta^*}{P_r}\frac{\partial^3\Psi_3}{\partial\zeta^{*3}} - \frac{2}{P_r}\frac{\partial^2\Psi_3}{\partial\zeta^{*2}} = 8Ra(1-\mu^2)\frac{\partial\Theta_0^*}{\partial\zeta^*}$$

(2.4.21)

which is subject to the boundary conditions

$$\Psi_3(\zeta^*,\mu) = \frac{\partial\Psi_3}{\partial\zeta^*}(\zeta^*,\mu) = \frac{\partial\Psi_3}{\partial\mu}(\zeta^*,\mu) = 0 \quad \text{at } \zeta^* = \frac{E_0}{\lambda^{1/2}}$$

(2.4.22)

and

$$\frac{\partial\Psi_3}{\partial\zeta^*}(\zeta^*,\mu) \longrightarrow 0 \quad \text{as } \zeta^* \longrightarrow \infty$$

(2.4.23)

A standard method of obtaining a solution to this type of partial differential equation is to assume that the variables are separable. Thus Φ_3 can be simplified by employing the separable variable as follows:

$$\Phi_3(\xi^*,\mu) = 8Ra\,(1-\mu^2).\,\bar{\Phi}_3(\xi^*) \qquad (2.4.24)$$

Hence the equation is reduced to a fourth order ordinary differential equation in which, it should be remembered, Θ_0 is dependent on ξ^* only. Thus $\bar{\Phi}_3$ satisfies,

$$\frac{d^4\bar{\Phi}_3}{d\xi^{*4}} + \frac{2\xi^*}{P_r}\frac{d^3\bar{\Phi}_3}{d\xi^{*3}} - \frac{2}{P_r}\frac{d^2\bar{\Phi}_3}{d\xi^{*2}} = \frac{d\Theta_0^*}{d\xi^*} \qquad (2.4.25)$$

and is subject to the boundary conditions,

$$\bar{\Phi}_3 = \frac{d\bar{\Phi}_3}{d\xi^*} = 0 \qquad \text{at } \xi^* = \frac{\varepsilon_0}{\lambda^{1/2}} \qquad (2.4.26)$$

and

$$\frac{d\Phi_3}{d\xi^*} \to 0 \quad \text{as} \quad \xi^* \to \infty \qquad (2.4.27)$$

Fourth Order

For the lower orders ($n \leq 3$) Θ_n and Θ_n^* have been dependent solely on ξ and ξ^* respectively and E_n has been a constant. That is, they have been independent of the polar angle Θ ($\mu = \cos\Theta$). However, on calculating the order τ^2 equations, the first dependency on μ of these perturbation functions is introduced. In particular, a term which governs the convective motion in the liquid thermal field is introduced. The equation for the liquid region is,

$$\frac{\partial^2 \Theta_4^*}{\partial \xi^{*2}} + 2\xi^* \frac{\partial \Theta_4^*}{\partial \xi^*} - 8\Theta_4^* = 32\xi^{*3} \frac{d\Theta_0^*}{d\xi^*} + 16\xi^{*2} \frac{d\Theta_1^*}{d\xi^*}$$

$$+ 8\xi^* \frac{d\Theta_2^*}{d\xi^*} + 4\frac{d\Theta_3^*}{d\xi^*} + 2\frac{\partial \Phi_3}{\partial \mu} \cdot \frac{d\Theta_0^*}{d\xi^*}$$

(2.4.28)

Substituting (2.4.24) into the term on the right hand side which contains Φ_3^*, it is found that this term becomes,

$$-32Ra\, \overline{\Phi}_3 \cdot \frac{d\Theta_0}{d\xi^*} \cdot \mu \qquad (2.4.29)$$

Since this is the only term containing μ, the following separable variables are employed.

$$\Theta_4(\xi, \mu) = \overline{\Theta}_4(\xi) + \mu \overline{\overline{\Theta}}_4(\xi) \qquad (2.4.30)$$

$$\Theta_4^*(\xi^*, \mu) = \overline{\Theta}_4^*(\xi^*) + \mu \overline{\overline{\Theta}}_4^*(\xi^*) \qquad (2.4.31)$$

and

$$E_4(\mu) = \overline{E}_4 + \mu \overline{\overline{E}}_4 \qquad (2.4.32)$$

Substitution into the fourth order thermal equations for the solid and liquid regions, together with their boundary conditions and also the interface equation, gives two systems of differential equations. These are the single bar and the double bar systems which are denoted by $\overline{\ }$ and $\overline{\overline{\ }}$ respectively.

Fourth Order Single Bar System

The solid thermal function $\bar{\Theta}_4$ satisfies the equation,

$$\frac{d^2\bar{\Theta}_4}{d\xi^2} + 2\xi\frac{d\bar{\Theta}_4}{d\xi} - 8\bar{\Theta}_4 = 32\xi^3\frac{d\Theta_0}{d\xi} + 16\xi^2\frac{d\Theta_1}{d\xi} + 8\xi\frac{d\Theta_2}{d\xi} + 4\frac{d\Theta_3}{d\xi} \tag{2.4.33}$$

which is subject to the boundary conditions,

$$\bar{\Theta}_4(0) = 0 \tag{2.4.34}$$

and

$$\left[\bar{\Theta}_4 + E_1\frac{d\Theta_3}{d\xi} + (E_2 - E_0E_1^2)\frac{d\Theta_2}{d\xi} + \left(E_3 + 2E_1^2 - 2E_1^3 - 2E_0E_1E_2 + \frac{2}{3}E_0^2E_1^3\right)\frac{d\Theta_1}{d\xi} + \left(4E_0E_1^2 - 2E_0E_1E_3 + \frac{19}{6}E_0E_1^4 - 5E_1^2E_2 - E_0E_2^2 + \bar{E}_4 + 4E_1E_2 - \frac{8}{3}E_0E_1^3 + 2E_0^2E_1^2E_2 - \frac{E_0^3E_1^4}{3}\right)\frac{d\Theta}{d\xi}\right]_{\xi=E_0} = 0$$

The liquid thermal function $\bar{\Theta}_4^*$ satisfies

$$\frac{d^2\bar{\Theta}_4^*}{d\xi^{*2}} + 2\xi^*\frac{d\bar{\Theta}_4^*}{d\xi^*} - 8\bar{\Theta}_4^* = 32\xi^{*3}\frac{d\Theta_0^*}{d\xi} + 16\xi^{*2}\frac{d\Theta_1^*}{d\xi^*} + 8\xi^*\frac{d\Theta_2^*}{d\xi^*} + 4\frac{d\Theta_3^*}{d\xi^*} \tag{2.4.35}$$

subject to the boundary conditions,

$$\left[\bar{\Theta}_4^* + \frac{E_1}{\lambda}\frac{d\Theta_3^*}{d\xi^*} + \left(\frac{E_2}{\lambda^{3/2}} - \frac{E_0E_1^2}{\lambda^{3/2}}\right)\frac{d\Theta_2^*}{d\xi^*} + \right.$$

$$+\left(\frac{E_3}{\lambda^2}+\frac{2E_1^2}{\lambda^2}-\frac{2E_1^3}{\lambda^3}-\frac{2E_0E_1E_2}{\lambda^3}+\frac{2}{3}\frac{E_0^2E_1^3}{\lambda^4}\right)\frac{d\overline{\otimes}_1^*}{d\xi^*}$$

$$+\left(\frac{\overline{E}_4}{\lambda^{5/2}}-\frac{2E_0E_1E_3}{\lambda^{7/2}}+\frac{4E_0E_1^2}{\lambda^{5/2}}+\frac{19}{6}\frac{E_0E_1^4}{\lambda^{9/2}}-\frac{5E_1^2E_2}{\lambda^{7/2}}-\frac{E_0E_2^2}{\lambda^{7/2}}+\right.$$

$$\left.+\frac{4E_1E_2}{\lambda^{5/2}}-\frac{8}{3}\frac{E_0E_1^3}{\lambda^{7/2}}+\frac{2E_0^2E_1^3E_2}{\lambda^{9/2}}-\frac{E_0^3E_1^4}{3\lambda^{11/2}}\right)\frac{d\overline{\otimes}_0^*}{d\xi^*}\Bigg]_{\xi^*=E^0/\lambda^{1/2}}=0$$

and (2.4.36)

$$\overline{\otimes}_4^*(\infty)=0$$

The interface equation which determines $\overline{E}_4$ is

$$10\beta\overline{E}_4=\left[\frac{d\overline{\otimes}_4}{d\xi}-2E_0E_1\frac{d\otimes_3}{d\xi}+\left(4E_1-5E_1^2\right.\right.$$

$$-2E_0E_2+2E_0^2E_1^2)\frac{d\otimes_2}{d\xi}+(8E_0E_1-10E_1E_2+\frac{32}{3}E_0E_1^3$$

$$+4E_2-2E_0E_3-8E_0E_1^2+4E_0^2E_1E_2-\frac{4}{3}E_0^3E_1^3)\frac{d\otimes_1}{d\xi}$$

$$+(16E_0^2E_1-10E_1E_3-\frac{56}{3}E_1^3+30E_0E_1^2E_2-\frac{34}{3}E_0^2E_1^4$$

$$+\frac{55}{6}E_1^4+8E_0E_2-5E_2^2+4E_3-2E_0\overline{E}_4+12E_1^2$$

$$-16E_0^2E_1^2+2E_0^2E_2^2-16E_0E_1E_2+4E_0^2E_1E_3+8E_0^2E_1^3$$

$$\left.\left.-4E_0^3E_1^2E_2+\frac{2}{3}E_0^4E_1^4)\frac{d\otimes_0}{d\xi}\right]\right|_{\xi=E_0}$$

$$-\lambda^{3/2}\gamma\left[\frac{d\overline{\otimes}_4^*}{d\xi^*}-\frac{2E_0E_1}{\lambda^{3/2}}\frac{d\otimes_3^*}{d\xi^*}+\left(\frac{4E_1}{\lambda}-\frac{5E_1^2}{\lambda^2}\right.\right.$$

$$\left.-\frac{2E_0E_2}{\lambda^2}+\frac{2E_0^2E_1^2}{\lambda^3}\right)\frac{d\otimes_2^*}{d\xi^*}+\left(\frac{8E_0E_1}{\lambda^{3/2}}-\frac{10E_1E_2}{\lambda^{5/2}}\right.$$

$$+\frac{32E_0E_1^3}{\lambda^{7/2}}+\frac{4E_2}{\lambda^{3/2}}-\frac{2E_0E_3}{\lambda^{5/2}}-\frac{8E_0E_1^2}{\lambda^{5/2}}+\frac{4E_0^2E_1E_2}{\lambda^{7/2}}$$

$$-\frac{4}{3}\frac{E_0^3E_1^3}{\lambda^{9/2}}\Big)\frac{d\bar{\bar{\Theta}}_1^*}{d\zeta^*} + \Big(\frac{16E_0^2E_1}{\lambda^3} - \frac{10E_1E_3}{\lambda^3} - \frac{56}{3}\frac{E_1^3}{\lambda^3}$$
$$+30\frac{E_0E_1^2E_2}{\lambda^4} - \frac{34}{3}\frac{E_0^2E_1^4}{\lambda^5} + \frac{55}{6}\frac{E_1^4}{\lambda^4} + 8\frac{E_0E_2}{\lambda^2} - 5\frac{E_2^2}{\lambda^3}$$
$$+\frac{4E_3}{\lambda^2} - 2\frac{E_0\bar{E}_4}{\lambda^3} + \frac{12E_1^2}{\lambda^2} - 16\frac{E_0^2E_1^2}{\lambda^3} + 2\frac{E_0^2E_2^2}{\lambda^4} + \frac{2}{3}\frac{E_0E_1}{\lambda^6}$$
$$-16\frac{E_0E_1E_2}{\lambda^3} + 4\frac{E_0^2E_1E_3}{\lambda^4} + 8\frac{E_0^2E_1^3}{\lambda^4} - 4\frac{E_0^3E_1^2E_2}{\lambda^5}\Big)\frac{d\bar{\bar{\Theta}}_0^*}{d\zeta^*}\Big]$$

(2.4.37)

Fourth Order Double Bar System

The governing equation for $\bar{\bar{\Theta}}_4$ in the solid region is,

$$\frac{d^2\bar{\bar{\Theta}}_4}{d\zeta^2} + 2\zeta\frac{d\bar{\bar{\Theta}}_4}{d\zeta} - 8\bar{\bar{\Theta}}_4 = 0 \qquad (2.4.38)$$

which is subject to the boundary conditions,

$$\bar{\bar{\Theta}}_4(0) = 0$$

and

$$\Big[\bar{\bar{\Theta}}_4 + \bar{\bar{E}}_4\frac{d\bar{\bar{\Theta}}_0}{d\zeta}\Big]_{\zeta=\epsilon_0} = 0 \qquad (2.4.39)$$

For the liquid, $\bar{\bar{\Theta}}_4^*$ satisfies the equation,

$$\frac{d^2\bar{\bar{\Theta}}_4^*}{d\zeta^{*2}} + 2\zeta^*\frac{d\bar{\bar{\Theta}}_4^*}{d\zeta^*} - 8\bar{\bar{\Theta}}_4^* = -32Ra\,\bar{\bar{\Psi}}_3\frac{d\bar{\bar{\Theta}}_0^*}{d\zeta^*} \qquad (2.4.40)$$

subject to the boundary conditions

$$\Big[\bar{\bar{\Theta}}_4^* + \frac{\bar{\bar{E}}_4}{\lambda^{5/2}}\frac{d\bar{\bar{\Theta}}_0}{d\zeta^*}\Big]_{\zeta^*=\frac{\epsilon_0}{\lambda^{1/2}}} = 0$$

and

$$\bar{\bar{\Theta}}_4^*(\infty) = 0 \qquad (2.4.41)$$

The double bar interface equation for $\bar{\bar{E}}_4$ is,

$$\left[\frac{d\bar{\bar{\Theta}}_4}{d\xi} - 2\epsilon_0 \bar{\bar{E}}_4 \frac{d\Theta_0}{d\xi} \right]_{\xi=\epsilon_0} - \lambda^{\frac{3}{2}}\gamma \left[\frac{d\bar{\bar{\Theta}}_4^*}{d\xi^*} - 2\frac{\epsilon_0}{\lambda^3}\bar{\bar{E}}_4 \frac{d\Theta_0^*}{d\xi^*} \right]_{\xi^*=\epsilon_0/\lambda^4} = 10\beta \bar{\bar{E}}_4 \tag{2.4.42}$$

Finally the perturbation function $\Phi_4(\xi^*, \mu)$ which is also given by collecting terms $O(\tau^{*2})$, satisfies the equation,

$$\frac{\partial^4 \Phi_4}{\partial \xi^{*4}} + 2\xi^* \frac{\partial^3 \Phi_4}{\partial \xi^{*3}} - \frac{4}{R} \frac{\partial^2 \Phi_4}{\partial \xi^{*2}} = 8Ra(1-\mu^2)\frac{d\Theta_1^*}{d\xi^*} - 16Ra(1-\mu^2)\xi^* \frac{d\Theta_0^*}{d\xi^*} \tag{2.4.43}$$

which is subject to the boundary conditions,

$$\left[\Phi_4 + \frac{\epsilon_1}{\lambda} \frac{\partial \Phi_3}{\partial \xi^{*2}} \right]_{\xi^*=\frac{\epsilon_0}{\lambda^4}} = 0 \tag{2.4.44}$$

and

$$\left[\frac{\partial \Phi_4}{\partial \xi^*} + \frac{\epsilon_1}{\lambda} \frac{\partial^2 \Phi_3}{\partial \xi^{*2}} \right]_{\xi^*=\frac{\epsilon_0}{\lambda^4}} = 0$$

and also

$$\frac{\partial \Phi_4}{\partial \xi^*} \to 0 \quad \text{as} \quad \xi^* \to 0 \tag{2.4.45}$$

Similarly to equation (2.4.21), the method of separation of variables is used, where

$$\Psi_4(\xi^*, \mu) = 8Ra(1-\mu^2)\,\bar{\Psi}_4(\xi^*) \tag{2.4.46}$$

This expression is substituted, together with (2.4.24), into the equation (2.4.43) and the boundary conditions (2.4.44) and (2.4.45). Hence the fourth order ordinary differential equation for $\bar{\Psi}_4$ is,

$$\frac{d^4\bar{\Psi}_4}{d\xi^{*4}} + \frac{2\xi^*}{P_r}\frac{d^3\bar{\Psi}_4}{d\xi^{*3}} - \frac{4}{P_r}\frac{d^2\bar{\Psi}_4}{d\xi^{*2}} = \frac{d\Theta_1^*}{d\xi^*} - 2\xi^*\frac{d\Theta_0^*}{d\xi^*} \tag{2.4.47}$$

and the boundary conditions are, noting that from (2.4.26) $\frac{\partial\Psi_3}{\partial\xi^*} = 0$ at $\xi^* = \frac{\epsilon_0}{\lambda^{1/2}}$.

$$\left.\begin{aligned} \bar{\Psi}_4 &= 0 \\ \left[\frac{d\bar{\Psi}_4}{d\xi^*} + \frac{\epsilon_1}{\lambda}\frac{d^2\bar{\Psi}_3}{d\xi^{*2}}\right] &= 0 \end{aligned}\right\} \text{at } \xi^* = \frac{\epsilon_0}{\lambda^{1/2}} \tag{2.4.48}$$

and

$$\frac{d\bar{\Psi}_4}{d\xi^*} \to 0 \quad \text{as} \quad \xi^* \to \infty \tag{2.4.49}$$

Fifth Order

In the fifth order thermal liquid equation there are an additional three terms which control the convective motion. This equation is,

$$\frac{\partial^2\Theta_5^*}{\partial\xi^{*2}} + 2\xi^*\frac{\partial\Theta_5^*}{\partial\xi^*} - 10\Theta_5^* = 64\xi^{*4}\frac{\partial\Theta_0^*}{\partial\xi^*} +$$

$$+32\xi^{*3}\frac{d\Theta_1^*}{d\xi^*} + 16\xi^{*2}\frac{d\Theta_2^*}{d\xi^*} + 8\xi^*\frac{d\Theta_3^*}{d\xi^*} + 4\frac{\partial\Theta_4^*}{\partial\xi^*}$$

$$+2\frac{\partial\Psi_4}{\partial\mu}\frac{d\Theta_0^*}{d\xi^*} + 2\frac{\partial\Psi_3}{\partial\mu}\frac{d\Theta_1^*}{d\xi^*} + 8\xi^*\frac{\partial\Psi_3}{\partial\mu}\frac{d\Theta_0^*}{d\xi^*} \qquad (2.4.50)$$

Substituting (2.4.24) and (2.4.46) for Ψ_3 and Ψ_4 respectively, these three terms become

$$-32\mu Ra\,\bar{\Psi}_4\frac{d\Theta_0^*}{d\xi^*} - 32\mu Ra\,\bar{\Psi}_3\frac{d\Theta_1^*}{d\xi^*}$$

$$-128\xi^*\bar{\Psi}_3\frac{d\Theta_0^*}{d\xi^*} \qquad (2.4.51)$$

Employing the same technique used for the fourth order equations, the functions Θ_5 , Θ_5^* and $E_5(\mu)$ can be written as,

$$\Theta_5(\xi,\mu) = \bar{\Theta}_5(\xi) + \mu\,\bar{\bar{\Theta}}_5(\xi) \qquad (2.4.52)$$

$$\Theta_5^*(\xi^*,\mu) = \bar{\Theta}_5^*(\xi^*) + \mu\,\bar{\bar{\Theta}}_5^*(\xi^*) \qquad (2.4.53)$$

and $$E_5(\mu) = \bar{E}_5 + \mu\bar{\bar{E}}_5 \qquad (2.4.54)$$

Again, as a consequence of these variables, there are two systems of equations - the single bar and the double bar.

Fifth Order Single Bar

For $\bar{\Theta}_5$, the thermal solid equation is

$$\frac{d^2\bar{\Theta}_5}{d\xi^2} + 2\xi\frac{d\bar{\Theta}_5}{d\xi} - 10\,\bar{\Theta}_5 = 64\xi^4\frac{d\Theta_0}{d\xi} + 32\xi^3\frac{d\Theta_1}{d\xi} + 16\xi^2\frac{d\Theta_2}{d\xi} + 8\xi\frac{d\Theta_3}{d\xi} + 4\frac{d\bar{\Theta}_4}{d\xi} \qquad (2.4.55)$$

subject to the conditions

$$\bar{\Theta}_5(0) = 0$$

and (2.4.56)

$$\Bigg[\bar{\Theta}_5 + \epsilon_1\frac{d\bar{\Theta}_4}{d\xi} + (\epsilon_2 - \epsilon_0\epsilon_1^2)\frac{d\Theta_3}{d\xi} + \Big(\epsilon_3 + 2\epsilon_1^2 + \cdots$$

$$-\frac{8}{3}\epsilon_1^3 - 2\epsilon_0\epsilon_1\epsilon_2 + \frac{2}{3}\epsilon_0^2\epsilon_1^3\Big)\frac{d\Theta_2}{d\xi} + (\bar{\epsilon}_4 + 4\epsilon_0\epsilon_1^2$$

$$-7\epsilon_1^2\epsilon_2 + \frac{9}{2}\epsilon_0\epsilon_1^4 - \epsilon_0\epsilon_2^2 + 4\epsilon_1\epsilon_2 - 2\epsilon_0\epsilon_1\epsilon_3 - \frac{8}{3}\epsilon_0\epsilon_1^3$$

$$+2\epsilon_0^2\epsilon_1^2\epsilon_2 - \frac{\epsilon_0^3\epsilon_1^4}{3}\Big)\frac{d\Theta_1}{d\xi} + (\bar{\epsilon}_5 + 8\epsilon_0^2\epsilon_1^2 - 6\epsilon_1^2\epsilon_3$$

$$-8\epsilon_1^4 + \frac{64}{15}\epsilon_1^5 + 2\epsilon_2^2 - 6\epsilon_1\epsilon_2^2 + 8\epsilon_0\epsilon_1\epsilon_2 + 4\epsilon_1\epsilon_3$$

$$-2\epsilon_0\epsilon_1\bar{\epsilon}_4 - 2\epsilon_0\epsilon_2\epsilon_3 + 4\epsilon_1^3 - \frac{16}{3}\epsilon_0^2\epsilon_1^3 + \frac{46}{3}\epsilon_0\epsilon_1^3\epsilon_2$$

$$+2\epsilon_0^2\epsilon_1\epsilon_2^2 - 8\epsilon_0\epsilon_1^2\epsilon_2 + 2\epsilon_0^2\epsilon_1^2\epsilon_3 + 2\epsilon_0^2\epsilon_1^4 - \frac{4}{3}\epsilon_0^3\epsilon_1^3\epsilon_2$$

$$+\frac{2}{15}\epsilon_0^4\epsilon_1^5 - \frac{61}{15}\epsilon_0^2\epsilon_1^5\Big)\frac{d\Theta_0}{d\xi}\Bigg]_{\xi=\epsilon_0} = 0$$

The equation for the liquid which governs the thermal function $\bar{\Theta}_5^*(\xi^*)$ is,

$$\frac{d\bar{\Theta}_5^*}{d\xi^{*2}} + 2\xi^* \frac{d\bar{\Theta}_5^*}{d\xi^*} - 10\,\bar{\Theta}_5^* = 64\xi^{*4}\frac{d\Theta_0^*}{d\xi^*} + 32\xi^{*3}\frac{d\Theta_1^*}{d\xi^*} + 16\xi^{*2}\frac{d\Theta_2^*}{d\xi^*} + 8\xi^*\frac{d\Theta_3^*}{d\xi^*} + 4\frac{d\Theta_4^*}{d\xi^*} \tag{2.4.57}$$

which is subject to the conditions

$$\left[\bar{\Theta}_5^* + \frac{E_1}{\lambda}\frac{d\bar{\Theta}_4^*}{d\xi^*} + \left(\frac{E_2}{\lambda^{3/2}} - \frac{E_0E_1^2}{\lambda^{5/2}}\right)\frac{d\Theta_3^*}{d\xi^*} + \right.$$

$$+ \left(\frac{E_3}{\lambda^2} + \frac{2E_1^2}{\lambda^2} - \frac{8}{3}\frac{E_1^3}{\lambda^3} - \frac{2E_0E_1E_2}{\lambda^3} + \frac{2}{3}\frac{E_0^2E_1^3}{\lambda^4}\right)\frac{d\Theta_2^*}{d\xi^*} +$$

$$+ \left(\frac{\bar{E}_4}{\lambda^{5/2}} + 4\frac{E_0E_1^2}{\lambda^{5/2}} - 7\frac{E_1^2E_2}{\lambda^{7/2}} + \frac{9}{2}\frac{E_0E_1^4}{\lambda^{9/2}} - \frac{E_0E_2^2}{\lambda^{7/2}} + 4\frac{E_1E_2}{\lambda^{5/2}} + \right.$$

$$\left. - 2\frac{E_0E_1E_3}{\lambda^{7/2}} - \frac{8}{3}\frac{E_0E_1^3}{\lambda^{7/2}} + 2\frac{E_0^2E_1^2E_2}{\lambda^{9/2}} - \frac{E_0^3E_1^4}{3\lambda^{11/2}}\right)\frac{d\Theta_1^*}{d\xi^*} +$$

$$+ \left(\frac{\bar{E}_5}{\lambda^3} + 8\frac{E_0^2E_1^2}{\lambda^3} - 6\frac{E_1^2E_3}{\lambda^4} - 8\frac{E_1^4}{\lambda^4} + \frac{64}{15}\frac{E_1^5}{\lambda^5} + 2\frac{E_2^2}{\lambda^3} - 6\frac{E_1E_2^2}{\lambda^4} + \right.$$

$$+ 8\frac{E_0E_1E_2}{\lambda^3} + 4\frac{E_1E_3}{\lambda^3} - 2\frac{E_0E_1\bar{E}_4}{\lambda^4} - 8\frac{E_0E_1^3E_2}{\lambda^4} + 2\frac{E_0^2E_1^3E_3}{\lambda^5} +$$

$$- 2\frac{E_0E_2E_3}{\lambda^4} + 4\frac{E_1^3}{\lambda^3} - \frac{16}{3}\frac{E_0^2E_1^3}{\lambda^4} + \frac{46}{3}\frac{E_0E_1^3E_2}{\lambda^5} + 2\frac{E_0^2E_1E_2^2}{\lambda^5} +$$

$$\left. \left. + 2\frac{E_0^2E_1^4}{\lambda^5} - \frac{4}{3}\frac{E_0^3E_1^3E_2}{\lambda^6} + \frac{2}{15}\frac{E_0^4E_1^5}{\lambda^9} - \frac{61}{15}\frac{E_0^2E_1^5}{\lambda^6}\right)\frac{d\Theta_0^*}{d\xi^*}\right]_{\xi_4 = \frac{E_0}{\lambda^{1/2}}} = 0$$

and (2.4.58)

$$\bar{\Theta}_5^*(\infty) = 0$$

The interface equation which determines the perturbation function $\bar{E}_5$ is,

$$12\beta\bar{E}_5 = \Big[\frac{d\bar{\Phi}_5}{d\xi} - 2\epsilon_0\epsilon_1\frac{d\bar{\Phi}_4}{d\xi} + \left(4\epsilon_1 - 6\epsilon_1^2 - 2\epsilon_0\epsilon_2 + 2\epsilon_0^2\epsilon_1^2\right)\frac{d\bar{\Phi}_3}{d\xi} + \left(8\epsilon_0\epsilon_1 - 12\epsilon_1\epsilon_2 + \frac{40}{3}\epsilon_0\epsilon_1^3 + 4\epsilon_3 - 2\epsilon_0\epsilon_3 - 8\epsilon_0\epsilon_1^2 + 4\epsilon_0^2\epsilon_1\epsilon_2 - \frac{4}{3}\epsilon_0^3\epsilon_1^3\right)\frac{d\bar{\Phi}_2}{d\xi} + \left(16\epsilon_1^4 - 12\epsilon_1\epsilon_3 - 24\epsilon_1^3 + 16\epsilon_0^2\epsilon_1 + 38\epsilon_0\epsilon_1^2\epsilon_2 + 8\epsilon_0^2\epsilon_1^3 + 8\epsilon_0\epsilon_2 - 6\epsilon_2^2 + 4\epsilon_3 - 2\epsilon_0\bar{\epsilon}_4 + 12\epsilon_1^2 - 16\epsilon_0^2\epsilon_1^2 - 15\epsilon_0^2\epsilon_1^4 + 2\epsilon_0^2\epsilon_2^2 + -16\epsilon_0\epsilon_1\epsilon_2 + 4\epsilon_0^2\epsilon_1\epsilon_3 - 4\epsilon_0^3\epsilon_1^2\epsilon_2 + \frac{2}{3}\epsilon_0^4\epsilon_1^4\right)\frac{d\bar{\Phi}_1}{d\xi} + \left(32\epsilon_0^3\epsilon_1 + 36\epsilon_0\epsilon_1^2\epsilon_3 - 12\epsilon_1\bar{\epsilon}_4 - \frac{200}{3}\epsilon_0\epsilon_1^3 + \frac{158}{3}\epsilon_0\epsilon_1^4 + -\frac{106}{3}\epsilon_0\epsilon_1^5 + 52\epsilon_1^3\epsilon_2 + 36\epsilon_0\epsilon_1\epsilon_2^2 - 68\epsilon_1^2\epsilon_2 - \frac{164}{3}\epsilon_0^2\epsilon_1^3\epsilon_2 + + \frac{34}{3}\epsilon_0^3\epsilon_1^5 + 16\epsilon_0^2\epsilon_2 - \frac{4}{15}\epsilon_0^5\epsilon_1^5 + \frac{8}{3}\epsilon_0^4\epsilon_1^3\epsilon_2 - 4\epsilon_0^3\epsilon_1^2\epsilon_3 + - \frac{16}{3}\epsilon_0^3\epsilon_1^4 - 12\epsilon_2\epsilon_3 + 4\bar{\epsilon}_4 + 8\epsilon_0\epsilon_3 - 2\epsilon_0\bar{\epsilon}_5 - 32\epsilon_0^3\epsilon_1^2 + -8\epsilon_0\epsilon_2^2 + 24\epsilon_1\epsilon_2 + 48\epsilon_0\epsilon_1^2 - 32\epsilon_0^2\epsilon_1\epsilon_2 - 16\epsilon_0\epsilon_1\epsilon_3 + +4\epsilon_0^2\epsilon_1\bar{\epsilon}_4 + 4\epsilon_0^2\epsilon_2\epsilon_3 - 4\epsilon_0^3\epsilon_1\epsilon_2^2 + 24\epsilon_0^2\epsilon_1^2\epsilon_2 + + 16\epsilon_0^3\epsilon_1^3\right)\frac{d\bar{\Phi}_0}{d\xi}\Big]_{\xi=\epsilon_0} +$$

$$-\lambda^2\gamma\Bigg[\frac{d\bar{\Theta}_5^*}{d\xi^*}-\frac{2E_0E_1}{\lambda^{3/2}}\frac{d\bar{\Theta}_4^*}{d\xi^*}+\Bigg(\frac{4E_1}{\lambda}-\frac{6E_1^2}{\lambda^2}+$$

$$-\frac{2E_0E_2}{\lambda^2}+\frac{2E_0^2E_1^2}{\lambda^3}\Bigg)\frac{d\bar{\Theta}_3^*}{d\xi^*}+\Bigg(\frac{8E_0E_1}{\lambda^{3/2}}-\frac{12E_1E_2}{\lambda^{5/2}}+$$

$$+\frac{40}{3}\frac{E_0E_1^3}{\lambda^{7/2}}+\frac{4E_2}{\lambda^{3/2}}-\frac{2E_0E_3}{\lambda^{5/2}}-\frac{8E_0E_1^2}{\lambda^{5/2}}+\frac{4E_0^2E_1E_2}{\lambda^{7/2}}+$$

$$-\frac{4}{3}\frac{E_0^3E_1^3}{\lambda^{9/2}}\Bigg)\frac{d\bar{\Theta}_2^*}{d\xi^*}+\Bigg(\frac{16E_1^4}{\lambda^4}-\frac{12E_1E_3}{\lambda^3}-\frac{24E_1^3}{\lambda^3}+\frac{16E_0^2E_1}{\lambda^2}+$$

$$+\frac{38E_0E_1^2E_2}{\lambda^4}+\frac{8E_0^2E_1^3}{\lambda^4}+\frac{8E_0E_2}{\lambda^2}-\frac{6E_2^2}{\lambda^3}+\frac{4E_3}{\lambda^2}-\frac{2E_0\bar{E}_4}{\lambda^3}+$$

$$+\frac{12E_1^2}{\lambda^2}-\frac{16E_0^2E_1^2}{\lambda^3}-\frac{15E_0^2E_1^4}{\lambda^5}+\frac{2E_0^2E_2^2}{\lambda^4}-\frac{16E_0E_1E_2}{\lambda^3}+$$

$$+\frac{4E_0^2E_1E_3}{\lambda^4}-\frac{4E_0^3E_1^2E_2}{\lambda^5}+\frac{2}{3}\frac{E_0^4E_1^4}{\lambda^6}\Bigg)\frac{d\bar{\Theta}_1^*}{d\xi^*}+\Bigg(\frac{32E_0^3E_1}{\lambda^{5/2}}$$

$$+\frac{36E_0E_1^2E_3}{\lambda^{9/2}}-\frac{12E_1\bar{E}_4}{\lambda^{7/2}}-\frac{200}{3}\frac{E_0E_1^3}{\lambda^{7/2}}+\frac{158}{3}\frac{E_0E_1^4}{\lambda^{9/2}}+$$

$$-\frac{106}{3}\frac{E_0E_1^5}{\lambda^{11/2}}+\frac{52E_1^3E_2}{\lambda^{9/2}}+\frac{36E_0E_1E_2^2}{\lambda^{9/2}}-\frac{68E_1^2E_2}{\lambda^{7/2}}-\frac{164E_0^2E_1^3E_2}{3\lambda^{11/2}}$$

$$+\frac{34}{3}\frac{E_0^3E_1^5}{\lambda^{13/2}}+\frac{16E_0^2E_2}{\lambda^{5/2}}-\frac{4}{15}\frac{E_0^5E_1^5}{\lambda^{13/2}}+\frac{8}{3}\frac{E_0^4E_1^3E_2}{\lambda^{13/2}}-\frac{4E_0^3E_1^2E_3}{\lambda^{11/2}}$$

$$-\frac{16}{3}\frac{E_0^3E_1^4}{\lambda^{11/2}}-\frac{12E_2E_3}{\lambda^{7/2}}+\frac{4\bar{E}_4}{\lambda^{5/2}}+\frac{8E_0E_3}{\lambda^{5/2}}-\frac{2E_0\bar{E}_5}{\lambda^{7/2}}$$

$$-\frac{32E_0^3E_1^2}{\lambda^{7/2}}-\frac{8E_0E_2^2}{\lambda^{7/2}}+\frac{4E_0^2E_3E_2}{\lambda^{9/2}}+\frac{24E_1E_2}{\lambda^{5/2}}+\frac{48E_0E_1^2}{\lambda^{5/2}}+$$

$$- 32\frac{E_0^2 E_1 E_2}{\lambda^{7/2}} - 16\frac{E_0 E_1 E_3}{\lambda^{7/2}} + 4\frac{E_0^2 E_1 \bar{E}_4}{\lambda^{13/2}} - 4\frac{E_0^3 E_1 E_2^2}{\lambda^{11/2}} +$$

$$+ 24\frac{E_0^2 E_1^2 E_2}{\lambda^{9/2}} + 16\frac{E_0^3 E_1^3}{\lambda^{9/2}} \Bigg) \frac{d\bar{\Theta}_0^*}{d\xi^*} \Bigg]_{\xi^* = \frac{E_0}{\lambda^{1/2}}} \qquad (2.4.59)$$

Fifth Order Double Bar System

For the solid region, $\bar{\bar{\Theta}}_5$ satisfies the equation,

$$\frac{d^2\bar{\bar{\Theta}}_5}{d\xi^2} + 2\xi \frac{d\bar{\bar{\Theta}}_5}{d\xi} - 10\bar{\bar{\Theta}}_5 = \frac{d\bar{\bar{\Theta}}_4}{d\xi} \qquad (2.4.60)$$

subject to the boundary conditions,

$$\bar{\bar{\Theta}}_5(0) = 0$$

and (2.4.61)

$$\left[\bar{\bar{\Theta}}_5 + E_1 \frac{d\bar{\bar{\Theta}}_4}{d\xi} + \bar{\bar{E}}_4 \frac{d\bar{\Theta}_1}{d\xi} + (\bar{\bar{E}}_5 - 2E_0E_1\bar{\bar{E}}_4)\frac{d\bar{\Theta}_0}{d\xi}\right]_{\xi = E_0} = 0$$

For the liquid region, $\bar{\bar{\Theta}}_5^*$ satisfies the equation,

$$\frac{d^2\bar{\bar{\Theta}}_5^*}{d\xi^{2*}} + 2\xi^* \frac{d\bar{\bar{\Theta}}_5^*}{d\xi^*} - 10\bar{\bar{\Theta}}_5^* = 4\frac{d\bar{\bar{\Theta}}_4^*}{d\xi^*} - 128Ra.\xi^*\bar{\Phi}_3\frac{d\bar{\Theta}_0^*}{d\xi^*}$$

$$-32\chi_4\bar{\Phi}_4\frac{d\bar{\Theta}_0^*}{d\xi^*} - 32Ra\,\bar{\Phi}_3\frac{d\bar{\Theta}_1^*}{d\xi^*}$$

(2.4.62)

subject to the boundary conditions,

$$\left[\bar{\bar{\Theta}}_5^* + \frac{E_1}{\lambda}\frac{d\bar{\bar{\Theta}}_4^*}{d\xi^*} + \frac{\bar{\bar{E}}_4}{\lambda^{5/2}}\frac{d\bar{\Theta}_1^*}{d\xi^*} + \left(\frac{\bar{\bar{E}}_5}{\lambda^3} - 2\frac{E_0E_1\bar{\bar{E}}_4}{\lambda^4}\right)\frac{d\bar{\Theta}_0^*}{d\xi^*}\right]_{\xi^* = \frac{E_0}{\lambda^{1/2}}} = 0$$

and (2.4.63)

$$\bar{\bar{\Theta}}_5^*(\infty) = 0$$

The interface equation which determines $\bar{\bar{E}}_5$ is,

$$\bar{12}\beta\bar{\bar{E}}_5 = \left[\frac{d\bar{\bar{\Theta}}_5}{d\xi} - 2E_0E_1\frac{d\bar{\bar{\Theta}}_4}{d\xi} - 2E_0\bar{\bar{E}}_4\frac{d\Theta_1}{d\xi} + \right.$$

$$\left. + (4\bar{\bar{E}}_4 + 4E_0^2E_1\bar{\bar{E}}_4 - 2E_0\bar{\bar{E}}_5 - 12E_1\bar{\bar{E}}_4)\frac{d\Theta_0}{d\xi} \right]_{\xi=E_0} +$$

$$-\lambda^2\gamma\left[\frac{d\bar{\bar{\Theta}}_5^*}{d\xi^*} - \frac{2E_0E_1}{\lambda^{3/2}}\frac{d\bar{\bar{\Theta}}_4^*}{d\xi^*} - \frac{2E_0\bar{\bar{E}}_4}{\lambda^3}\frac{d\Theta_1^*}{d\xi^*} + \right.$$

$$\left. + \left(\frac{4\bar{\bar{E}}_4}{\lambda^{5/2}} + \frac{4E_0^2E_1\bar{\bar{E}}_4}{\lambda^{9/2}} - \frac{2E_0\bar{\bar{E}}_5}{\lambda^{7/2}} - \frac{12E_1\bar{\bar{E}}_4}{\lambda^{7/2}}\right)\frac{d\Theta_0^*}{d\xi^*} \right]_{\xi^*=\frac{E_0}{\lambda^4}}$$

(2.4.64)

The fifth order equation and boundary conditions governing the flow field is not determined because Ψ_5 does not feature in any of the other equations.

It can be clearly seen that, as the exponent of τ increases, the equations of the thermal fields, their boundary conditions and the interface equations become lengthy and complicated. This is mainly due to the resolution of the perturbation procedure by the Van Dyke method.

Before these equations for the sphere are solved, the equations governing the thermal fields and convective motion in a cylinder are also derived, since both of these problems are solved using the same techniques.

Chapter 3

The Effects of Natural Convection During Solidification in a Liquid Cylinder

3.1 The Derivation of the Governing Equations

The derivation of the equations governing the heat and mass transfer of a liquid undergoing the process of phase-change in a cylinder is similar to that in the case of the sphere. Nevertheless, although the equations for the sphere and the cylinder could be established at the same time by a general derivation, due to some subtle differences in the analyses, the equations are derived separately in order to highlight these differences.

The three assumptions made on page 18 are again assumed and figure 1 is also the same, although the frame of reference is, of course, polar cylindrical and not a spherical coordinate system. Yet, due to the similarity between these two coordinate systems, the generalised form of the heat balance equation - see appendix A - gives the same equation as (2.1.18). Thus, at the interface $C(\underline{r},t)$, which is represented by

$$C(\underline{r},t) = r - r_F(\mu,t) \tag{3.1.1}$$

the Stefan condition is

$$K\left(\frac{\partial T}{\partial r} - \frac{(1-\mu^2)}{r^2}\frac{\partial T}{\partial \mu}\cdot\frac{\partial r_F}{\partial \mu}\right) - K^*\left(\frac{\partial T^*}{\partial r} + \right.$$

$$\left. -\frac{(1-\mu^2)}{r^2}\frac{\partial T^*}{\partial \mu}\cdot\frac{\partial r_F}{\partial \mu}\right) = \rho L \frac{\partial r_F}{\partial t} \tag{3.1.2}$$

Although this equation is the same heat balance equation as derived for the sphere, it is included throughout this cylindrical problem in order to complete the model.

In the solid region, the equation for the heat conduction is

$$k\left\{\frac{1}{r}\frac{\partial}{\partial r}\left(r\frac{\partial T}{\partial r}\right) + \frac{(1-\mu^2)^{\frac{1}{2}}}{r^2}\frac{\partial}{\partial \mu}\left[(1-\mu^2)^{\frac{1}{2}}\frac{\partial T}{\partial \mu}\right]\right\} = \frac{\partial T}{\partial r} \qquad (3.1.3)$$

where $T(r,\mu,t)$ is the temperature distribution and k is the thermal diffusivity. This heat equation is subject to the boundary conditions,

$$T(a,\mu,t) = T_0$$

and (3.1.4)

$$T(r_F(\mu,t),\mu,t) = T_F$$

At this stage the Boussinesq approximation is invoked on the equations of motion and heat in the liquid. This gives the following equations for the energy, continuity and momentum.

The thermal energy equation is,

$$k^*\left\{\frac{1}{r}\frac{\partial}{\partial r}\left(r\frac{\partial T}{\partial r}\right) + \frac{(1-\mu^2)^{\frac{1}{2}}}{r^2}\frac{\partial}{\partial \mu}\left[(1-\mu^2)^{\frac{1}{2}}\frac{\partial T^*}{\partial \mu}\right]\right\}$$

$$= \frac{\partial T^*}{\partial t} + v_r\frac{\partial T^*}{\partial r} - \frac{(1-\mu^2)^{\frac{1}{2}}}{r}\frac{\partial T^*}{\partial \mu}v_\mu \qquad (3.1.5)$$

and the equation of continuity is,

$$\frac{1}{r}\frac{\partial}{\partial r}(rv_r) - \frac{(1-\mu^2)^{\frac{1}{2}}}{r}\frac{\partial}{\partial \mu}(v_\mu) = 0 \qquad (3.1.6)$$

and finally the Navier-Stokes equation is,

$$\rho_F^*\left[\frac{\partial \underline{v}}{\partial t} - \underline{v}\times\underline{\nabla}\times\underline{v}\right] = -\underline{\nabla}\left(p + \tfrac{1}{2}\rho_F^*\underline{v}^2\right) +$$

$$-\nu^*\rho_F^*(\underline{\nabla}\times\underline{\nabla}\times\underline{v}) + \rho^*\underline{F} \qquad (3.1.7)$$

In these equations $\underline{v} = (v_r, v_\mu)$ is the velocity in the fluid, $T^*(r, \mu, t)$ the liquid temperature distribution, p the pressure and ρ^* the density of the fluid.

As in the case of the sphere, the force exerted due to gravity is,

$$\underline{F} = (-g\mu\,,\ g(1-\mu^2)^{\frac{1}{2}},\ 0) \tag{3.1.8}$$

and the equation of state, where ρ_F^* is the density of the liquid at fusion temperature and α is the coefficient of cubical expansion, is

$$\rho^* = \rho_F^* \left[1 - \alpha (T - T_F) \right] \tag{3.1.9}$$

Substitution of these two equations into the equation (3.1.7), and taking the curl, eliminates the pressure term to give

$$\underline{\nabla} \times \frac{\partial \underline{v}}{\partial t} - \underline{\nabla} \times \left[\underline{v} \times \underline{\nabla} \times \underline{v} \right] = -\nu^* \underline{\nabla} \times \underline{\nabla} \times \underline{v} + \underline{\nabla} \times \left\{ \left[1 - \alpha (T - T_F) \right] \underline{F} \right\} \tag{3.1.10}$$

The stream function $\psi(r, \mu, t)$, on examination of the continuity equation, is given as

$$v_\mu = -\frac{\partial \psi}{\partial r} \quad \text{and} \quad v_r = -\frac{(1-\mu^2)^{\frac{1}{2}}}{r} \frac{\partial \psi}{\partial \mu} \tag{3.1.11}$$

Substitution of (3.1.11) into (3.1.10) followed by some further analysis yields,

$$\nu^* D_r^4 \psi = \frac{\partial D_r^2 \psi}{\partial t} + \frac{(1-\mu^2)^{\frac{1}{2}}}{r} \frac{\partial (\psi, D_r^2 \psi)}{\partial (r, \mu)} + g\alpha (1-\mu^2)^{\frac{1}{2}} \left\{ \mu \frac{\partial T^*}{\partial \mu} - \frac{\partial T^*}{\partial r} \right\} \tag{3.1.12}$$

where the operator D_r^2 is defined by

$$D_r^2 \cdot = \frac{1}{r}\frac{\partial}{\partial r}\left(r\frac{\partial \cdot}{\partial r}\right) + \frac{(1-\mu^2)^{\frac{1}{2}}}{r^2}\frac{\partial}{\partial \mu}\left[(1-\mu^2)^{\frac{1}{2}}\frac{\partial \cdot}{\partial \mu}\right] \qquad (3.1.13)$$

and the Jacobian is defined by (2.1.14).

The boundary conditions for the equations in the liquid domain are

(i) initially,

$$\left.\begin{aligned} T^* &= T_I \\ \underline{v} &= 0 \end{aligned}\right\} \text{ at } t=0,\ 0 \leq r \leq a \qquad (3.1.14)$$

(ii) at the interface,

$$\left.\begin{aligned} T^* &= T_F \\ \psi = \frac{\partial \psi}{\partial r} &= 0 \end{aligned}\right\} \text{ at } r = r_F(\mu,t),\ t>0 \qquad (3.1.15)$$

At this point it is worth comparing these equations with the corresponding equations in Chapter 2. Comparison of (3.1.11) with (2.1.10) shows that the velocity of the liquid in the cylinder can be expected to be less at the centre than it would be in the sphere. The operator D_r^2 has different definitions for the two geometries, yet it is not surprising to note that the boundary conditions for both problems are identical.

3.2 Dimensionless and Neumann Variables

The dimensionless variables (2.2.1) and (2.2.2) are introduced for the solid region and liquid region respectively together with the dimensionless parameter λ. However, due to the differing analyses, the dimensionless stream function is now given as

$$\Psi = \frac{\Psi}{k^*} \tag{3.2.1}$$

And so, on employing these variables the governing equations are transformed to become:

for the solid region the heat conduction equation,

$$\frac{1}{R}\frac{\partial}{\partial R}\left(R\frac{\partial \Theta}{\partial R}\right) - \frac{(1-\mu^2)^{\frac{1}{2}}}{R^2}\frac{\partial}{\partial \mu}\left[(1-\mu^2)^{\frac{1}{2}}\frac{\partial \Theta}{\partial \mu}\right] = \frac{\partial \Theta}{\partial \tau'} \tag{3.2.2}$$

which is subject to the boundary conditions

$$\Theta(1,\mu,\tau') = 0$$

and

$$\Theta(R_F(\mu,\tau'),\mu,\tau') = 1 \tag{3.2.3}$$

for the liquid region the heat conduction and convection equation,

$$\frac{1}{R}\frac{\partial}{\partial R}\left(R\frac{\partial \Theta^*}{\partial R}\right) - \frac{(1-\mu^2)^{\frac{1}{2}}}{R^2}\frac{\partial}{\partial \mu}\left[(1-\mu^2)^{\frac{1}{2}}\frac{\partial \Theta^*}{\partial \mu}\right] + \frac{(1-\mu^2)^{\frac{1}{2}}}{R}\frac{\partial(\Psi,\Theta^*)}{\partial(R,\mu)} = \frac{\partial \Theta^*}{\partial \tau^*}, \tag{3.2.4}$$

which is subject to the boundary conditions

$$\Theta^*(R,\mu,0) = 1$$

and

$$\Theta^*(R_F,\mu,\tau) = 0 \tag{3.2.5}$$

The equation governing the convective motion is

$$D_R^4\,\Psi = \frac{1}{Pr}\left\{\frac{\partial D_R^2 \Psi}{\partial \tau^*} + \frac{(1-\mu^2)^{\frac{1}{2}}}{R}\frac{\partial(\Psi, D_R^2\Psi)}{\partial(R,\mu)}\right.$$

$$\left. + Ra\,(1-\mu^2)^{\frac{1}{2}}\left\{\frac{\mu}{R}\frac{\partial \Theta^*}{\partial \mu} - \frac{\partial \Theta^*}{\partial R}\right\}\right. \tag{3.2.6}$$

where Ψ satisfies the boundary conditions

$$\Psi = \frac{\partial \Psi}{\partial R} = \frac{\partial \Psi}{\partial \mu} = 0 \quad \text{at} \quad R = R_F \tag{3.2.7}$$

and the initial condition

$$\frac{\partial \Psi}{\partial R}(R, \mu, 0) = 0 \tag{3.2.8}$$

The dimensionless numbers Pr and Ra are defined by (2.2.10) and the operator D_R^2 is defined by

$$D_R^2 \cdot = \frac{1}{R} \frac{\partial}{\partial R}\left(R \frac{\partial \cdot}{\partial R}\right) + \frac{(1-\mu^2)^{\frac{1}{2}}}{R^2} \frac{\partial}{\partial \mu}\left[(1-\mu^2)^{\frac{1}{2}} \cdot \frac{\partial \cdot}{\partial \mu}\right] \tag{3.2.9}$$

The latent heat condition at the interface is

$$\beta \frac{\partial R_F}{\partial t'} = \left[\frac{\partial \Theta}{\partial R} - \frac{(1-\mu^2)}{R^2} \frac{\partial \Theta}{\partial \mu} \frac{\partial R_F}{\partial \mu}\right] + \\ - \gamma \left[\frac{\partial \Theta^*}{\partial R} - \frac{(1-\mu^2)}{R^2} \frac{\partial \Theta^*}{\partial \mu} \frac{\partial R_F}{\partial \mu}\right] \tag{3.2.10}$$

For the same reasons as those given in section 2.2, the Neumann variables (2.2.17) and (2.2.18) together with the interface variable

$$E(\mu, \tau) = \frac{(1 - R_F)}{2\tau^{\frac{1}{2}}} \tag{3.2.11}$$

are introduced. The previously established equations now become, for the solid,

$$\frac{\partial}{\partial \xi}\left[(1-2\tau^{1/2}\xi)\frac{\partial \Theta}{\partial \xi}\right] - \frac{(1-\mu^2)^{1/2}}{(1-2\tau^{1/2}\xi)} 4\tau \frac{\partial}{\partial \mu}\left[(1-\mu^2)^{1/2}\frac{\partial \Theta}{\partial \mu}\right]$$

$$= (1-2\tau^{1/2}\xi)\left[4\tau\frac{\partial \Theta}{\partial \tau} - 2\xi\frac{\partial \Theta}{\partial \xi}\right] \qquad (3.2.12)$$

This equation must satisfy the boundary conditions

$$\Theta(0,\mu,\tau) = 0$$

and (3.2.13)

$$\Theta(E,\mu,\tau) = 1$$

In the liquid region, Θ^* is governed by the conduction-convection equation

$$\frac{\partial}{\partial \xi^*}\left[(1-2\tau^{*1/2}\xi^*)\frac{\partial \Theta^*}{\partial \xi^*}\right] + (1-\mu^2)^{1/2} 2\tau^{*1/2}\frac{\partial(\Psi,\Theta^*)}{\partial(\xi^*,\mu)}$$

$$- \frac{(1-\mu^2)^{1/2}\,4\tau^*}{(1-2\tau^{*1/2}\xi^*)}\frac{\partial}{\partial \mu}\left[(1-\mu^2)^{1/2}\frac{\partial \Theta^*}{\partial \mu}\right]$$

$$= (1-2\tau^{*1/2}\xi^*)\left\{4\tau^*\frac{\partial \Theta^*}{\partial \tau^*} - 2\xi^*\frac{\partial \Theta^*}{\partial \xi^*}\right\} \qquad (3.2.14)$$

subject to the conditions,

$$\Theta^*(\infty,\mu,0) = 1$$

and (3.2.15)

$$\Theta^*\left(\frac{E}{\lambda^{1/2}},\mu,\tau^*\right) = 0$$

and also

$$\frac{\partial \Theta^*}{\partial \xi^*}(\infty,\mu,0) = \frac{\partial \Theta^*}{\partial \mu}(\infty,\mu,0) = 0 \qquad (3.2.16)$$

The equation which governs the flow field is,

$$D^4_{\xi^*}\Psi = \frac{1}{Pr}\left\{\left(\frac{\partial}{\partial\tau^*} - \frac{\xi^*}{2\tau^*}\frac{\partial}{\partial\xi^*}\right)D^2_{\xi^*}\Psi + \right.$$

$$-\frac{(1-\mu^2)^{\frac{1}{2}}}{(1-2\tau^{*\frac{1}{2}}\xi^*)}\frac{\partial(\Psi, D^2_{\xi^*}\Psi)}{\partial(\xi^*,\mu)}$$

$$\left. + Ra(1-\mu^2)^{\frac{1}{2}}\left\{\frac{\mu}{(1-2\tau^{*\frac{1}{2}}\xi^*)}\frac{\partial\Theta^*}{\partial\mu} + \frac{1}{2\tau^{*\frac{1}{2}}}\frac{\partial\Theta^*}{\partial\xi^*}\right\}\right. \qquad (3.2.17)$$

where Ψ satisfies the boundary conditions,

$$\Psi = \frac{\partial\Psi}{\partial R} = \frac{\partial\Psi}{\partial\mu} = 0 \quad \text{at} \quad \xi^* = \frac{E_0}{\lambda^{\frac{1}{2}}}$$

and (3.2.18)

$$\frac{\partial\Psi}{\partial\xi^*}(\infty,\mu,0) = 0$$

The operator $D^2_{\xi^*}\cdot$ is now defined by

$$D^2_{\xi^*}\cdot = \frac{1}{4\tau^*}\frac{\partial^2\cdot}{\partial\xi^{*2}} - \frac{1}{2\tau^{*\frac{1}{2}}(1-2\tau^{*\frac{1}{2}}\xi^*)}\frac{\partial\cdot}{\partial\xi^*} +$$

$$+\frac{(1-\mu^2)^{\frac{1}{2}}}{(1-2\tau^{*\frac{1}{2}}\xi^*)}\frac{\partial}{\partial\mu}\left[(1-\mu^2)^{\frac{1}{2}}\frac{\partial\cdot}{\partial\mu}\right] \qquad (3.2.19)$$

whilst the Jacobian is again defined by (2.2.28).

Finally the latent heat condition at the interface is

$$\left[\frac{1}{2\tau^{\frac{1}{2}}}\frac{\partial\Theta}{\partial\xi} - \frac{2\tau^{\frac{1}{2}}(1-\mu^2)^{\frac{1}{2}}}{(1-2\tau^{\frac{1}{2}}\xi)}\frac{\partial\Theta}{\partial\mu}\frac{\partial E}{\partial\mu}\right]_{\xi=E} +$$

$$-\gamma\left[\frac{1}{2\tau^{*\frac{1}{2}}}\frac{\partial\Theta^*}{\partial\xi^*}-\frac{2\tau^{*\frac{1}{2}}(1-\mu^2)^{\frac{1}{2}}}{(1-2\tau^{*\frac{1}{2}}\xi^*)}\frac{\partial\Theta^*}{\partial\mu}\frac{\partial E}{\partial\mu}\right]_{\xi^*=\frac{\xi}{\lambda^{\frac{1}{2}}}}$$

$$=2\beta\frac{\partial(E\tau^{\frac{1}{2}})}{\partial\tau} \qquad (3.2.20)$$

The initial condition on E is,

$$E(\mu,0)=0 \qquad (3.2.21)$$

3.3 The Perturbation Procedure

The regular perturbation expansion as used to solve the equations for the spherical problem are used to solve this cylindrical problem. Nevertheless, before a summary of these expansions is given - purely for completeness - the form of the perturbation expansion for the stream function Ψ must also be resolved. Suppose that this function can be written as

$$\Psi(\xi^*,\mu,\tau^*)=\Psi_n(\xi^*,\mu)\,\tau^{*n_2} \qquad (3.3.1)$$

so that, substituting into the equation which governs the convective motion (3.2.14) and expanding for small τ^*, the following equation is obtained:

$$\frac{1}{16\tau^{*2}}\frac{\partial^4(\Psi_n\tau^{*n})}{\partial\xi^{*4}}-\frac{1}{P_1}\left\{-\frac{1}{4\tau^{*2}}\frac{\partial^2(\Psi_n\tau^{*n})}{\partial\xi^{*2}}+\right.$$

$$\left.+\frac{n}{4\tau^*}\frac{\partial^2(\Psi_n\tau^{*n})}{\partial\xi^{*2}}-\frac{\xi^*}{8\tau^{*2}}\frac{\partial^3(\Psi_n\tau^{*n})}{\partial\xi^{*3}}\right\}+O(\tau^{*n-1})$$

$$=Ra\,\frac{(1-\mu^2)^{\frac{1}{2}}}{2\tau^{*\frac{1}{2}}}\frac{\partial\Theta^*}{\partial\xi^*}+O(1) \qquad (3.3.2)$$

Comparing both sides of this equation, it can be seen that again n = 3/2. Thus the perturbation expansion for the stream function is written as

$$\Psi(\xi^*, \mu, \tau^*) = \sum_{n=3}^{\infty} \Psi_n(\xi^*, \mu)\, \tau^{*\frac{n}{2}} \qquad (3.3.3)$$

Whilst the form of the perturbation expansion for Ψ is the same for both the spherical and cylindrical problems, it is interesting to compare equations (3.3.2) and (2.3.6). In particular, the terms on the right hand side differ by $(1-\mu^2)^{\frac{1}{2}}(1-2\xi^*\tau^{*\frac{1}{2}})$, a factor which will become more apparent later.

As in the case of the sphere, before all the boundary conditions can be found at the interface, Van Dyke's method must be employed to release τ from the argument of each of the perturbation functions.

And so, to recapitulate, the expansions are

$$\Omega(\xi, \mu, \tau) = \Omega_0(\xi) + \tau^{\frac{1}{2}}\Omega_1(\xi) + \tau\,\Omega_2(\xi) + \\ + \tau^{\frac{3}{2}}\Omega_3(\xi) + \tau^2\Omega_4(\xi, \mu) + \tau^{5/2}\Omega_5(\xi, \mu) + \cdots \qquad (3.3.4)$$

$$\Omega(\xi^*, \mu, \tau^*) = \Omega_0^*(\xi^*) + \tau^{*\frac{1}{2}}\Omega_1^*(\xi^*) + \\ + \tau^*\Omega_2^*(\xi^*) + \tau^{*\frac{3}{2}}\Omega_3^*(\xi^*) + \\ + \tau^{*2}\Omega_4^*(\xi^*, \mu) + \tau^{*5/2}\Omega_5^*(\xi^*, \mu) + \cdots \qquad (3.3.5)$$

$$E(\mu, \tau) = E_0 + \tau^{\frac{1}{2}}E_1 + \tau E_2 + \tau^{\frac{3}{2}}E_3 + \\ + \tau^2 E_4(\mu) + \tau^{5/2}E_5(\mu) + \cdots \qquad (3.3.6)$$

$$\Psi(\xi^*, \mu, \tau^*) = \Psi_3(\xi^*, \mu)\tau^{*\frac{3}{2}} + \Psi_4(\xi^*, \mu)\tau^{*2} + \cdots \qquad (3.3.7)$$

3.4 Determination of the Perturbation Functions

Substitution of these expansions into the equations governing the thermal field in the solid (3.2.12), the thermal field (3.2.14) and the convective motion (3.2.17) in the liquid as well as the latent heat condition at the interface gives the following differential equations on collecting terms of like powers of τ :

Zeroth Order

Collection of terms O(1) gives the equation in the solid region which governs Θ_0. That is,

$$\frac{\partial^2 \Theta_0}{\partial \xi^2} + 2\xi \frac{\partial \Theta_0}{\partial \xi} = 0 \qquad (3.4.1)$$

which is subject to the boundary conditions

$$\Theta_0(0) = 0$$

and (3.4.2)

$$\Theta_0(E_0) = 1$$

For the liquid region, the zeroth order perturbation function must satisfy the equation,

$$\frac{\partial^2 \Theta_0^*}{\partial \xi^{*2}} + 2\xi^* \frac{\partial \Theta_0^*}{\partial \xi^*} = 0 \qquad (3.4.3)$$

subject to the boundary conditions,

$$\Theta_0^*\left(\frac{E_0}{\lambda^{1/2}}\right) = 0$$

and

$$\Theta_0^*(\infty) = 1 \qquad (3.4.4)$$

It is not surprising that these equations and the boundary conditions

are the same as those for the zeroth order in the spherical problem.

E_o is determined by the latent heat condition

$$2\beta E_o = \left[\frac{\partial \Theta_o}{\partial \xi}\right]_{\xi=\epsilon_o} - \frac{\gamma}{\lambda^{\frac{1}{2}}}\left[\frac{\partial \Theta_o^*}{\partial \xi^*}\right]_{\xi^*=\frac{\epsilon_o}{\lambda^{\frac{1}{2}}}} \qquad (3.4.5)$$

So, for the zeroth order, the value of E_o obtained is the same for both the cylinder and the sphere. However, for higher orders it will be seen that the different geometries will produce differing equations and hence different results.

First Order

On equating terms $O(\tau^{\frac{1}{2}})$, the following equations for the first order perturbation functions Θ_1, Θ_1^* and E_1 are obtained:
for the solid region the thermal function Θ_1 satisfies

$$\frac{d^2\Theta_1}{d\xi^2} + 2\xi\frac{d\Theta_1}{d\xi} - 2\Theta_1 = 2\frac{d\Theta_o}{d\xi} \qquad (3.4.6)$$

subject to the boundary conditions

$$\Theta_1(0) = 0$$

and

$$\left[\Theta_1 + \epsilon_1\frac{d\Theta_o}{d\xi}\right]_{\xi=\epsilon_o} = 0 \qquad (3.4.7)$$

for the liquid region, Θ_1^* satisfies the equation

$$\frac{d^2\Theta_1^*}{d\xi^{*2}} + 2\xi^*\frac{d\Theta_1^*}{d\xi^*} - 2\Theta_1^* = 2\frac{d\Theta_o^*}{d\xi^*} \qquad (3.4.8)$$

subject to the boundary conditions

$$\left[\Theta_1^* + \frac{E_1}{\lambda} \frac{d\Theta_0^*}{d\xi^*} \right]_{\xi^* = \frac{\epsilon_0}{\lambda^{1/2}}} = 0$$

and

$$\Theta_1^*(\infty) = 0 \qquad (3.4.9)$$

In the interface equation E_1 satisfies

$$4\beta E_1 = \left[\frac{d\Theta_1}{d\xi} - 2E_0E_1 \frac{d\Theta_0}{d\xi} \right]_{\xi=\epsilon_0} +$$

$$-\gamma \left[\frac{d\Theta_1^*}{d\xi^*} - 2\frac{E_0E_1}{\lambda^{3/2}} \frac{d\Theta_0^*}{d\xi^*} \right]_{\xi^* = \frac{\epsilon_0}{\lambda^{1/2}}} \qquad (3.4.10)$$

Second Order

The collection of terms of order τ gives the equations:

For the solid region, Θ_2 satisfies,

$$\frac{d^2\Theta_2}{d\xi^2} + 2\xi \frac{d\Theta_2}{d\xi} - 4\Theta_2 = 4\xi \frac{d\Theta_0}{d\xi} + 2\frac{d\Theta_1}{d\xi} \qquad (3.4.11)$$

subject to the boundary conditions

$$\Theta_2(0) = 0$$

and

$$\left[\Theta_2 + E_1 \frac{d\Theta_1}{d\xi} + (E_2 - E_0E_1^2) \frac{d\Theta_0}{d\xi} \right]_{\xi=\epsilon_0} = 0 \qquad (3.4.12)$$

and for the liquid region, Θ_2^* satisfies,

$$\frac{d^2\Theta_2^*}{d\xi^{*2}} + 2\xi^* \frac{d\Theta_2^*}{d\xi^*} - 4\Theta_2^* = 4\xi^* \frac{d\Theta_0^*}{d\xi^*} + 2\frac{d\Theta_1^*}{d\xi^*} \qquad (3.4.13)$$

subject to the boundary conditions

$$\left[\Theta_2^* + \frac{E_1}{\lambda} \frac{d\Theta_1^*}{d\xi^*} + \left(\frac{E_2}{\lambda^{3/2}} - \frac{E_0 E_1^2}{\lambda^{5/2}} \right) \frac{d\Theta_0^*}{d\xi^*} \right]_{\xi^* = \frac{\epsilon_0}{\lambda^{1/2}}} = 0$$

and

$$\Theta_2^*(\infty) = 0 \tag{3.4.14}$$

Finally, for this order, the interface equation which determines E_2 is,

$$6\beta E_2 = \left[\frac{d\Theta_2}{d\xi} - 2E_0 E_1 \frac{d\Theta_1}{d\xi} + \left(2E_1 - 3E_1^2 + E_0^2 E_1^2 - 2E_0 E_2 \right) \frac{d\Theta_0}{d\xi} \right]_{\xi = \epsilon_0} - \lambda^{1/2} \gamma \left[\frac{d\Theta_2^*}{d\xi^*} - 2\frac{E_0 E_1}{\lambda^{3/2}} \frac{d\Theta_1^*}{d\xi^*} + \left(\frac{2E_1}{\lambda} - \frac{3E_1^2}{\lambda^2} + \frac{E_0^2 E_1^2}{\lambda^3} - \frac{2E_0 E_2}{\lambda^2} \right) \frac{d\Theta_0^*}{d\xi^*} \right]_{\xi^* = \frac{\epsilon_0}{\lambda^{1/2}}} \tag{3.4.15}$$

Third Order

As with the sphere, equating terms of order $\tau^{3/2}$ (or equivalently $\tau^{*3/2}$) gives the equation which determines the flow field perturbation function $\Psi_3(\xi^*, \mu)$.

For the solid region the thermal function Θ_3 satisfies the equation,

$$\frac{d^2\Theta_3}{d\xi^2} + 2\xi \frac{d\Theta_3}{d\xi^2} - 6\Theta_3 = B\xi^2 \frac{d\Theta_0}{d\xi} + 4\xi \frac{d\Theta_1}{d\xi} + 2\frac{d\Theta_2}{d\xi} \tag{3.4.16}$$

and is subject to the boundary conditions,

$$\Theta_3(0) = 0$$

and (3.4.17)

$$\left[\Theta_3 + E_1 \frac{d\Theta_2}{d\xi} + (E_2 - E_0E_1^2) \frac{d\Theta_1}{d\xi} + \left(E_1^2 - \frac{4}{3}E_1^3 + \frac{2}{3}E_0^2E_1^3 + E_3 - 2E_0E_1E_2\right) \frac{d\Theta_0}{d\xi} \right]_{\xi=E_0} = 0$$

For the liquid region, Θ_3^* satisfies the equation

$$\frac{d^2\Theta_3^*}{d\xi^{*2}} + 2\xi^* \frac{d\Theta_3^*}{d\xi^*} - 6\Theta_3^* = 8\xi^{*2} \frac{d\Theta_0^*}{d\xi^*} + 4\xi^* \frac{d\Theta_1^*}{d\xi^*} + 2\frac{d\Theta_2^*}{d\xi^*} \quad (3.4.18)$$

subject to the conditions,

$$\left[\Theta_3^* + \frac{E_1}{\lambda} \frac{d\Theta_2^*}{d\xi^*} + \left(\frac{E_2}{\lambda^{3/2}} - \frac{E_0E_1^2}{\lambda^{5/2}}\right) \frac{d\Theta_1^*}{d\xi^*} + \left(\frac{E_1^2}{\lambda^2} - \frac{4}{3}\frac{E_1^3}{\lambda^3} + \frac{E_3}{\lambda^2} + \frac{2}{3}\frac{E_1^3E_0^2}{\lambda^4} - \frac{2E_0E_1E_2}{\lambda^3}\right) \frac{d\Theta_0^*}{d\xi^*} \right]_{\xi^*=\frac{E_0}{\lambda^{1/2}}} = 0$$

and (3.4.19)

$$\Theta_3^*(\infty) = 0$$

E_3 is determined by the interface equation

$$8\beta E_3 = \left[\frac{d\Theta_3}{d\xi} - 2E_0E_1 \frac{d\Theta_2}{d\xi} + (2E_1 - 4E_1^2 + -2E_0E_2 + 2E_0^2E_1^2) \frac{d\Theta_1}{d\xi} + (4E_0E_1 - 4E_0E_1^2 - 2E_0E_3 + +8E_0E_1^3 - 8E_1E_2 - \frac{4}{3}E_0^3E_1^3 + 2E_2 + 4E_0^2E_1E_2) \frac{d\Theta_0}{d\xi} \right]_{\xi=E_0}$$

$$-\lambda\gamma \left[\frac{d\Theta_3^*}{d\xi^*} - \frac{2E_0E_1}{\lambda^{3/2}} \frac{d\Theta_2^*}{d\xi^*} + \left(\frac{2E_1}{\lambda} - \frac{4E_1^2}{\lambda^2} + \right.\right.$$

$$+\frac{2E_0E_2}{\lambda^2}+\frac{2E_0^2E_1^3}{\lambda^3}\Big)\frac{d\Theta_1^*}{d\xi^*}+\Big(\frac{4E_0E_1}{\lambda^{3/2}}-\frac{4E_0E_1^2}{\lambda^{5/2}}-\frac{2E_0E_3}{\lambda^{5/2}}$$

$$+\frac{8E_0E_1^3}{\lambda^{7/2}}-\frac{8E_1E_2}{\lambda^{5/2}}-\frac{4}{3}\frac{E_0^3E_1^3}{\lambda^{3/2}}+\frac{2E_2}{\lambda^{3/2}}+\frac{4E_0^2E_1E_3}{\lambda^{7/2}}\Big)\frac{d\Theta_0^*}{d\xi^*}\Big]_{\xi^*=\frac{E_0}{\lambda^{1/2}}}$$

(3.4.20)

The function Ψ_3 is governed by the fourth order partial differential equation,

$$\frac{\partial^4\Psi_3}{\partial\xi^{*4}}+\frac{2\xi^*}{P_r}\frac{\partial^3\Psi_3}{\partial\xi^{*3}}-\frac{2}{P_r}\frac{\partial^2\Psi_3}{\partial\xi^{*2}}=8Ra(1-\mu^2)^{\frac{1}{2}}\frac{\partial\Theta_0^*}{\partial\xi^*} \qquad (3.4.21)$$

and is subject to the conditions,

$$\Psi_3\left(\frac{E_0}{\lambda^{1/2}},\mu\right)=\frac{\partial\Psi_3}{\partial\xi^*}\left(\frac{E_0}{\lambda^{1/2}},\mu\right)=\frac{\partial\Psi_3}{\partial\mu}\left(\frac{E_0}{\lambda^{1/2}},\mu\right)=0 \qquad (3.4.22)$$

and

$$\frac{\partial\Psi_3(\xi^*,\mu)}{\partial\xi^*}\longrightarrow 0 \quad \text{as} \quad \xi^*\longrightarrow\infty \qquad (3.4.23)$$

Utilising the method of separation of variables, this equation can be simplified by writing the flow field perturbation function Ψ_3 as,

$$\Psi_3(\xi^*,\mu)=8Ra(1-\mu^2)^{\frac{1}{2}}\,\bar{\Psi}_3(\xi^*) \qquad (3.4.24)$$

Substitution of (3.4.24) into (3.4.21) and the conditions (3.4.22) and (3.4.23) gives the fourth order ordinary differential equation,

$$\frac{d^4\bar{\Psi}_3}{d\xi^{*4}}+\frac{2\xi^*}{P_r}\frac{d^3\bar{\Psi}_3}{d\xi^{*3}}-\frac{2}{P_r}\frac{d^2\bar{\Psi}_3}{d\xi^{*2}}=\frac{d\Theta_0^*}{d\xi^*} \qquad (3.4.25)$$

which is subject to the boundary conditions,

$$\bar{\Psi}_3 = \frac{d\bar{\Psi}_3}{d\xi^*} = 0 \qquad \text{at} \quad \xi^* = \frac{\varepsilon_0}{\lambda^2} \tag{3.4.26}$$

and

$$\frac{d\bar{\Psi}_3}{d\xi^*} \to 0 \quad \text{as} \quad \xi^* \to \infty \tag{3.4.27}$$

Fourth Order

The dependency of the perturbation functions Θ_4, Θ_4^* and E_4 on μ becomes apparent in the equations obtained from the terms of order τ^2. Investigation of the fourth order thermal field equation for the liquid reveals the inclusion of a term,

$$2(1-\mu^2)^{\frac{1}{2}} \frac{\partial \bar{\Psi}_3}{\partial \mu} \cdot \frac{d\Theta_0^*}{d\xi^*} \tag{3.4.28}$$

Substitution of (3.4.24) into (3.4.28) gives,

$$-16 Ra \cdot \bar{\Psi}_3 \frac{d\Theta_0^*}{d\xi^*} \cdot \mu \tag{3.4.29}$$

It is interesting at this point to compare this term with (2.4.29).

Again, the separation of variables technique is employed and the following variables are introduced:

$$\Theta_4(\xi,\mu) = \bar{\Theta}_4(\xi) + \mu\, \bar{\bar{\Theta}}_4(\xi) \tag{3.4.30}$$

$$\Theta_4^*(\xi^*,\mu) = \bar{\Theta}_4^*(\xi^*) + \mu\, \bar{\bar{\Theta}}_4^*(\xi^*) \tag{3.4.31}$$

and $$E_4(\mu) = \bar{E}_4 + \mu \bar{\bar{E}}_4 \qquad (3.4.32)$$

Substitution of these variables into the fourth order equations produces two systems of differential equations; the single bar and the double bar. These are denoted, as in the case of the sphere, by — and = respectively.

Fourth Order Single Bar System

The solid thermal function $\bar{\Theta}_4$ satisfies the equation,

$$\frac{d^2\bar{\Theta}_4}{d\zeta^2} + 2\zeta\frac{d\bar{\Theta}_4}{d\zeta} - 8\bar{\Theta}_4 = 16\zeta^3\frac{d\Theta_0}{d\zeta} + 8\zeta^2\frac{d\Theta_1}{d\zeta} + 4\zeta\frac{d\Theta_2}{d\zeta} + 2\frac{d\Theta_3}{d\zeta} \qquad (3.4.33)$$

which is subject to the boundary conditions,

$$\bar{\Theta}_4(0) = 0$$

and $$(3.4.34)$$

$$\left[\bar{\Theta}_4 + E_1\frac{d\Theta_3}{d\zeta} + (E_2 - E_0E_1^2)\frac{d\Theta_2}{d\zeta} + \left(E_3 + E_1^2 - 2E_1^3 - 2E_0E_1E_2 + \frac{2}{3}E_0^2E_1^3\right)\frac{d\Theta_1}{d\zeta} + \left(2E_0E_1^2 + \frac{19}{6}E_0E_1^4 - 2E_0E_1E_3 - 5E_1^2E_2 - E_0E_2^2 + 2E_1E_2 + \bar{E}_4 - \frac{4}{3}E_0E_1^3 + 2E_0^2E_1^2E_2 - \frac{E_0^3E_1^4}{3}\right)\frac{d\Theta_0}{d\zeta}\right]_{\zeta=\zeta_0} = 0$$

The liquid thermal function $\bar{\Theta}_4^*$ satisfies the equation,

$$\frac{d^2\bar{\Theta}_4^*}{d\xi^{*2}} + 2\xi^* \frac{d\bar{\Theta}_4^*}{d\xi^*} - 8\bar{\Theta}_4^* = 16\xi^{*3}\frac{d\Theta_0^*}{d\xi^*} + 8\xi_*^2\frac{d\Theta_1^*}{d\xi^*} + 4\xi^*\frac{d\Theta_2^*}{d\xi^*} + 2\frac{d\Theta_3^*}{d\xi^*} \qquad (3.4.35)$$

subject to the boundary conditions,

$$\left[\bar{\Theta}_4^* + \frac{E_1}{\lambda}\frac{d\Theta_3^*}{d\xi^*} + \left(\frac{E_2}{\lambda^{3/2}} - \frac{E_0E_1^2}{\lambda^{5/2}}\right)\frac{d\Theta_2^*}{d\xi^*} + \left(\frac{E_3}{\lambda^2} + \frac{E_1^2}{\lambda^2} - \frac{2E_1^3}{\lambda^3} - \frac{2E_0E_1E_2}{\lambda^3} + \frac{2}{3}\frac{E_0^2E_1^3}{\lambda^4}\right)\frac{d\Theta_1^*}{d\xi^*} + \left(\frac{2E_0E_1^2}{\lambda^{5/2}} + \frac{19}{6}\frac{E_0E_1^4}{\lambda^{9/2}} - \frac{2E_0E_1E_3}{\lambda^{7/2}} - \frac{5E_1^2E_2}{\lambda^{7/2}} - \frac{E_0E_2^2}{\lambda^{7/2}} + \frac{2E_1E_2}{\lambda^{4/2}} + \frac{\bar{E}_4}{\lambda^{5/2}} - \frac{4}{3}\frac{E_0E_1^3}{\lambda^{7/2}} + \frac{2E_0^2E_1^2E_2}{\lambda^{9/2}} - \frac{E_0^3E_1^4}{3\lambda^{11/2}}\right)\frac{d\Theta_0^*}{d\xi^*}\right]_{\xi^*=E_0/\lambda^{1/2}} = 0$$

and

$$\bar{\Theta}^*(\infty) = 0 \qquad (3.4.36)$$

$\bar{E}_4$ is determined by the interface equation

$$10\beta\bar{E}_4 = \left[\frac{d\bar{\Theta}_4}{d\xi} - 2E_0E_1\frac{d\Theta_3}{d\xi} + \left(2E_1 - 5E_1^2 - 2E_0E_2 + 2E_0^2E_1^2\right)\frac{d\Theta_2}{d\xi} + \left(4E_0E_1 - 10E_1E_2 + \frac{32}{3}E_0E_1^3 + 2E_2 - 2E_0E_3 - 4E_0E_1^2 + 4E_0^2E_1E_2 - \frac{4}{3}E_0^3E_1^3\right)\frac{d\Theta_1}{d\xi} + \left(8E_0^2E_1 - 10E_1E_3 - \frac{28}{3}E_1^3 + 30E_0E_1^2E_2 - \frac{34}{3}E_0^2E_1^4 + \frac{55}{6}E_1^4 + 4E_0E_2 - 5E_2^2 + 2E_3 - 2E_0\bar{E}_4 + 4E_1^2 - 8E_0^2E_1^2 + 2E_0^2E_2^2 - 8E_0E_1E_2 + 4E_0^2E_1E_3 + 4E_0^2E_1^3 - 4E_0^3E_1^2E_2 + \frac{2}{3}E_0^4E_1^4\right)\frac{d\Theta_0}{d\xi}\right]_{\xi=E_0} +$$

$$-\lambda^{\frac{3}{2}}\gamma\left[\frac{d\bar{\bar{\otimes}}_4^*}{d\xi^*}-\frac{2E_0E_1}{\lambda^{3/2}}\frac{d\bar{\bar{\otimes}}_3^*}{d\xi^*}+\left(\frac{2E_1}{\lambda}-\frac{5E_1^2}{\lambda^2}-\frac{2E_0E_2}{\lambda^2}+\right.\right.$$

$$+\frac{2E_0^2E_1^2}{\lambda^3}\Bigg)\frac{d\bar{\bar{\otimes}}_2^*}{d\xi^*}+\left(\frac{4E_0E_1}{\lambda^{3/2}}-\frac{10E_1E_2}{\lambda^{5/2}}+\frac{32E_0E_1^3}{\lambda^{7/2}}+\frac{2E_2}{\lambda^{3/2}}+\right.$$

$$-\frac{2E_0E_3}{\lambda^{5/2}}-\frac{4E_0E_1^2}{\lambda^{5/2}}+\frac{4E_0^2E_1E_2}{\lambda^{7/2}}-\frac{4}{3}\frac{E_0^3E_1^3}{\lambda^{9/2}}\Bigg)\frac{d\bar{\bar{\otimes}}_1^*}{d\xi^*}+\left(\frac{8E_0^2E_1}{\lambda^2}\right.$$

$$-\frac{10E_1E_3}{\lambda^3}-\frac{28}{3}\frac{E_1^3}{\lambda^3}+\frac{30E_0E_1^2E_2}{\lambda^4}-\frac{34}{3}\frac{E_0^2E_1^4}{\lambda^5}+\frac{55}{6}\frac{E_1^4}{\lambda^4}+$$

$$+\frac{4E_0E_2}{\lambda^2}-\frac{5E_2^2}{\lambda^3}+\frac{2E_3}{\lambda^2}-\frac{2E_0\bar{E}_4}{\lambda^3}+\frac{4E_1^2}{\lambda^2}-\frac{8E_0^2E_1^2}{\lambda^3}+$$

$$+\frac{2E_0^2E_2^2}{\lambda^4}-\frac{8E_0E_1E_2}{\lambda^3}+\frac{4E_0^2E_1E_3}{\lambda^4}+\frac{4E_0^2E_1^3}{\lambda^4}+$$

$$\left.\left.-\frac{4E_0^3E_1^2E_2}{\lambda^5}+\frac{2}{3}\frac{E_0^4E_1^4}{\lambda^6}\right)\frac{d\bar{\bar{\otimes}}_0^*}{d\xi^*}\right]_{\xi^*=\frac{E_0}{\lambda^{1/2}}} \qquad (3.4.37)$$

Fourth Order Double Bar System

The fourth order functions $\bar{\bar{\otimes}}_4$, $\bar{\bar{\otimes}}_4^*$ and $\bar{E}_4$ satisfy the following equations:

for the solid region,

$$\frac{d^2\bar{\bar{\otimes}}_4}{d\xi^2}+2\xi\frac{d\bar{\bar{\otimes}}_4}{d\xi}-8\bar{\bar{\otimes}}_4=0 \qquad (3.4.38)$$

subject to the boundary conditions,

$$\bar{\bar{\otimes}}_4(0)=0 \qquad (3.4.39)$$

and

$$\left[\bar{\bar{\otimes}}_4+\bar{\bar{E}}_4\frac{d\bar{\otimes}_0}{d\xi}\right]_{\xi=\epsilon_0}=0$$

and for the liquid region,

$$\frac{d^2\bar{\bar{\otimes}}_4^*}{d\xi^{*2}}+2\xi^*\frac{d\bar{\bar{\otimes}}_4^*}{d\xi^*}-8\bar{\bar{\otimes}}_4^*=-16R_a\bar{\Psi}_3\frac{d\bar{\otimes}_0^*}{d\xi^*} \qquad (3.4.40)$$

subject to the boundary conditions

$$\left[\bar{\bar{\Theta}}_4^* + \frac{E_4}{\lambda^{5/2}} \frac{d\Theta_0^*}{d\xi^*} \right]_{\xi^* = \frac{\epsilon_0}{\lambda^{1/2}}} = 0$$

and

$$\bar{\bar{\Theta}}_4^*(\infty) = 0 \qquad (3.4.41)$$

The interface equation which determines $\bar{\bar{E}}_4$ is,

$$10\beta \bar{\bar{E}}_4 = \left[\frac{d\bar{\bar{\Theta}}_4}{d\xi} - 2\epsilon_0 \bar{\bar{E}}_4 \frac{d\Theta_0}{d\xi} \right]_{\xi = \epsilon_0} +$$

$$-\lambda^{3/2}\gamma \left[\frac{d\bar{\bar{\Theta}}_4^*}{d\xi^*} - \frac{2\epsilon_0 \bar{\bar{E}}_4}{\lambda^3} \frac{d\Theta_0^*}{d\xi^*} \right]_{\xi^* = \frac{\epsilon_0}{\lambda^{1/2}}} \qquad (3.4.42)$$

On equating terms of order τ^{*2} in the flow field equation, the perturbation function Ψ_4 is found to be governed by the equation,

$$\frac{\partial^4 \Psi_4}{\partial \xi^{*4}} + \frac{2\xi^*}{P_r} \frac{\partial^3 \Psi_4}{\partial \xi^{*3}} - \frac{4}{P_r} \frac{\partial^2 \Psi_4}{\partial \xi^{*2}} = 8Ra(1-\mu^2)^{1/2} \frac{d\Theta_1^*}{d\xi^*}$$

(3.4.43)

The boundary conditions are,

$$\left[\Psi_4 + \frac{E_1}{\lambda} \frac{\partial \Psi_3}{\partial \xi^*} \right]_{\xi^* = \frac{\epsilon_0}{\lambda^{1/2}}} = 0$$

and (3.4.44)

$$\left[\frac{\partial \Psi_4}{\partial \xi^*} + \frac{E_1}{\lambda} \frac{\partial^2 \Psi_3}{\partial \xi^{*2}} \right]_{\xi^* = \frac{\epsilon_0}{\lambda^{1/2}}} = 0$$

and also

$$\frac{\partial \Psi_4}{\partial \xi^*} \to 0 \quad \text{as} \quad \xi^* \to \infty \tag{3.4.45}$$

Introducing the separable variables

$$\Psi_4(\xi^*, \mu) = 8Ra(1-\mu^2)^{\frac{1}{2}} \bar{\Psi}_4(\xi^*) \tag{3.4.46}$$

and again utilising (3.4.24), the fourth order differential equation (3.4.43) becomes,

$$\frac{d^4\Psi_4}{d\xi^{*4}} + \frac{2\xi^*}{P_r}\frac{d^3\Psi_4}{d\xi^{*3}} - \frac{4}{P_r}\frac{d^2\Psi_4}{d\xi^{*2}} = \frac{d\Theta_1^*}{d\xi^*} \tag{3.4.47}$$

subject to the conditions

$$\bar{\Psi}_4\left(\frac{\epsilon_0}{\lambda^{\frac{1}{3}}}\right) = 0$$

$$\left[\frac{d\bar{\Psi}_4}{d\xi^*} + \frac{\epsilon_1}{\lambda}\frac{d^2\bar{\Psi}_3}{d\xi^{*2}}\right]_{\xi^* = \frac{\epsilon_0}{\lambda^{\frac{1}{3}}}} = 0 \tag{3.4.48}$$

and

$$\frac{d\bar{\Psi}_4}{d\xi^*} \to 0 \quad \text{as} \quad \xi^* \to \infty \tag{3.4.49}$$

where the second boundary condition in (3.4.26) has been used to simplify the first boundary condition in (3.4.44).

Fifth Order

Investigation of the thermal field equation for the liquid reveals the presence of the terms

$$(1-\mu^2)^{\frac{1}{2}}\left(2\frac{\partial\Phi_3}{\partial\mu}\frac{d\Theta_1^*}{d\xi^*}+4\xi^*\frac{\partial\Phi_3}{\partial\mu}\frac{d\Theta_0^*}{d\xi^*}+2\frac{\partial\Phi_4}{\partial\mu}\frac{d\Theta_0^*}{d\xi^*}\right) \tag{3.4.50}$$

Substituting (3.4.24) and (3.4.46) into these terms gives,

$$-8Ra\left(2\bar{\Phi}_3\frac{d\Theta_1^*}{d\xi^*}+4\xi^*\bar{\Phi}_3\frac{d\Theta_0^*}{d\xi^*}+2\bar{\Phi}_4\frac{d\Theta_0}{d\xi^*}\right)\mu \tag{3.4.51}$$

and so the fifth order perturbation functions can be written as,

$$\Theta_5(\xi,\mu)=\bar{\Theta}_5(\xi)+\mu\,\bar{\bar{\Theta}}_5(\xi) \tag{3.4.52}$$

$$\Theta_5^*(\xi^*,\mu)=\bar{\Theta}_5^*(\xi^*)+\mu\,\bar{\bar{\Theta}}_5^*(\xi^*) \tag{3.4.53}$$

and
$$E_5(\mu)=\bar{E}_5+\bar{\bar{E}}_5.\mu \tag{3.4.54}$$

Substitution of these variables together with (3.4.30) - (3.4.32) gives the single and double bar systems of differential equations.

Fifth Order Single Bar System

For the solid region $\bar{\Theta}_5$ satisfies the equation,

$$\frac{d^2\bar{\Theta}_5}{d\xi^2}+2\xi\frac{d\bar{\Theta}_5}{d\xi}-10\bar{\Theta}_5=32\xi^4\frac{d\Theta_0}{d\xi}+$$
$$+16\xi^3\frac{d\Theta_1}{d\xi}+8\xi^2\frac{d\Theta_2}{d\xi}+4\xi\frac{d\Theta_3}{d\xi}+2\frac{d\bar{\Theta}_4}{d\xi} \tag{3.4.55}$$

subject to the boundary conditions

$$\bar{\Theta}_5(0) = 0$$

and (3.4.56)

$$\Big[\bar{\Theta}_5 + \epsilon_1 \frac{d\bar{\Theta}_4}{d\xi} + (\epsilon_2 - \epsilon_0\epsilon_1^2)\frac{d\bar{\Theta}_3}{d\xi} + (\epsilon_3 + \epsilon_1^2 + -\frac{8}{3}\epsilon_1^3 - 2\epsilon_0\epsilon_1\epsilon_2 + \frac{2}{3}\epsilon_0^2\epsilon_1^3)\frac{d\bar{\Theta}_2}{d\xi} + (\bar{\epsilon}_4 + 2\epsilon_0\epsilon_1^2 + -7\epsilon_1^2\epsilon_2 + \frac{9}{2}\epsilon_0\epsilon_1^4 - \epsilon_0\epsilon_2^2 + 2\epsilon_1\epsilon_2 - 2\epsilon_0\epsilon_1\epsilon_3 - \frac{4}{3}\epsilon_0\epsilon_1^3 + 2\epsilon_0^2\epsilon_1^2\epsilon_2 - \frac{\epsilon_0^3\epsilon_1^4}{3}\Big)\frac{d\bar{\Theta}_1}{d\xi} + \Big(\bar{\epsilon}_5 + 4\epsilon_0^2\epsilon_1^3 - 6\epsilon_1^2\epsilon_3 - 4\epsilon_1^4 + \frac{64}{15}\epsilon_1^5 + \epsilon_2^2 - 6\epsilon_1\epsilon_2^2 + 4\epsilon_0\epsilon_1\epsilon_2 + 2\epsilon_1\epsilon_3 + - 2\epsilon_0\epsilon_1\bar{\epsilon}_4 - 2\epsilon_0\epsilon_2\epsilon_3 + \frac{4}{3}\epsilon_1^3 - \frac{8}{3}\epsilon_0^2\epsilon_1^3 + \frac{46}{3}\epsilon_0\epsilon_1^3\epsilon_2 + 2\epsilon_0^2\epsilon_1\epsilon_2^2 - 4\epsilon_0\epsilon_1^2\epsilon_2 + 2\epsilon_0^2\epsilon_1^2\epsilon_3 + \epsilon_0^2\epsilon_1^4 + -\frac{4}{3}\epsilon_0^3\epsilon_1^3\epsilon_2 + \frac{2}{15}\epsilon_0^4\epsilon_1^5 - \frac{61}{15}\epsilon_0^2\epsilon_1^5\Big)\frac{d\bar{\Theta}_0}{d\xi}\Big]_{\xi=\epsilon_0} = 0$$

For the liquid region $\bar{\Theta}_5^*$ satisfies the equation,

$$\frac{d^2\bar{\Theta}_5^*}{d\xi^{*2}} + 2\xi^*\frac{d\bar{\Theta}_5^*}{d\xi^*} - 10\,\bar{\Theta}_5^* = 32\xi^{*4}\frac{d\bar{\Theta}_0^*}{d\xi^*} + 16\xi^{*3}\frac{d\bar{\Theta}_1^*}{d\xi^*} + 8\xi^{*2}\frac{d\bar{\Theta}_2^*}{d\xi^*} + 4\xi^*\frac{d\bar{\Theta}_3^*}{d\xi^*} + 2\frac{d\bar{\Theta}_4^*}{d\xi^*} \quad (3.4.57)$$

subject to the conditions

$$\left[\bar{\Theta}_5^* + \frac{\epsilon_1}{\lambda}\frac{d\bar{\Theta}_4^*}{d\xi^+} + \left(\frac{E_2}{\lambda^{3/2}} - \frac{E_0E_1^2}{\lambda^{5/2}}\right)\frac{d\Theta_3^*}{d\xi^+} + \right.$$

$$+\left(\frac{E_3}{\lambda^2} + \frac{E_1^2}{\lambda^2} - \frac{8E_1^3}{3\lambda^3} - \frac{2E_0E_1E_2}{\lambda^3} + \frac{2}{3}\frac{E_0^2E_1^3}{\lambda^4}\right)\frac{d\Theta_2^*}{d\xi^+} +$$

$$+\left(\frac{\bar{E}_4}{\lambda^{5/2}} + \frac{2E_0E_1^2}{\lambda^{5/2}} - \frac{7E_1^2E_2}{\lambda^{7/2}} + \frac{9}{2}\frac{E_0E_1^4}{\lambda^{9/2}} - \frac{E_0E_2^2}{\lambda^{7/2}} + \frac{2E_1E_2}{\lambda^{5/2}} + \right.$$

$$\left. - \frac{2E_0E_1E_3}{\lambda^{7/2}} - \frac{4}{3}\frac{E_0E_1^3}{\lambda^{7/2}} + \frac{2E_0^2E_1^2E_2}{\lambda^{9/2}} - \frac{E_0^3E_1^4}{3\lambda^{11/2}}\right)\frac{d\Theta_1^*}{d\xi^+} +$$

$$+\left(\frac{\bar{E}_5}{\lambda^3} + \frac{4E_0^2E_1^2}{\lambda^3} - \frac{6E_1^2E_3}{\lambda^4} - \frac{4E_1^4}{\lambda^4} + \frac{64}{15}\frac{E_1^5}{\lambda^5} + \frac{E_2^2}{\lambda^3} - \frac{6E_1E_2^2}{\lambda^4}\right.$$

$$+\frac{4E_0E_1E_2}{\lambda^3} + \frac{2E_1E_3}{\lambda^3} - \frac{2E_0E_1\bar{E}_4}{\lambda^4} - \frac{2E_0E_2E_3}{\lambda^4} + \frac{4}{3}\frac{E_1^3}{\lambda^3} +$$

$$-\frac{8}{3}\frac{E_0^2E_1^3}{\lambda^4} + \frac{46}{3}\frac{E_0E_1^3E_2}{\lambda^5} + \frac{2E_0^2E_1E_2^2}{\lambda^5} - \frac{4E_0E_1^2E_2}{\lambda^4} + \frac{2E_0^3E_1^2E_3}{\lambda^5}$$

$$\left.\left. + \frac{E_0^2E_1^4}{\lambda^5} - \frac{4}{3}\frac{E_0^3E_1^3E_2}{\lambda^6} + \frac{2}{15}\frac{E_0^4E_1^5}{\lambda^7} - \frac{61}{15}\frac{E_0^3E_1^5}{\lambda^6}\right)\frac{d\Theta_0^*}{d\xi^+}\right]_{\xi^+=\frac{E_0}{\lambda^4}} = 0$$

and (3.4.58)

$$\bar{\Theta}^*(\infty) = 0$$

The interface equation which determines the perturbation function $\bar{E}_5$ is,

$$12\beta\bar{E}_5 = \left[\frac{d\bar{\Theta}_5}{d\xi} - 2E_0E_1\frac{d\bar{\Theta}_4}{d\xi} + (2E_1 - 6E_1^2 + \right.$$

$$\left. -2E_0E_2 + 2E_0^2E_1^2)\frac{d\Theta_3}{d\xi} + \left(4E_0E_1 - 12E_1E_2 + \frac{40}{3}E_0E_1^3 + \right.\right.$$

$$+2E_2 - 2E_0E_3 - 4E_0E_1^2 + 4E_0^2E_1E_2 - \frac{4}{3}E_0^3E_1^3\Big)\frac{d\Theta_2}{d\zeta} +$$

$$+\Big(16E_1^4 - 12E_1E_3 - 12E_1^3 + 8E_0^2E_1 + 38E_0E_1^2E_2 + 4E_0^3E_1^3 +$$

$$+4E_0E_2 - 6E_2^2 + 2E_3 - 2E_0\bar{E}_4 + 4E_1^2 - 8E_0^2E_1^2 - 15E_0^2E_1^4 +$$

$$+2E_0^2E_2^2 - 8E_0E_1E_2 + 4E_0^2E_1E_3 - 4E_0^3E_1^2E_2 + \frac{2}{3}E_0^4E_1^4\Big)\frac{d\Theta_1}{d\zeta} +$$

$$+\Big(16E_0^3E_1 + 36E_0E_1^2E_3 - 12E_1\bar{E}_4 - \frac{88}{3}E_0E_1^3 + \frac{79}{3}E_0E_1^4 +$$

$$-\frac{106}{3}E_0E_1^5 + 52E_1^3E_2 + 36E_0E_1E_2^2 - 34E_1^2E_2 - \frac{164}{3}E_0^2E_1^3E_2$$

$$+\frac{34}{3}E_0^3E_1^5 + 8E_0^2E_2 - \frac{4}{15}E_0^5E_1^5 + \frac{8}{3}E_0^4E_1^3E_2 - 4E_0^3E_1^2E_3 +$$

$$-\frac{8}{3}E_0^3E_1^4 - 12E_2E_3 + 2\bar{E}_4 + 4E_0E_3 - 2E_0\bar{E}_5 - 16E_0^3E_1^2 +$$

$$-4E_0E_2^2 + 8E_1E_2 + 16E_0E_1^2 - 16E_0^2E_1E_2 - 8E_0E_1E_3 +$$

$$+4E_0^2E_1\bar{E}_4 + 4E_0^2E_2E_3 - 4E_0^3E_1E_2^2 + 12E_0^2E_1^2E_2 +$$

$$+8E_0^3E_1^3\Big)\frac{d\Theta_0}{d\zeta}\Bigg|_{\zeta=E_0} - \lambda^2\gamma\Bigg[\frac{d\bar{\Theta}_5^*}{d\zeta} +$$

$$-\frac{2E_0E_1}{\lambda^{3/2}}\frac{d\bar{\Theta}_4^*}{d\zeta} + \Big(\frac{2E_1}{\lambda} - \frac{6E_1^2}{\lambda^2} - \frac{2E_0E_2}{\lambda^2} + \frac{2E_0^2E_1^2}{\lambda^3}\Big)\frac{d\Theta_3^*}{d\zeta^*}$$

$$+\Big(\frac{4E_0E_1}{\lambda^{3/2}} - \frac{12E_1E_2}{\lambda^{5/2}} + \frac{40}{3}\frac{E_0E_1^3}{\lambda^{7/2}} + \frac{2E_2}{\lambda^{3/2}} - \frac{2E_0E_3}{\lambda^{5/2}} +$$

$$-\frac{4E_0E_1^2}{\lambda^{5/2}} + \frac{4E_0^2E_1E_2}{\lambda^{7/2}} - \frac{4}{3}\frac{E_0^3E_1^3}{\lambda^{9/2}}\Big)\frac{d\Theta_2^*}{d\zeta^*} +$$

$$+\left(\frac{16E_1^4}{\lambda^4}-\frac{12E_1E_3}{\lambda^3}-\frac{12E_1^3}{\lambda^3}+\frac{8E_0^2E_1}{\lambda^2}+\frac{38E_0E_1^2E_2}{\lambda^4}+\right.$$

$$+\frac{4E_0^2E_1^3}{\lambda^4}+\frac{4E_0E_2}{\lambda^2}-\frac{6E_2^2}{\lambda^3}+\frac{2E_3}{\lambda^2}-\frac{2E_0\bar{E}_4}{\lambda^3}+\frac{4E_1^2}{\lambda^3}-\frac{8E_0^2E_1^2}{\lambda^3}$$

$$-\frac{15E_0^2E_1^4}{\lambda^5}+\frac{2E_0^2E_2^2}{\lambda^3}-\frac{8E_0E_1E_2}{\lambda^3}+\frac{4E_0^2E_1E_3}{\lambda^4}-\frac{4E_0^3E_1^2E_2}{\lambda^5}$$

$$\left.+\frac{2}{3}\frac{E_0^4E_1^4}{\lambda^6}\right)\frac{d\Theta_1^*}{d\xi^*}+\left(\frac{16E_0^3E_1}{\lambda^{5/2}}+\frac{36E_0E_1^2E_3}{\lambda^{9/2}}-\frac{12E_1\bar{E}_4}{\lambda^{7/2}}\right.$$

$$-\frac{88}{3}\frac{E_0E_1^3}{\lambda^{7/2}}+\frac{79}{3}\frac{E_0E_1^4}{\lambda^{9/2}}-\frac{106}{3}\frac{E_0E_1^5}{\lambda^{11/2}}+\frac{52E_1^3E_2}{\lambda^{9/2}}+\frac{36E_0E_1E_2^2}{\lambda^{9/2}}$$

$$-\frac{34E_1^2E_2}{\lambda^{7/2}}-\frac{164}{3}\frac{E_0^2E_1^3E_2}{\lambda^{11/2}}+\frac{34}{3}\frac{E_0^3E_1^5}{\lambda^{13/2}}+\frac{8E_0^2E_2}{\lambda^{5/2}}+$$

$$-\frac{4}{15}\frac{E_0^5E_1^5}{\lambda^{15/2}}+\frac{8}{3}\frac{E_0^4E_1^3E_2}{\lambda^{13/2}}-\frac{4E_0^3E_1^2E_2}{\lambda^{11/2}}-\frac{8}{3}\frac{E_0^3E_1^4}{\lambda^{11/2}}+$$

$$-\frac{12E_2E_3}{\lambda^{7/2}}+\frac{2\bar{E}_4}{\lambda^{5/2}}+\frac{4E_0E_3}{\lambda^{5/2}}-\frac{2E_0\bar{E}_5}{\lambda^{7/2}}-\frac{16E_0^3E_1^2}{\lambda^{7/2}}+$$

$$-\frac{4E_0E_2^2}{\lambda^{7/2}}+\frac{8E_1E_2}{\lambda^{5/2}}+\frac{16E_0E_1^2}{\lambda^{5/2}}-\frac{16E_0^2E_1E_2}{\lambda^{7/2}}-\frac{8E_0E_1E_3}{\lambda^{7/2}}+$$

$$+\frac{4E_0^2E_1\bar{E}_4}{\lambda^{9/2}}+\frac{4E_0^2E_2E_3}{\lambda^{9/2}}-\frac{4E_0^3E_1E_2^2}{\lambda^{11/2}}+\frac{12E_0^2E_1^2E_3}{\lambda^{9/2}}+$$

$$\left.+\frac{8E_0^3E_1^3}{\lambda^{9/2}}\right]_{\xi^*=\frac{E_0}{\lambda^{1/2}}} \qquad (3.4.59)$$

Fifth Order Double Bar System

For the solid region, $\bar{\bar{\otimes}}_5$ satisfies the equation,

$$\frac{d^2\bar{\bar{\otimes}}_5}{d\xi^2} + 2\xi\frac{d\bar{\bar{\otimes}}_5}{d\xi} - 10\bar{\bar{\otimes}}_5 = 2\frac{d\bar{\bar{\otimes}}_4}{d\xi} \qquad (3.4.60)$$

subject to the boundary conditions,

$$\bar{\bar{\otimes}}_5(0) = 0$$

and (3.4.61)

$$\left[\bar{\bar{\otimes}}_5 + \epsilon_1\frac{d\bar{\bar{\otimes}}_4}{d\xi} + \bar{\bar{E}}_4\frac{d\otimes_1}{d\xi} + (\bar{\bar{E}}_5 - 2\epsilon_0\epsilon_1\bar{\bar{E}}_4)\frac{d\otimes_0}{d\xi}\right]_{\xi=\epsilon_0} = 0$$

For the liquid region, $\bar{\bar{\otimes}}_5^*$ satisfies the equation,

$$\frac{d^2\bar{\bar{\otimes}}_5^*}{d\xi^{*2}} + 2\xi\frac{d\bar{\bar{\otimes}}_5^*}{d\xi^*} - 10\bar{\bar{\otimes}}_5^* = 2\frac{d\bar{\bar{\otimes}}_4^*}{d\xi^*} +$$

$$-16Ra\bar{\Psi}_3\frac{d\otimes_1^*}{d\xi^*} - 32Ra\xi^*\bar{\Psi}_3\frac{d\otimes_0^*}{d\xi^*} - 16Ra\bar{\Psi}_4\frac{d\otimes_0^*}{d\xi^*} \qquad (3.4.62)$$

subject to the boundary conditions,

$$\left[\bar{\bar{\otimes}}_5^* + \frac{E_1}{\lambda}\frac{d\bar{\bar{\otimes}}_4^*}{d\xi^*} + \frac{\bar{\bar{E}}_4}{\lambda^{5/2}}\frac{d\otimes_1^*}{d\xi^*} + \left(\frac{\bar{\bar{E}}_5}{\lambda^3} - \frac{2\epsilon_0\epsilon_1\bar{\bar{E}}_4}{\lambda^4}\right)\frac{d\otimes_0^*}{d\xi^*}\right]_{\xi^*=\frac{\epsilon_0}{\lambda}} = 0$$

and (3.4.63)

$$\bar{\bar{\otimes}}_5(\infty) = 0$$

The interface equation which determines $\bar{\bar{E}}_5$ is,

$$\left[\frac{d\bar{\bar{\otimes}}_5}{d\xi} - 2\epsilon_0\epsilon_1\frac{d\bar{\bar{\otimes}}_4}{d\xi} - 2\epsilon_0\bar{\bar{E}}_4\frac{d\otimes_1}{d\xi} + \left(2\bar{\bar{E}}_4 + \right.\right.$$

$$\left.\left. -2\epsilon_0\bar{\bar{E}}_5 - 12\epsilon_1\bar{\bar{E}}_4 + 4\epsilon_0^2\epsilon_1\bar{\bar{E}}_4\right)\frac{d\otimes_0}{d\xi}\right]_{\xi=\epsilon_0} +$$

$$-\lambda^2\gamma\left[\frac{d\bar{\bar{\Phi}}_5^*}{d\xi^+} - \frac{2E_0E_1}{\lambda^{3/2}}\frac{d\bar{\bar{\Phi}}_4^*}{d\xi^+} - \frac{2E_0\bar{E}_4}{\lambda^3}\frac{d\bar{\Phi}_1^*}{d\xi^+} + \left(\frac{2\bar{\bar{E}}_4}{\lambda^{5/2}} - \frac{2E_0\bar{\bar{E}}_5}{\lambda^{7/2}} - \frac{12E_1\bar{\bar{E}}_4}{\lambda^{7/2}} + \frac{4E_0^2E_1\bar{\bar{E}}_4}{\lambda^{9/2}}\right)\frac{d\bar{\Phi}_0^*}{d\xi^+}\right]_{\xi^+=\frac{E_0}{\lambda^{1/2}}} = 0$$

(3.4.64)

It can be seen that these derived equations are of the same form as the corresponding equations for the spherical problem. Hence, the method of solution for either case uses the same techniques and these are considered in the next chapter.

Chapter 4

Solutions and Results for Solidification Problems

4.1 Analytical Solutions

The equations which were obtained in the two previous chapters and which govern the thermal field functions can all be solved analytically, see Stead [30]. However, from a practical viewpoint this procedure turns out to be limited and rather laborious. Indeed the computation of the analytical solutions for the fixed values of the dimensionless parameters γ, β, λ, Pr and Ra is just as awkward as their derivation. Moreover, the numerical evaluation of such solutions is tedious and liable to errors. Even when analytical solutions are sought for large β they are found to be unsuitable for computation. Nevertheless, in this section the zeroth and first order equations are solved analytically since the solutions of the lower orders are not as complex as those for the higher orders.. These solutions can then be used to check the accuracy of the numerical computations.

The general structure of all the equations governing the thermal fields Θ_n and Θ_n^* is now discussed. Each of these equations can be written either as

$$H_\zeta^n \Theta_n(\zeta) = f_n(\zeta) \tag{4.1.1}$$

or

$$H_{\zeta^*}^n \Theta_n^*(\zeta^*) = f_n^*(\zeta^*) \tag{4.1.2}$$

where the operator on the left hand side of each of these equations is defined by

$$H_\zeta^n \cdot = \frac{d^2 \cdot}{d\zeta^2} + 2\zeta \frac{d \cdot}{d\zeta} - 2n \cdot \tag{4.1.3}$$

It can be readily shown that one solution to the homogeneous differential

equation

$$H_\xi^\wedge \otimes_n(\xi) = 0 \tag{4.1.4}$$

is given by

$$\otimes_n(\xi) = i^n \operatorname{erfc} \xi \tag{4.1.5}$$

where the repeated integrals are defined by

$$i^n \operatorname{erfc} \xi = \int_\xi^\infty i^{n-1} \operatorname{erfc} x \, dx \quad , \; n = 1,2.. \tag{4.1.6}$$

and

$$i^0 \operatorname{erfc} \xi = \operatorname{erfc} \xi \tag{4.1.7}$$

Another obvious solution to this differential equation is of the form,

$$\otimes_n(\xi) = i^n \operatorname{erfc}(-\xi) \tag{4.1.8}$$

However, this second solution can also be determined in the form of a Hermite type polynomial of degree n. Accordingly, a general solution to the differential equation (4.1.1) is,

$$\otimes_n(\xi) = A_n i^n \operatorname{erfc} \xi + B_n \left[\xi^n + \frac{n(n-1)}{4} \xi^{n-2} + (n-1)(n-2)(n-3)\xi^{n-4} \right] + p_n(\xi) \tag{4.1.9}$$

where A_n and B_n are constants to be determined by the boundary conditions and $p_n(\xi)$ is the particular integral. Similarly, the solution to the differential equation for the liquid region (4.1.2) is,

$$\Theta_n^*(\xi^*) = A_n^* i^n \operatorname{erfc} \xi^* + B_n^* \left[\xi^{*n} + \frac{n(n-1)}{4} \xi^{*n-2} + \frac{(n-1)(n-2)(n-3)}{32} \xi^{*n-4} \right] + p_n^*(\xi^*)$$

(4.1.10)

Analytical Solutions for the Sphere

The solution of the zeroth order thermal perturbation equation in the solid region is,

$$\Theta_o(\xi) = \frac{\operatorname{erfc} \xi - \operatorname{erfc}(-\xi)}{\operatorname{erfc} \varepsilon_o - \operatorname{erfc}(-\varepsilon_o)} \qquad (4.1.11)$$

or, expressed more simply,

$$\Theta_o(\xi) = \frac{\operatorname{erf} \xi}{\operatorname{erf} \varepsilon_o} \qquad (4.1.12)$$

For the liquid region the zeroth order thermal perturbation function is given as,

$$\Theta_o^*(\xi^*) = \frac{\operatorname{erf} \xi^* - \operatorname{erf}\left(\frac{\varepsilon_o}{\lambda^{1/2}}\right)}{\operatorname{erfc}\left(\frac{\varepsilon_o}{\lambda^{1/2}}\right)} \qquad (4.1.13)$$

or,

$$\Theta_o^*(\xi^*) = 1 - \frac{\operatorname{erfc}(\xi^*)}{\operatorname{erfc}\left(\frac{\varepsilon_o}{\lambda^{1/2}}\right)} \qquad (4.1.14)$$

In order to determine the value of E_o these functions are substituted

into the zeroth order interface equation (2.4.5) to give the transcendental equation,

$$\sqrt{\pi}\beta E_o = \frac{e^{-E_o^2}}{\text{erf}\, E_o} - \left(\frac{\gamma}{\lambda^{\frac{1}{2}}}\right) \frac{e^{-\frac{E_o^2}{\lambda}}}{\text{erfc}\left(\frac{E_o}{\lambda^{\frac{1}{2}}}\right)} \qquad (4.1.15)$$

E_o is then obtained using an iterative procedure.

First Order Solution

Using the solutions for Θ_1 and Θ_1^* in the first order thermal equations, it is found that for the solid region, equation (2.4.6) becomes,

$$\frac{d^2\Theta_1}{d\xi^2} + 2\xi \frac{d\Theta_1}{d\xi} - 2\Theta_1 = \frac{8 e^{-\xi^2}}{\sqrt{\pi}\, \text{erf}\, E_o} \qquad (4.1.16)$$

subject to the boundary conditions

$$\Theta_1(0) = 0$$

and

$$\Theta_1(E_o) = -\frac{2E_o}{\sqrt{\pi}} \frac{e^{-E_o^2}}{\text{erf}\, E_o} \qquad (4.1.17)$$

Whilst for the liquid region, the first order equation (2.4.8) becomes,

$$\frac{d^2\Theta_1^*}{d\xi^{*2}} + 2\xi^* \frac{d\Theta_1^*}{d\xi^*} - 2\Theta_1^* = \frac{8\, e^{-\xi^{*2}}}{\sqrt{\pi}\, \text{erfc}\left(\frac{E_o}{\lambda^{\frac{1}{2}}}\right)} \qquad (4.1.18)$$

subject to the conditions

$$\Theta_1^*\left(\frac{E_o}{\lambda^{\frac{1}{2}}}\right) = -\frac{2}{\sqrt{\pi}} \frac{E_1}{\lambda} \frac{e^{-\frac{E_o^2}{\lambda}}}{\text{erfc}\left(\frac{E_o}{\lambda^{\frac{1}{2}}}\right)}$$

and

$$\Theta_1^*(\infty) = 0 \qquad (4.1.19)$$

The solutions for these first order equations are, for the solid,

$$\Theta_1(\xi) = \frac{2\xi}{\operatorname{erf} E_0}\left[\operatorname{erfc} E_0 - \operatorname{erfc}\xi - \frac{E_1}{E_0}\frac{e^{-E_0^2}}{\sqrt{\pi}}\right] \tag{4.1.20}$$

and, for the liquid,

$$\Theta_1^*(\xi^*) = \frac{2}{\sqrt{\pi}}\left[\frac{\left(1-\frac{E_1}{\lambda}\right)e^{\frac{E_0^2}{\lambda}}\operatorname{ierfc}\xi^* - e^{-\xi^{*2}}\operatorname{ierfc}\left(\frac{E_0}{\lambda^{1/2}}\right)}{\operatorname{erfc}\left(\frac{E_0}{\lambda^{1/2}}\right)\cdot\operatorname{ierfc}\left(\frac{E_0}{\lambda^{1/2}}\right)}\right] \tag{4.1.21}$$

Substituting these functions into the first order interface equation (2.4.10), E_1 is found to satisfy the transcendental equation

$$2\pi\beta E_1 = \frac{e^{-E_0^2}}{E_0\operatorname{erf}E_0}\left[2E_0^2 - E_1(1+2E_0^2)\right] +$$

$$-\gamma e^{-\frac{E_0^2}{\lambda}}\left(1-\frac{E_1}{\lambda}\right)\left[\frac{2E_0}{\lambda^{1/2}\operatorname{erfc}\left(\frac{E_0}{\lambda^{1/2}}\right)} - \frac{1}{\operatorname{ierfc}\left(\frac{E_0}{\lambda^{1/2}}\right)}\right] \tag{4.1.22}$$

Solving for E_1 the equation can be simplified to become,

$$E_1 =$$

$$\frac{\dfrac{2E_0 e^{-E_0^2}}{\operatorname{erf}E_0} - \gamma e^{-\frac{E_0^2}{\lambda}}\left[\dfrac{E_0}{\lambda^{1/2}}\dfrac{2}{\operatorname{erfc}\left(\frac{E_0}{\lambda^{1/2}}\right)} - \dfrac{1}{\operatorname{ierfc}\left(\frac{E_0}{\lambda^{1/2}}\right)}\right]}{2\pi\beta + \dfrac{(1+2E_0^2)}{E_0\operatorname{erf}E_0}e^{-E_0^2} - \left(\dfrac{\gamma}{\lambda}\right)e^{-\frac{E_0^2}{\lambda}}\left[\dfrac{E_0}{\lambda^{1/2}}\dfrac{2}{\operatorname{erfc}\left(\frac{E_0}{\lambda^{1/2}}\right)} - \dfrac{1}{\operatorname{ierfc}\left(\frac{E_0}{\lambda^{1/2}}\right)}\right]} \tag{4.1.23}$$

Analytical Solutions for the Cylinder

Since the general structure of the thermal field equations for the cylinder are of the same form as the corresponding equations for the sphere, then the same methods for the analytical, as well as the numerical solutions, are used. In fact, the zeroth order equations, boundary conditions and interface equation, which are identical, obviously give the same solutions. However, with increasing exponent of τ, the differences soon become apparent.

First Order Solutions

Substitution of (4.1.12) and (4.1.14) into the first order thermal equations (3.4.6) and (3.4.8) and their respective boundary conditions (3.4.7) and (3.4.9) yields, for the solid,

$$\frac{d^2\Theta_1}{d\xi^2} + 2\xi\frac{d\Theta_1}{d\xi} - 2\Theta_1 = \frac{4}{\sqrt{\pi}}\frac{e^{-\xi^2}}{\operatorname{erf} E_0} \tag{4.1.24}$$

subject to

$$\Theta_1(0) = 0$$

and

$$\left[\Theta_1 + \frac{2}{\sqrt{\pi}}E_1\frac{e^{-E_0^2}}{\operatorname{erf} E_0}\right] = 0 \tag{4.1.25}$$

and for the liquid,

$$\frac{d^2\Theta_1^*}{d\xi^{*2}} + 2\xi^*\frac{d\Theta_1^*}{d\xi^*} - 2\Theta_1^* = \frac{4}{\sqrt{\pi}}\frac{e^{-\xi^{*2}}}{\operatorname{erfc}\left(\frac{E_0}{\lambda^{1/2}}\right)} \tag{4.1.26}$$

subject to

$$\left[\Theta_1^* + \frac{2}{\sqrt{\pi}}\frac{E_1}{\lambda}\frac{e^{-\frac{E_0^2}{\lambda}}}{\operatorname{erfc}\left(\frac{E_0}{\lambda^{1/2}}\right)}\right]_{\xi^* = \frac{E_0}{\lambda^{1/2}}} = 0$$

and

$$\Theta_1^*(\infty) = 0 \tag{4.1.27}$$

The solutions of these equations are, for the solid,

$$\Theta_1(\xi) = \frac{\xi}{\operatorname{erf} E_0}\left\{ \operatorname{erfc} E_0 - \operatorname{erfc}\xi - \frac{2E_1}{\sqrt{\pi}E_0} e^{-E_0^2} \right\} \qquad (4.1.28)$$

and for the liquid,

$$\Theta_1^*(\xi^*) = \frac{1}{\sqrt{\pi}}\left\{ \frac{\left(1 - \frac{2E_1}{\lambda}\right) i\operatorname{erfc}\xi^* . e^{-\frac{E_0^2}{\lambda}} - e^{-\xi^{*2}} i\operatorname{erfc}\left(\frac{E_0}{\lambda^{1/2}}\right)}{i\operatorname{erfc}\left(\frac{E_0}{\lambda^{1/2}}\right) . \operatorname{erfc}\left(\frac{E_0}{\lambda^{1/2}}\right)} \right\} \qquad (4.1.29)$$

Substitution of these functions into the first order interface equation (3.4.10) gives the following:

$$2\beta E_1 = \frac{e^{-E_0^2}}{\sqrt{\pi}} \frac{1}{E_0 \operatorname{erf} E_0}\left[E_0^2 - E_1(1 + 2E_0^2) \right]$$

$$- \frac{\gamma e^{-\frac{E_0^2}{\lambda}}}{\sqrt{\pi}}\left(\frac{1}{2} - \frac{E_1}{\lambda}\right)\left[\frac{2E_0}{\lambda^{1/2}\operatorname{erfc}\left(\frac{E_0}{\lambda^{1/2}}\right)} - \frac{1}{i\operatorname{erfc}\left(\frac{E_0}{\lambda^{1/2}}\right)} \right] \qquad (4.1.30)$$

or, solving for E_1,

$$E_1 =$$

$$\frac{\frac{E_0 e^{-E_0^2}}{\operatorname{erf} E_0} - \frac{\gamma e^{-\frac{E_0^2}{\lambda}}}{2\sqrt{\pi}}\left[\frac{E_0\ 2}{\lambda^{1/2}\operatorname{erfc}\left(\frac{E_0}{\lambda^{1/2}}\right)} - \frac{1}{i\operatorname{erfc}\left(\frac{E_0}{\lambda^{1/2}}\right)} \right]}{2\sqrt{\pi}\beta + \frac{(1 + 2E_0^2)e^{-E_0^2}}{\sqrt{\pi}E_0 \operatorname{erf} E_0} - \frac{\gamma}{\lambda}\frac{e^{-\frac{E_0^2}{\lambda}}}{\sqrt{\pi}}\left[\frac{E_0\ 2}{\lambda^{1/2}\operatorname{erfc}\frac{E_0}{\lambda^{1/2}}} - \frac{1}{i\operatorname{erfc}\left(\frac{E_0}{\lambda^{1/2}}\right)} \right]}$$

(4.1.31)

Comparison of this equation with (4.1.23) will reveal the fact that

$$2E_1^c = E_1^s \tag{4.1.32}$$

where E_1^c and E_1^s are the values of E_1 obtained from the interface equations for the cylinder and sphere respectively.

4.2 Numerical Solutions

To simplify the computer implementation of the established equations a final change of variable is made. For the solid region, the following variable is introduced,

$$q = \frac{\xi}{E_0} \tag{4.2.1}$$

and hence the solutions are to be found over the interval $0 \leqslant q \leqslant 1$. For the liquid region, the new variable employed is,

$$q^* = \frac{\xi^*}{(E_0/\lambda^2)} - 1 \tag{4.2.2}$$

and the range of integration is $0 \leqslant q^* \leqslant \infty$. However, integrating the system of equations over the interval $[0,4]$, by the method described later, and integrating the same system over the interval $[0,6]$, it is found that there is good agreement (5 decimal places) between the two sets of results. The reason is due to the exponential decay of the solutions which can be seen from (4.1.10). Thus the value of the finite upper bound used in the calculation of the liquid equations is 5.

The systems of differential equations are now solved numerically with the aid of a computer using the Runge-Kutta-Merson method. This method is made available by the Numerical Algorithm Group (NAG) library. The reasons for using this numerical scheme are threefold and are given as follows:

(i) the method is self-starting, requiring only the initial values of

the dependent variables;

(ii) the evaluation of the truncation error enables the step width to be made as large as possible, or adjusts it automatically as the solution proceeds with the aim of keeping the error within a predetermined tolerance at each step;

(iii) the estimate of this truncation error is asymptotically correct for linear equations.

With regard to the first reason, it should be noted that the systems of equations which have been derived are all boundary value problems and not, as this method requires, initial value problems. To alleviate this problem the method of complementary functions is employed (see appendix B) which transforms these systems of equations into initial value problems.

Calculation of E_n

To determine the value of the n^{th} order perturbation function E_n an iterative procedure is used. Firstly, the system of n second order differential equations for the solid and liquid regions, which can be written in the general form

$$\frac{d^2\Theta_i}{dx^2} = f_i\left(x, \Theta_0, \frac{d\Theta_0}{dx}, \ldots, \Theta_n, \frac{d\Theta_n}{dx}\right) \qquad i = 0,1,\ldots,n \qquad (4.2.3)$$

are rewritten as the 2n first order differential system,

$$\frac{dy_{i1}}{dx} = y_{i2}$$

$$\frac{dy_{i2}}{dx} = f_i(x, y_{02}, y_{12}, \ldots, y_{i1}, y_{i2}) \qquad (4.2.4)$$

where y_{ij} is defined as

$$y_{i1} = \Theta_i \qquad \text{and} \qquad y_{i2} = \frac{dy_{i1}}{dx} \tag{4.2.5}$$

The independent variable is either q or q*, depending on which region is being considered. A similar method is used for solving the fourth order differential equation governing the flow field functions.

An initial estimate $E_n^{(o)}$ is made for E_n and is used to solve the solid and liquid equations by the method described earlier. The results obtained from these equations, namely $\frac{d\Theta_i}{dq}$ and $\frac{d\Theta_i^*}{dq^*}$, are substituted into the corresponding interface equation which can be written in the form,

$$E_n = Q_n(E_n) \tag{4.2.6}$$

and the following function is calculated,

$$\Phi_n(E_n^{(o)}) = E_n^{(o)} - Q_n(E_n^{(o)}) \tag{4.2.7}$$

where $\Phi_n(E^x) = 0$, E^x being the exact value of E_n.

The solid and liquid equations are then integrated again but the value of E_n is now $\varepsilon E_n^{(o)}$, where $0 < \varepsilon < 1$. The function

$$\Phi_n(\varepsilon E_n^{(o)}) = \varepsilon E_n^{(o)} - Q_n(\varepsilon E_n^{(o)}) \tag{4.2.8}$$

is calculated and the new value of E_n is obtained from

$$E_n^{(1)} = E_n^{(o)} \left\{ \frac{\varepsilon \Phi_n(E_n^{(o)}) - \Phi_n(\varepsilon E_n^{(o)})}{\Phi_n(E_n^{(o)}) - \Phi_n(\varepsilon E_n^{(o)})} \right\} \tag{4.2.9}$$

This scheme is terminated at the m^{th} iteration by predetermined tolerances which are imposed on

$$\left| \Phi_n(\varepsilon E_n^{(m)}) - \Phi_n(E_n^{(m)}) \right| \tag{4.2.10}$$

and

$$\left| E_n^{(m+1)} - E_n^{(m)} \right| \tag{4.2.11}$$

4.3 Comparison of Solutions

In order to compare the numerical solutions obtained by the method described in section 4.2 with the analytical solutions obtained from section 4.1, the case when $\gamma = 0.1$, $\beta = 3.0$, $\lambda = 0.1$, Ra = 8000 and Pr = 13.4 is investigated. Using an iterative procedure on (4.1.15) and the subsequent result for E_o in (4.1.23), it is found that the analytical solution for the sphere gives,

$$E_o = 0.328791$$

and

$$E_1 = 0.084834$$

On the other hand, solving the thermal field and interface equations numerically, it is calculated that (where $|E_n^{(m+1)} - E_n^{(m)}| \leq 10^{-6}$)

$$E_o = 0.328790$$

and

$$E_1 = 0.084834$$

Obviously the agreement between these two sets of results is extremely good and, from (4.1.32) it can be seen that similar agreement would be obtained for the cylinder.

4.4 Results and Discussion

The numerical results for the depth of solidification and the temperature and velocity distributions can now be computed as a function of the dimensionless parameters γ, β, λ, Ra and Pr for a specified liquid. Because of the assumptions made in the formulation of the model, some care must be exercised in interpreting these results. For instance, in the case of water if the initial temperature is above the inversion temperature the actual natural convective flow will be quite different from that predicted by the present model. The numerical study by

Watson [28] on the natural convective motion of water in a rectangular enclosure shows how a flaw lies with the Boussinesq approximation. When this approximation is invoked, see pages 20 and 56, it greatly simplifies the analysis but, unfortunately, variations in fluid properties cannot, in reality, always be neglected. Watson cites, for example, how the viscosity of water varies by about 35% over the temperature range 0 to 10°C, whilst the maximum density occurs at 3.98°C.

Another complication which arises as a direct result of ignoring the density changes is, of course, the change of volume. As solidification occurs the volume of the solidified region can, in the case of steel, contract and create a small gap, or void, between the solid region and the surface of the container. A thermal resistance is thus introduced between the surface and solid and this can affect the rest of the solidification process. Also, depending on the width of the shrinkage gap and the level of the temperature, the heat transfer across this gap can be by a combination of radiation and conduction or, alternatively by radiation and convection. In other words, the condition of constant temperature which is normally applied must be replaced by one of radiative heat transfer.

Alternatively, in the case of water, the volume can expand on solidification and thus creates extra stress within the container, particularly in a radial direction. Consider, for example, water in a copper pipe; as the temperature drops and the water freezes and expands, the radial stress against the pipe wall increases the pressure within the ice and thus lowers the melting point.

The shrinkage or expansion of a substance on solidification can be an important factor in the design of moulds. The structure of ingot moulds for the British Steel Corporation and the shape of ice-lolly

moulds in the frozen food industry are two of many examples.

Due to the similarities of the geometries of the sphere and cylinder, it is probably more instructive to give the numerical results obtained from their respective analyses in the same results section. In both cases it will be seen from the subsequent results that the shape of the solidification front is as predicted in section 1.3. That is, in general, the natural convective flow rises in the form of a jet along the axis from the south pole ($\theta = \pi$) to the north pole ($\theta = 0$) and forms a forward stagnation point at the north pole. The flow then returns downwards (symmetrically about this axis) bathing the inside of the solidification front. These down flows collide to give a (backward) stagnation point at the south pole. As the volume of liquid decreases and loses its sensible heat, the density differences increase leading to increased natural convective velocities. This form of 'spin-up' in the early part of the solidification process initiates the formation of a cusp at the lower pole. As the solidification and natural convective processes evolve, the temperature of the liquid will approach the fusion temperature and the circulation in the liquid will cease.

For selecting values for the dimensionless parameters to be used in the numerical computation, data is obtained for the metal and alloy systems, see Chiesa and Guthrie [26] and for latent heat thermal storage systems, see Sparrow et al. [13]. The latter system is examined first and, as an illustration, the values that the parameters take are as follows: $\gamma = 0.1$, $\beta = 3$, $\lambda = 0.1$, Ra = 8000 and Pr = 13.4.

Interfacial Positions

The depth of solidification at any time τ is given by

$$E(\mu,\tau) = 2\tau^{1/2}\left[E_0 + \tau^{1/2}E_1 + \tau E_2 + \tau^{3/2}E_3 + \tau^2 E_4 + \tau^{5/2}E_5 + \cdots\right]$$

And so, substituting the separable variables (2.4.32) and (2.4.54) for E_4 and E_5 respectively, it is readily seen that the position of the interface can be written as:

$$R(\mu,\tau) = 1 - E(\mu,\tau)$$

or

$$R(\mu,\tau) = a(\tau) + \mu\, b(\tau)$$

where

$$a(\tau) = 1 - 2\tau^{1/2}(E_0 + \tau^{1/2}E_1 + \tau E_2 + \tau^{3/2}E_3 + \tau^2\bar{E}_4 + \tau^{5/2}\bar{E}_5 + \cdots)$$

and

$$b(\tau) = 2\tau^{1/2}(\tau^2\bar{\bar{E}}_4 + \tau^{5/2}\bar{\bar{E}}_5 + \cdots)$$

The equation for $R(\mu,\tau)$ is the equation for the limacon of Pascal and obviously the present analysis becomes invalid for times when $b(\tau) \leq a(\tau)$. When this condition does occur the cusp will be located above the centre of the container; when $b(\tau) = a(\tau)$ the shape of the interface is a cardioid.

Figure 2 displays the position of the transient interface for the sphere. Initially the interface is located at the surface and its position is shown at (dimensionless) time intervals of 0.1 until the (formal) small time expansions break down. In this case, this occurs at approximately $\tau = 0.8$ when the cusp reaches the neighbourhood of the centre. During the early stages of the solidification process the interface is symmetrical since the heat transfer is dominated by conduction. As the natural convective motion increases the interface moves towards the centre at a slightly faster rate at the south pole than at the north pole. Thus the shape of the interface is deformed into the aforementioned limacon of Pascal with the cusp forming at the south pole.

Volume of Liquid

It is interesting to compute the volume of liquid remaining in the container at any time during the solidification process. Since the changes in density have been ignored except in the calculation of the buoyancy force, the volume of liquid in the sphere is,

$$V_{\ell}(\tau) = -2\pi a^3 \int_{+1}^{\mu=1} \int_{0}^{R=1-\xi(\mu,\tau)} R^2 \, dR \, d\mu$$

The graph in figure 3 displays the volume of liquid remaining in the sphere for the present case. The broken line in this graph is the volume remaining when the convection, and its effects, are ignored. The results obtained from this graph show very good agreement with those obtained from the analytical solution of Stewartson and Waechter [8] and the numerical solution of Tao [4]. It can also be seen from this graph that the natural convective motion of the liquid slows down the solidification process. This is not surprising since the convection is governed, in part, by the initial temperature of the liquid; the higher this temperature is, the greater the convective effects.

Streamlines and Velocity Distributions

The stream function can be calculated as a function of the (physical) dimensionless variables R and Θ for any time τ. Curves of constant Ψ are then obtained by interpolation to yield the streamlines for the natural convective motion. Figure 4 displays the curves when Ψ = 0.1, 0.7, 1.3 and 2.0 at τ = 0.1; the smaller magnitude of Ψ being the outer streamline.

The dimensionless velocities of the liquid are also given in this

diagram. Since the shape of the interface is initially symmetrical, the magnitude of the velocities is also symmetrical. The direction of these velocities is as described earlier, with the velocity reaching a maximum at the centre of the sphere. As the central column of the flow reaches the north pole its velocity decreases. It then flows down the inside of the solidification front and its velocity increases as it nears $\Theta = \frac{\pi}{2}$.

A later stage in the solidification process is given in figure 5. The streamlines shown in this diagram are $\Psi = 0.1, 0.7$ and 1.5. Although the velocities shown in this diagram appear to be symmetrical, the velocity at the south pole is in fact greater than that at the north pole; this is because of the non-symmetrical shape of the interface due to convection. It can also be seen from this diagram that the effect of thermal 'spin-up' has increased the magnitudes of the velocities, leading to a greater degree of non-uniform heat transfer at the interface.

Temperature Distribution

The dimensionless temperature distribution along the radius is given in figure 6 for the solid and liquid regions. The two diagrams given describe the distributions at the times $\tau = 0.1$ and $\tau = 0.4$ and at various polar angles $\Theta = 0, \frac{\pi}{2}$ and π; the broken lines indicate the position of the interface at these various angles. Clearly in the early stages of solidification, the temperature profiles are symmetrical. However, as time proceeds these profiles vary between the poles and, in particular, in the regions adjacent to the interface. This variation is more noticeable in the solid region. Also it should be noted that there is a drop in the dimensionless liquid temperature, as expected, below the initial temperature at the centre of the circle when $\tau = 0.4$.

Heat Transfer

The dimensionless Nusselt numbers $Nu = \frac{\partial T}{\partial n}\frac{a}{(T-T_R)}$ at the solid and liquid interface and also at the surface of the sphere are displayed in figure 7; n measures the outward normal to a surface; in the liquid $T = T_l$, $T_R = T_F$ and in the solid $T = T_F$ and $T_R = T_o$. For both of the phases the Nusselt numbers are given at the polar angles $\theta = 0, \frac{\pi}{2}$ and π.

Initially there is very little convection and the heat transfer between the two phases is dominated by conduction. As time passes, and the convection becomes more prominent, there is a marked variation with θ of the heat transfer from the liquid to the interface. There is less transfer of heat at the south pole than the north; at $\theta = 0$ there appears to be a minimum and then the heat transfer increases as the final time of solidification is approached. The variation in the heat transfer with polar angle θ from the interface to the solid and from the solid to the surface is seen to be very small.

Cylinder

The results and the diagrams obtained for the effects of natural convection during solidification in a cylinder are very similar to those obtained for the sphere. Due to the differences in geometric shape, the effect of the convection is not so apparent. For example, the shape of the solidification fronts in figure 8, although limacons of Pascal, do not have such a noticeable cusp forming at the south pole compared with the fronts at corresponding times in figure 2. This means that, in this case, the analysis does not break down until τ is approximately 1.1.

Figure 9 gives the volume of the liquid remaining at any time with and without the convective effects. This volume is given by,

$$V_{ol}(\tau) = -2a^2 \int_{+1}^{\mu=-1} \int_{0}^{R=1-\epsilon(\mu,\tau)} R(1-\mu^2)^{-\frac{1}{2}} dR d\mu$$

Once again the results obtained from the broken line show good agreement with other works which ignore convection.

The streamlines and velocity distributions for the dimensionless times $\tau = 0.1$ and $\tau = 0.4$ are given in figures 10 and 11 respectively. The curves of constant $\bar{\Psi}$ are obtained for the same values as used in the sphere. It can be seen that whilst smaller values of $\bar{\Psi}$ appear to give similar streamlines, larger values give streamlines closer to the centre for the sphere than for the cylinder. The velocities in the cylinder are smaller than those in the sphere. Although near to the interface this does not seem apparent, it should be noted that the velocities in both diagrams are not necessarily given at the same positions for the same times. The thermal spin-up is again seen to occur as the solidification proceeds.

The diagrams in figure 12 showing the temperature distributions are very much the same as the corresponding diagrams in figure 6. However, at time $\tau = 0.4$ the variations in the distributions, particularly in the solid region, are less pronounced at the different polar angles. Of course, the position of the solidification front is not as far advanced in the case of the cylinder and this should be remembered when comparing these results with the sphere. The drop in the liquid temperature at the centre of the cylinder is also less pronounced than that in the sphere.

The graph of the dimensionless Nusselt number against time is given in figure 13. Comparing the diagram with figure 7, it can be seen that the heat transfer coefficients at the surface of the containers and at the interface in the solid region are similar. However, at the interface

in the liquid region the variations between the poles are less for the cylinder than for the sphere.

Another set of results has been computed from data which was used by Chiesa and Guthrie [26]. The solidification of lead in a sphere and a cylinder is studied, where

$C_p = 161$ $\qquad$ $L = 23340$

$\nu = 2.28 \times 10^{-7}$ $\qquad$ $\alpha = 1.14 \times 10^{-4}$

$k = 9.5 \times 10^{-6}$ $\qquad$ $k^* = 24.3 \times 10^{-6}$

The fusion temperature T_F of lead is 327.3°C. The diameter of the container to be examined is 26mm and it is assumed that the initial temperature T_1 of the liquid lead is 335°C and the reduced temperature T_o is 300°C. Hence, the dimensionless parameters are,

$\gamma = 0.5$, $\beta = 5.3$, $\lambda = 0.39$, Ra = 8717 and Pr = 0.02

It is,perhaps, of more interest to present some of the results in dimensional terms although, for simplicity, the graphs are displayed with non-dimensional variables.

The shape of the solidification fronts for the sphere and the cylinder are seen in figures 14 and 20 respectively. In both cases the fronts are given at time intervals of 1.78 seconds up to a final time (the time at which this analysis breaks down) of 16 seconds for the sphere and 17.8 seconds for,the cylinder.

The volume of liquid remaining in either container is given as a function of time in figures 15 and 21.

The streamlines and velocity distributions are displayed in figures 16 and 17 for the sphere and figures 22 and 23 for the cylinder. These results are given at times 1.78 seconds and 7.12 seconds and the velocities are given in metres/second.

The temperature distributions are probably the most interesting of the set of results. Figure 18 displays these distributions for the sphere at times 1.78 seconds and 7.12 seconds; figure 24 displays the distributions for the cylinder. In both of these figures it is seen that there is a considerable reduction in the temperature of the liquid after 7.12 seconds. At this time the depth of solidification in the sphere is 4.8mm and 5.5mm at $\Theta = 0$ and $\frac{\pi}{2}$ respectively and the temperature at the centre is 329.8°C, only 2.5°C above the fusion temperature. At the same time in the cylinder, the depth of solidification varies between 4.4mm at the north pole and 4.8mm at the south pole; the temperature at the centre is 332.3°C, slightly higher than the temperature in the sphere. Although the analysis breaks down for both geometries before total solidification, it is seen from the graphs that the temperature of the liquid would soon approach the fusion temperature and the circulation of the liquid in the container would cease.

Figures 19 and 25 show the dimensionless heat transfer coefficients for the sphere and cylinder.

The depth of solidification is now studied for various values of the parameters γ, β and Ra. Before these are given it should be remembered that for any specified liquid these parameters depend on the values taken by T_o, T_1 and T_F, the ambient, initial and fusion temperatures. Although these parameters are interrelated, the computation of the depth of solidification is still made, for while the actual values of the parameters may not relate to any particular liquid, the size or order may do so.

Table 1 displays the depth of solidification for the sphere with the values $\gamma = 0.1$, $\beta = 5.0$, $\lambda = 0.1$, Ra = 8000 and Pr = 13.4 at angular intervals of 30° over the dimensionless time 0.1(0.1)1.0 .

The solidification depth is also given when $T_1 = T_F$ and there is no convection. Hence the Rayleigh number Ra is zero and so too is the thermal head θ. Table 2 displays similar results for the cylinder.

Tables 3 and 4 give the solidification depths for the sphere and cylinder for various values of the parameters as time passes until $\tau = 1.0$ or the analysis breaks down. From these results it is seen that the speed of the moving solidification front increases for small Stefan number. The effect of convection on the solidification process is greatly influenced by the size of the initial Rayleigh number. This is to be expected since Ra gives a measure of the buoyancy force which drives the convective motion. Thus the larger this number, the more noticeable the effect of convection becomes, leading to a greater deformation in the front.

In conclusion, it is worth mentioning that the British Steel Corporation has shown interest in the results obtained from this work. This interest arises in connection with the solidification of steel ingots, a study of which has been made by Schulze [24]. Due to the complications described in chapter 1, this study neglected the effects of convection. It is hoped that the analysis and results obtained from this present work will be useful and help to improve our understanding of the effects of natural convection during such solidification processes.

ANGLE/TIME	0.1	0.2	0.3	0.4	0.5	0.6	0.7	0.8	0.9	1.0
0	0.18590	0.27177	0.34093	0.40069	0.45355	0.50059	0.54227	0.57873	0.60996	0.63582
30	0.18594	0.27205	0.34174	0.40241	0.45668	0.50568	0.54997	0.58975	0.62509	0.65595
60	0.18607	0.27281	0.34394	0.40713	0.46522	0.51959	0.57099	0.61986	0.66646	0.71095
90	0.18624	0.27385	0.34696	0.41357	0.47689	0.53858	0.59971	0.66099	0.72298	0.78607
120	0.18641	0.27488	0.34996	0.42002	0.48856	0.55758	0.62842	0.70211	0.77947	0.86120
150	0.18653	0.27564	0.35216	0.42474	0.49710	0.57148	0.64947	0.73222	0.82083	0.91620
180	0.18658	0.27592	0.35297	0.42647	0.50023	0.57657	0.65714	0.74324	0.83597	0.93633
γ = Ra = 0	0.20783	0.30471	0.38524	0.45843	0.52787	0.59444	0.66236	0.72942	0.79726	0.86636

Table 1. Depth of Solidification for the Sphere when $\gamma = 0.1$, $\beta = 5.0$, $\lambda = 0.1$, Ra = 8000 and Pr = 13.4

ANGLE/TIME	0.1	0.2	0.3	0.4	0.5	0.6	0.7	0.8	0.9	1.0
0	0.17897	0.25711	0.31827	0.37010	0.41537	0.45538	0.49079	0.52197	0.54907	0.57216
30	0.17899	0.25725	0.31867	0.37096	0.41693	0.45791	0.49463	0.52746	0.55661	0.58219
60	0.17905	0.25763	0.31977	0.37331	0.42119	0.46484	0.50510	0.54246	0.57721	0.60958
90	0.17914	0.25814	0.32128	0.37653	0.42700	0.47431	0.51941	0.56294	0.60536	0.64700
120	0.17922	0.25866	0.32278	0.37974	0.43282	0.48378	0.53372	0.58343	0.63351	0.68442
150	0.17928	0.25904	0.32388	0.38209	0.43708	0.49071	0.54420	0.59843	0.65412	0.71182
180	0.17931	0.25918	0.32428	0.38295	0.43864	0.49324	0.54803	0.60392	0.66166	0.72184
γ = Ra = 0	0.20056	0.28855	0.35864	0.41984	0.47563	0.52782	0.57750	0.62537	0.67195	0.71762

Table 2. Depth of Solidification for the Cylinder when $\gamma = 0.1$, $\beta = 5.0$, $\lambda = 0.1$, Ra = 8000 and Pr = 13.4

γ	β	Ra	θ	0.1	0.2	0.3	0.4	0.5	0.6	0.7	0.8	0.9	1.0
0.0		0		0.20782	0.30471	0.38524	0.45843	0.52787	0.59544	0.66236	0.72942	0.79726	0.86636
		80	0	0.18623	0.27383	0.34689	0.41344	0.47666	0.53820	0.59913	0.66016	0.72183	0.78457
			180	0.18624	0.27387	0.34701	0.41370	0.47712	0.53896	0.60028	0.66181	0.72409	0.78758
	5.0	800	0	0.18620	0.27364	0.34635	0.41228	0.47456	0.53479	0.58396	0.65276	0.71166	0.77105
			180	0.18627	0.27405	0.34755	0.41486	0.47922	0.54238	0.60545	0.66921	0.73427	0.80120
0.1			0	0.18590	0.27177	0.34093	0.40068	0.54355	0.50059	0.54227	0.57873	0.60996	0.63582
			180	0.18658	0.27592	0.35297	0.42647	0.50023	0.57657	0.65714	0.74324	0.83597	0.93633
	10.0		0	0.13670	0.19762	0.24551	0.28597	0.32098	0.35138	0.37759	0.39975	0.41792	0.43203
			180	0.13710	0.20001	0.25242	0.30071	0.34755	0.39449	0.44258	0.49259	0.54519	0.60090
	3.0	8000	0	0.22825	0.33734	0.42756	0.50771	0.58086	0.64834	0.71075	0.76832		
			180	0.22918	0.34302	0.44408	0.54317	0.64518	0.75318	0.86946	0.99588		
0.5			0	0.13256	0.19071	0.23061	0.25530	0.26462					
			180	0.13511	0.20616	0.27534	0.35087	0.43735					
1.0	5.0		0	0.09866	0.13933	0.16147	0.16570						
			180	0.10216	0.16053	0.22283	0.29675						

Table 3. Depth of Solidification for the Sphere for Various Values of the Parameters γ, β, Ra as a Function of Time when $\lambda = 0.1$ and $Pr = 13.4$

γ	β	Ra	Θ	0.1	0.2	0.3	0.4	0.5	0.6	0.7	0.8	0.9	1.0
0.0		0		0.20056	0.28855	0.35864	0.41984	0.47563	0.52782	0.57750	0.62537	0.67195	0.71762
		80	0	0.17914	0.25813	0.32125	0.37646	0.42689	0.47412	0.51912	0.56254	0.60480	0.64625
			180	0.17914	0.25815	0.32131	0.37660	0.42712	0.47450	0.51970	0.56335	0.60593	0.64775
	5.0	800	0	0.17912	0.25804	0.32097	0.37588	0.42584	0.47242	0.51655	0.55885	0.59973	0.63952
			180	0.17915	0.25825	0.32158	0.37717	0.42817	0.47620	0.52227	0.56704	0.61099	0.65449
0.1			0	0.17897	0.25711	0.31827	0.37010	0.41537	0.45538	0.49079	0.52197	0.54907	0.57216
			180	0.17931	0.25918	0.32428	0.38295	0.43864	0.49324	0.54803	0.60392	0.66166	0.72184
	10.0		0	0.13303	0.19012	0.23437	0.27157	0.30387	0.33229	0.35738	0.37944	0.39865	0.41509
			180	0.13323	0.19132	0.13787	0.27896	0.31720	0.35392	0.38999	0.42604	0.46253	0.49986
	3.0	8000	0	0.21771	0.31437	0.39096	0.45666	0.51479	0.56691	0.61379	0.65586	0.69330	0.72619
			180	0.21818	0.31721	0.39923	0.47441	0.54699	0.61939	0.69326	0.76980	0.85001	0.93475
0.5			0	0.12684	0.18070	0.21939	0.24725	0.26531	0.27358				
			180	0.12811	0.18837	0.24158	0.29463	0.35087	0.41253				
1.0	5.0		0	0.09399	0.13259	0.15754	0.17126	0.17379					
			180	0.09572	0.14304	0.18771	0.32557	0.28980					

Table 4. Depth of Solidification for the Cylinder for Various Values of the Parameters γ, β, Ra as a Function of Time when $\lambda = 0.1$ and Pr = 13.4

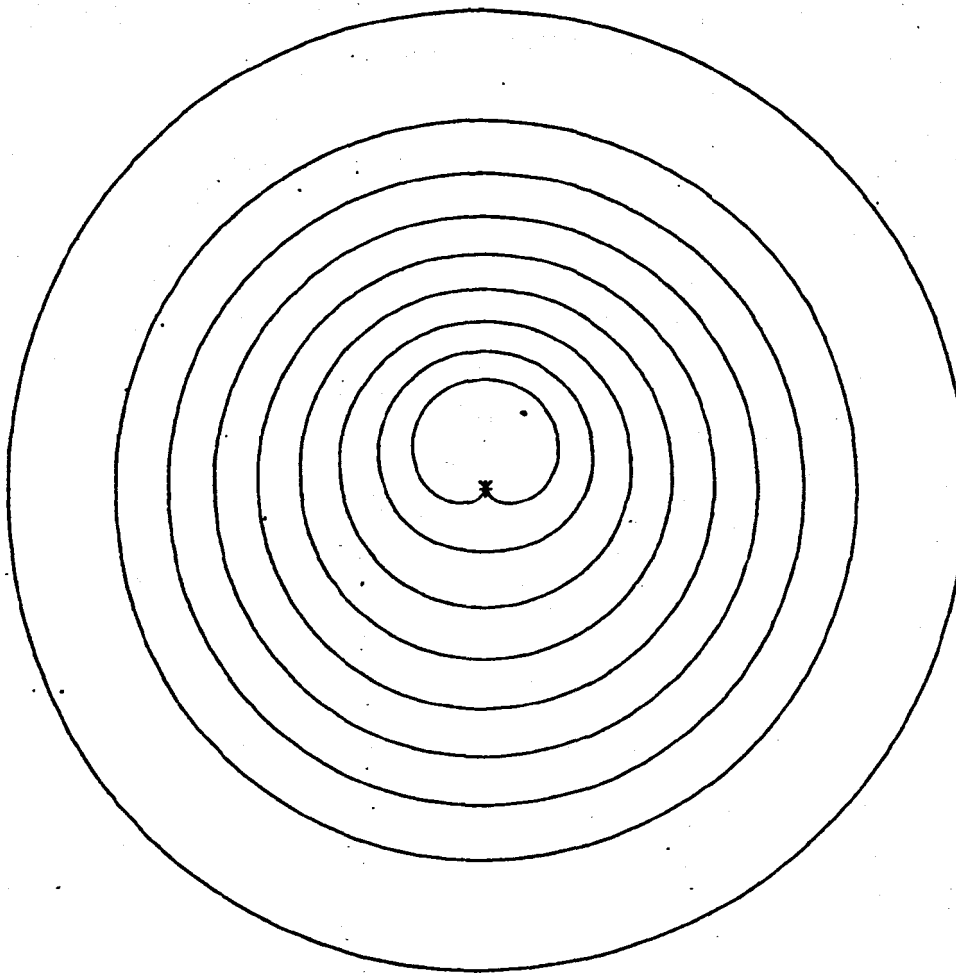

Figure 2. Interfacial Positions for the Sphere

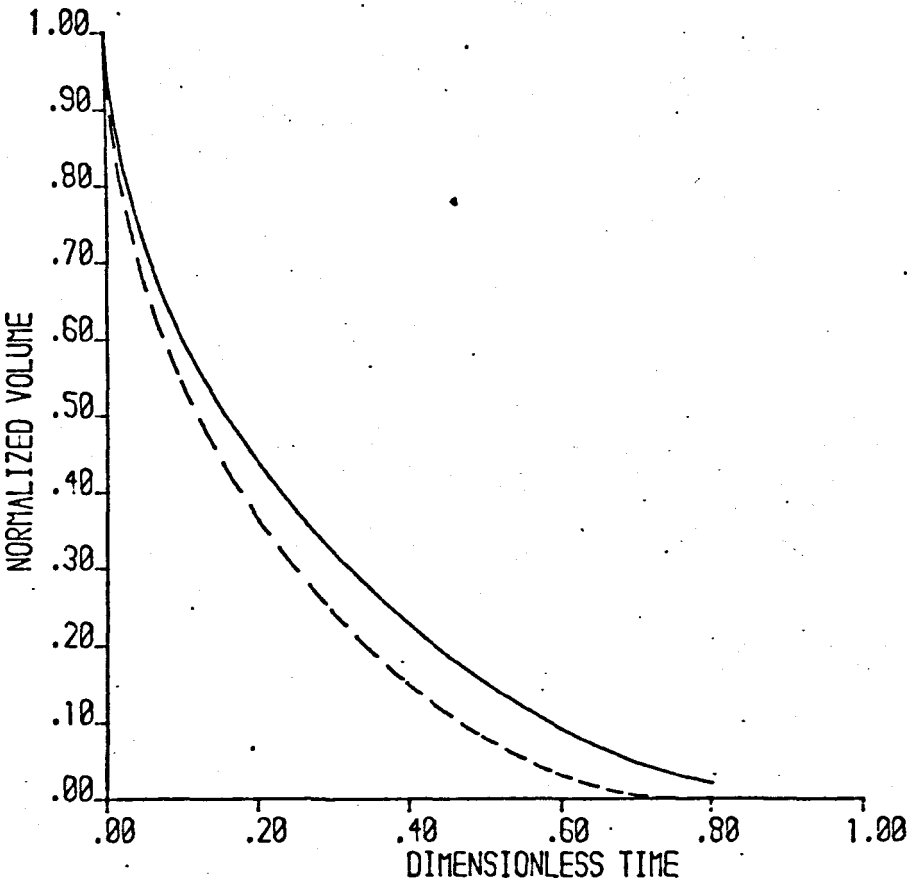

Figure 3. Volume of Liquid remaining in the Sphere

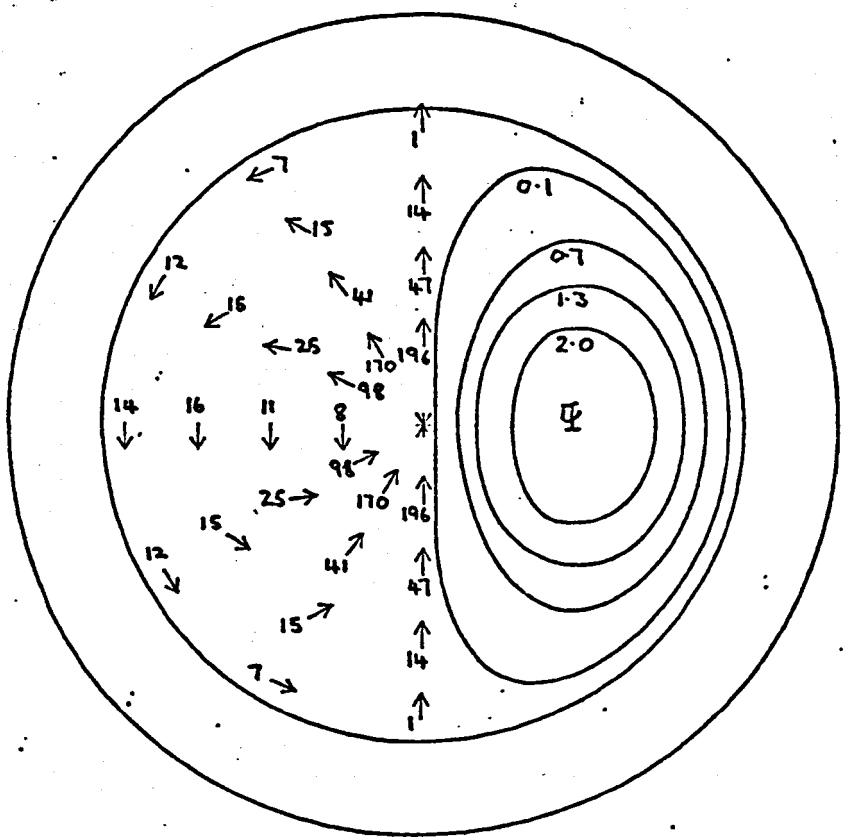

Figure 4. Streamlines and Dimensionless Velocity Vector for the Sphere at $\tau = 0.1$

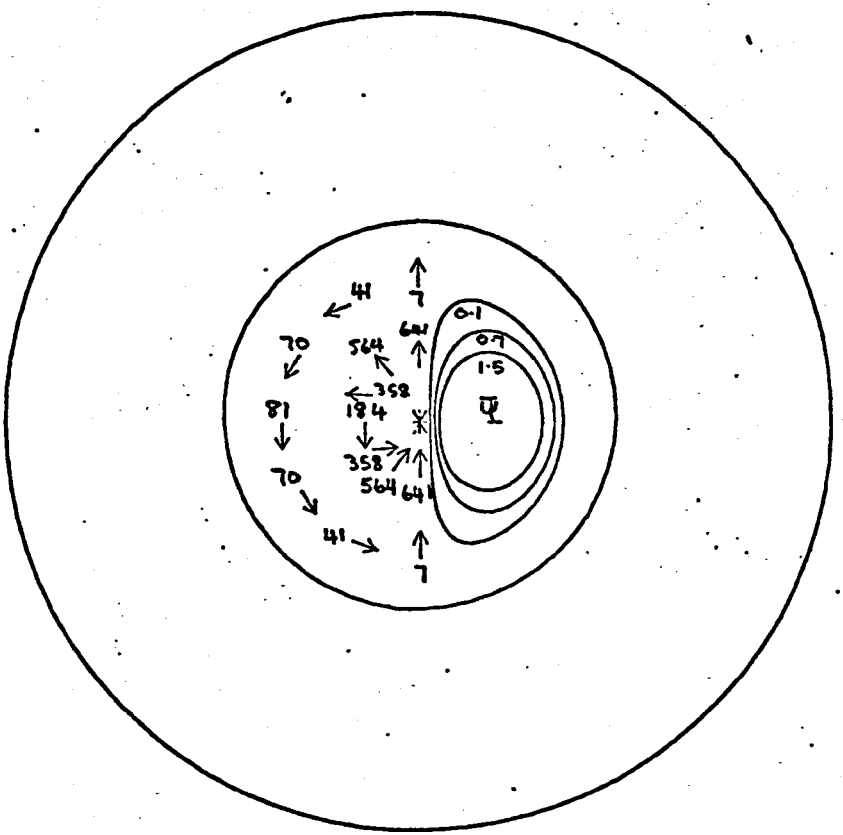

Figure 5. Streamlines and Dimensionless Velocity Vector for the Sphere at $\tau = 0.4$

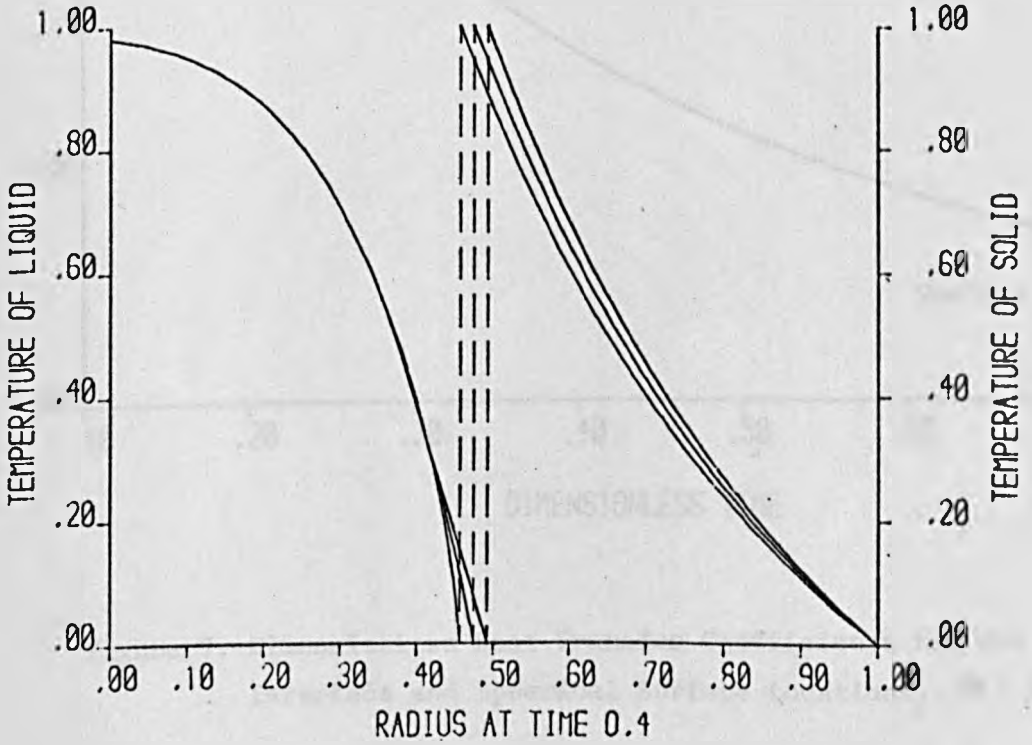

Figure 6. Temperature Distributions for the Sphere

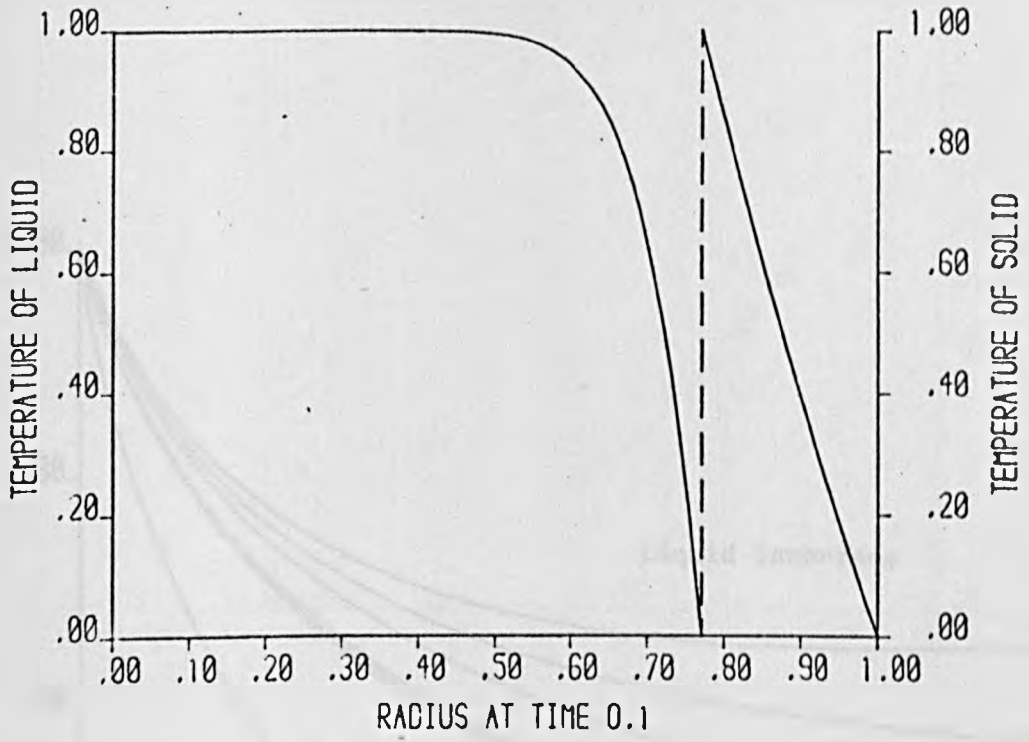
1.00
.80
.60
.40
.20
.00
TEMPERATURE OF LIQUID
1.00
.80
.60
.40
.20
.00
TEMPERATURE OF SOLID
.00 .10 .20 .30 .40 .50 .60 .70 .80 .90 1.00
RADIUS AT TIME 0.1

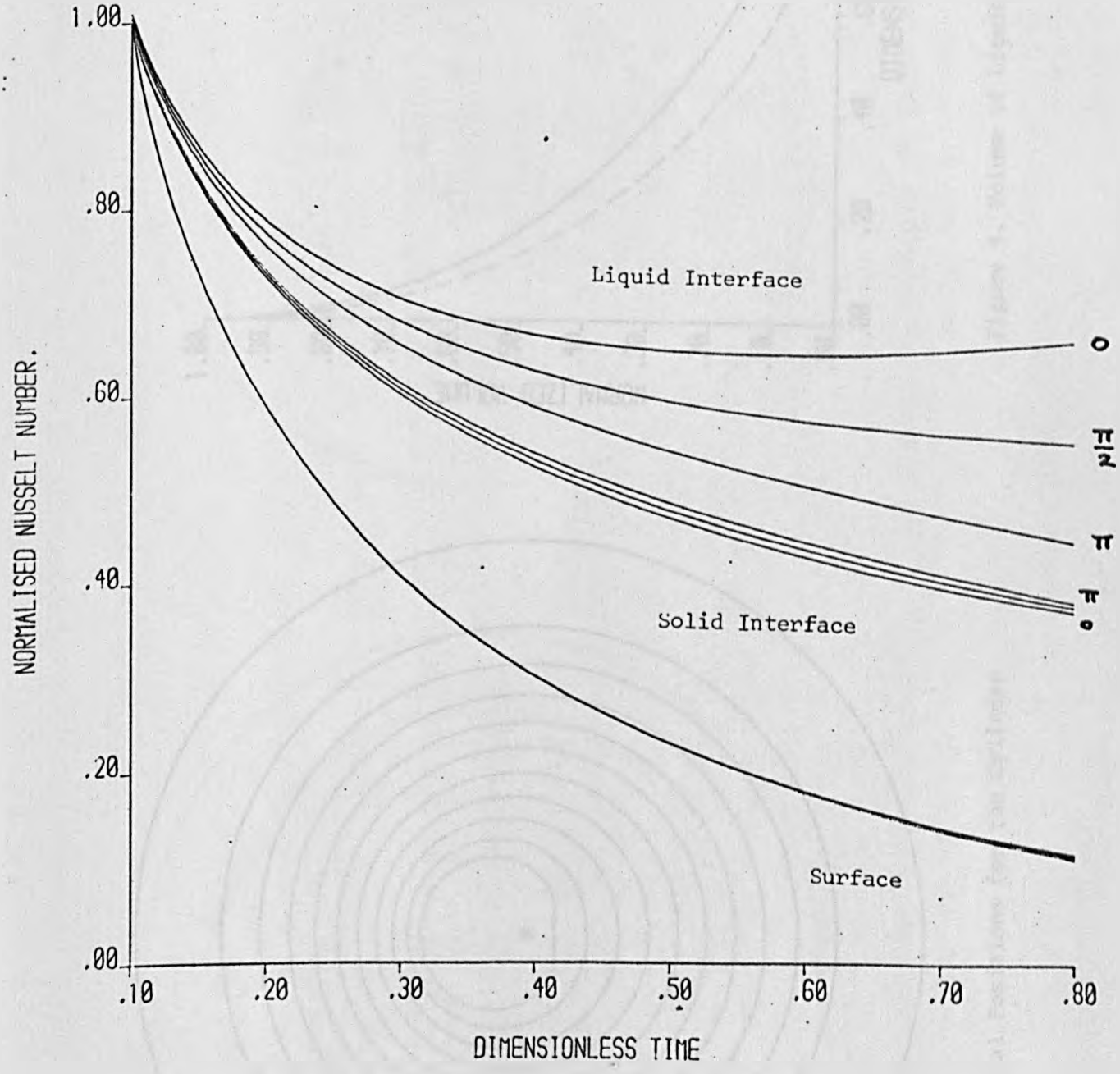

Figure 7. Dimensionless Heat Transfer Coefficients for the Sphere at the Interface and Spherical Surface Locations, $\Theta = 0, \frac{\pi}{2}$ and π

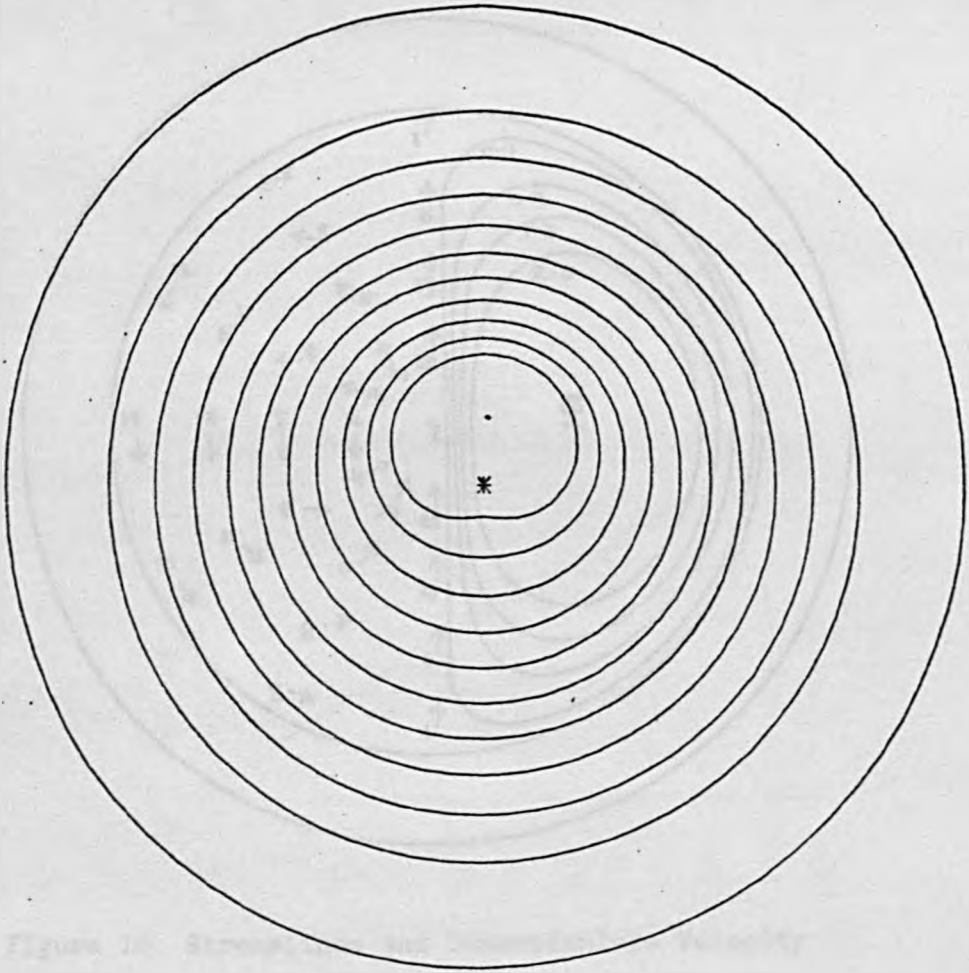

Figure 8. Interfacial Positions for the Cylinder

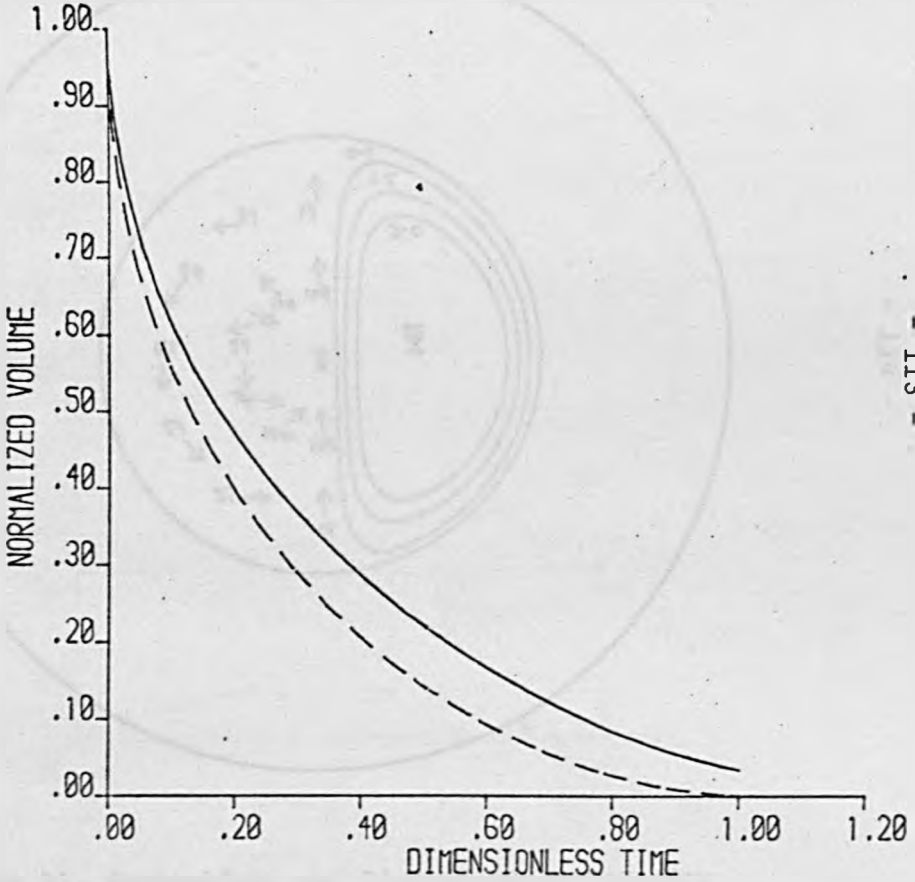

Figure 9. Volume of Liquid remaining in the Cylinder

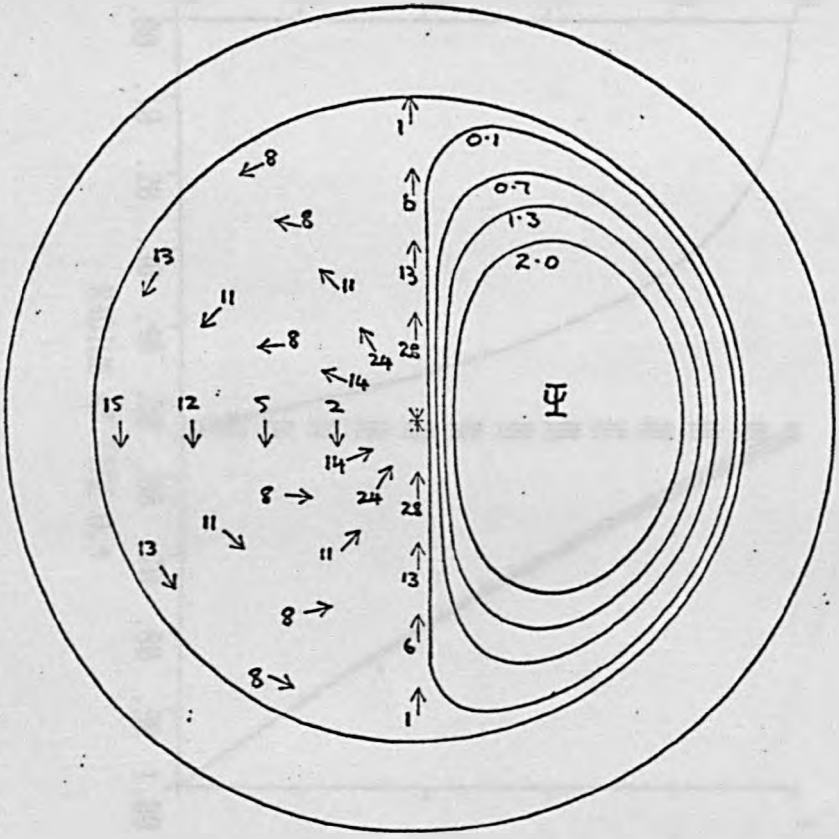

Figure 10. Streamlines and Dimensionless Velocity Vector for the Cylinder at $\tau = 0.1$

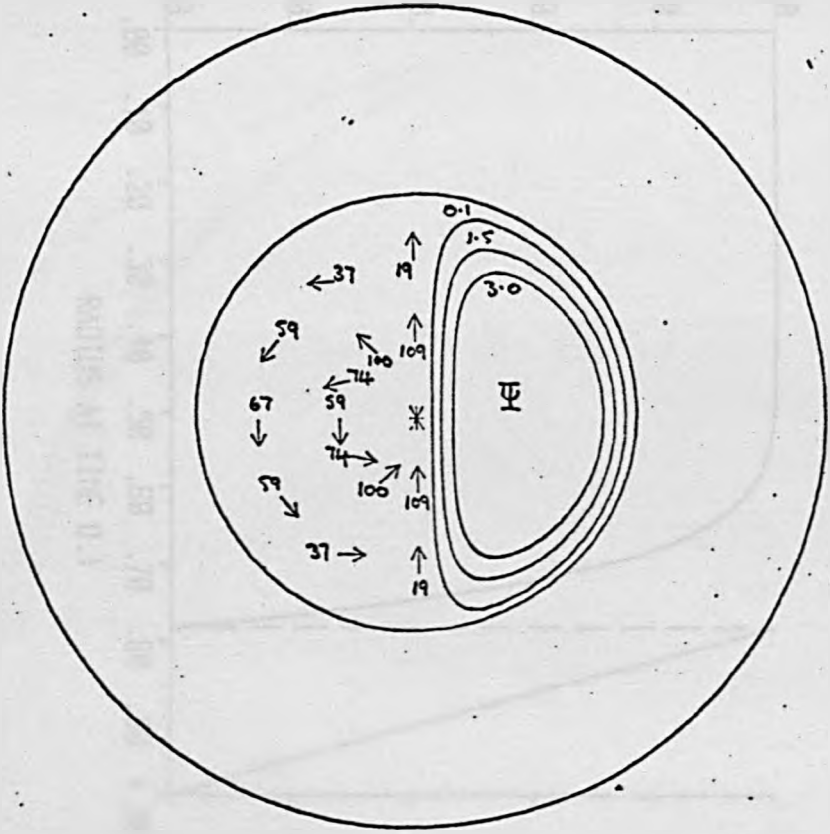

Figure 11. Streamlines and Dimensionless Velocity Vector for the Cylinder at $\tau = 0.4$

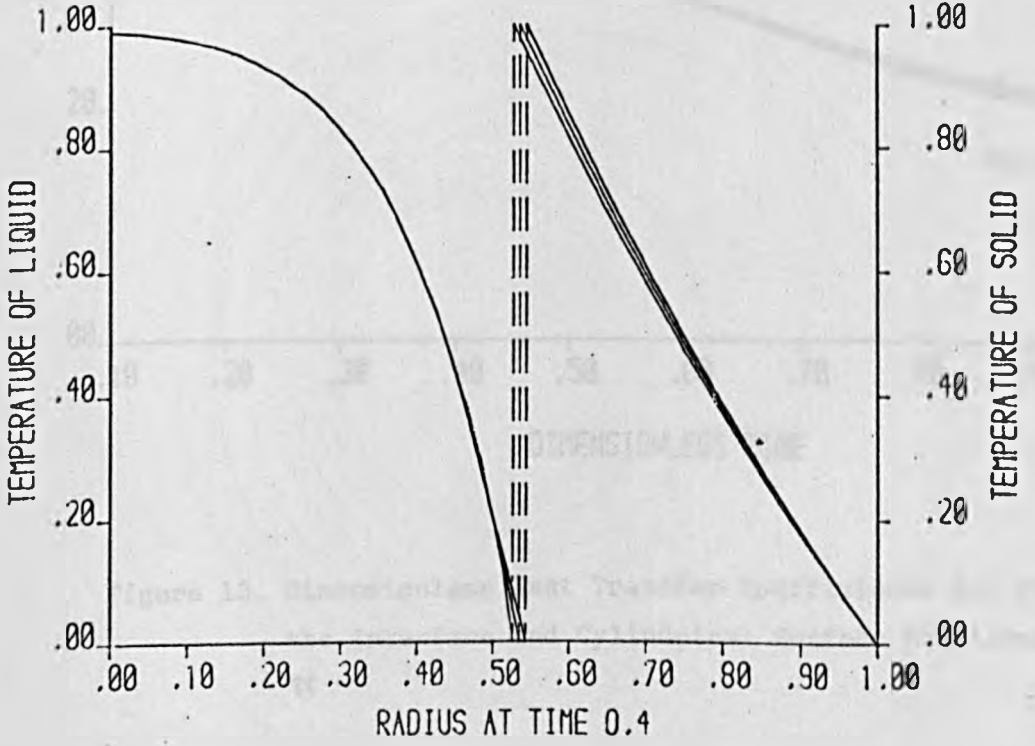

Figure 12. Temperature Distributions for the Cylinder

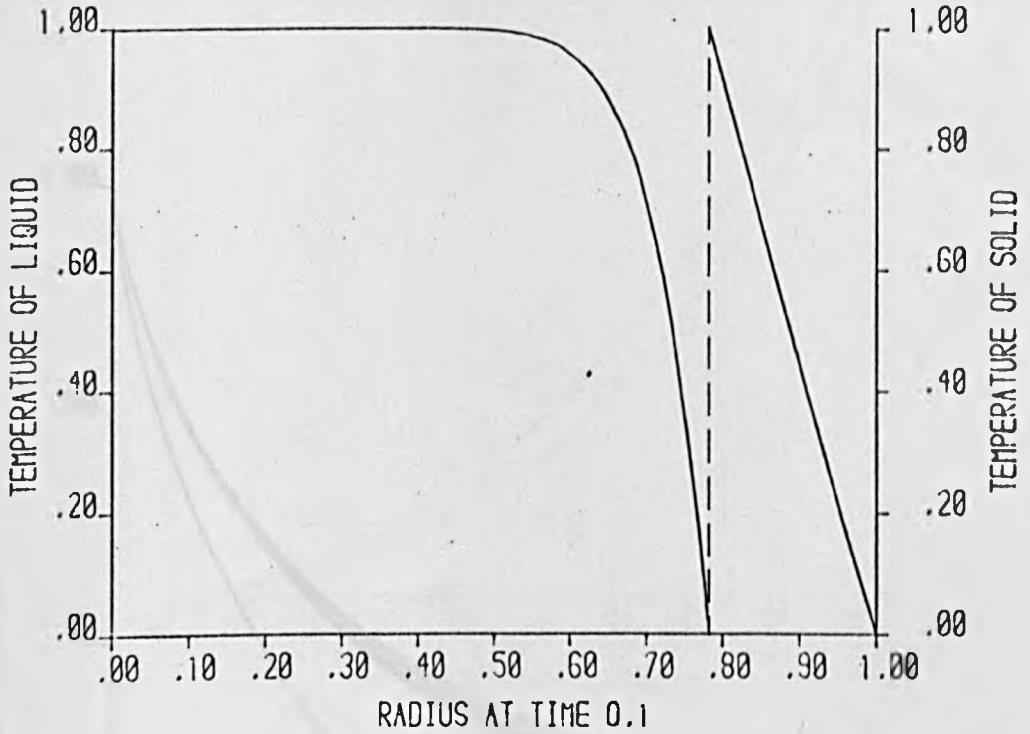
1.00
.80
.60
.40
.20
.00
TEMPERATURE OF LIQUID
1.00
.80
.60
.40
.20
.00
TEMPERATURE OF SOLID
.00 .10 .20 .30 .40 .50 .60 .70 .80 .90 1.00
RADIUS AT TIME 0.1

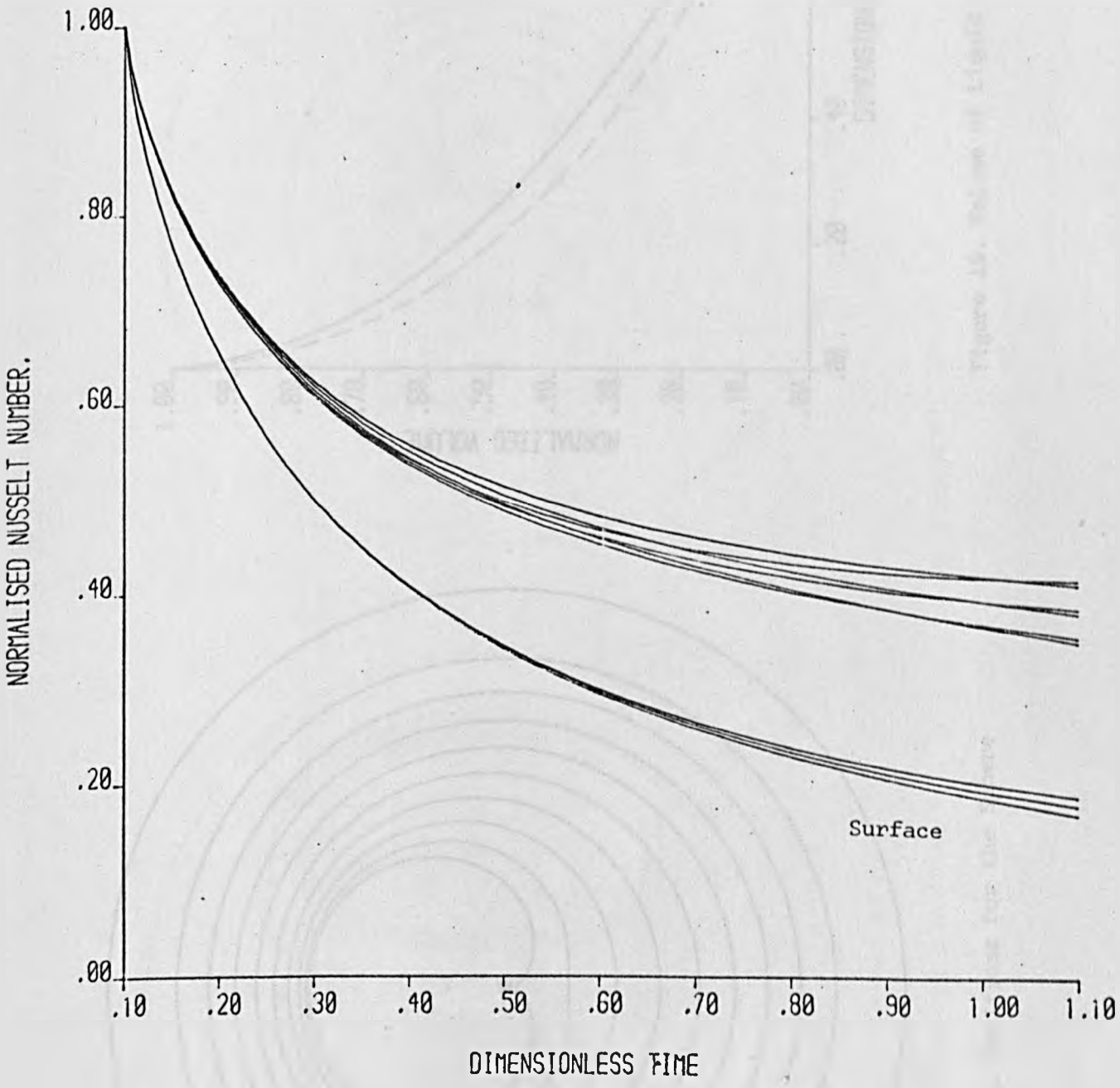

Figure 13. Dimensionless Heat Transfer Coefficients for the Cylinder at the Interface and Cylindrical Surface Locations, $\Theta = 0$, $\frac{\pi}{2}$ and π

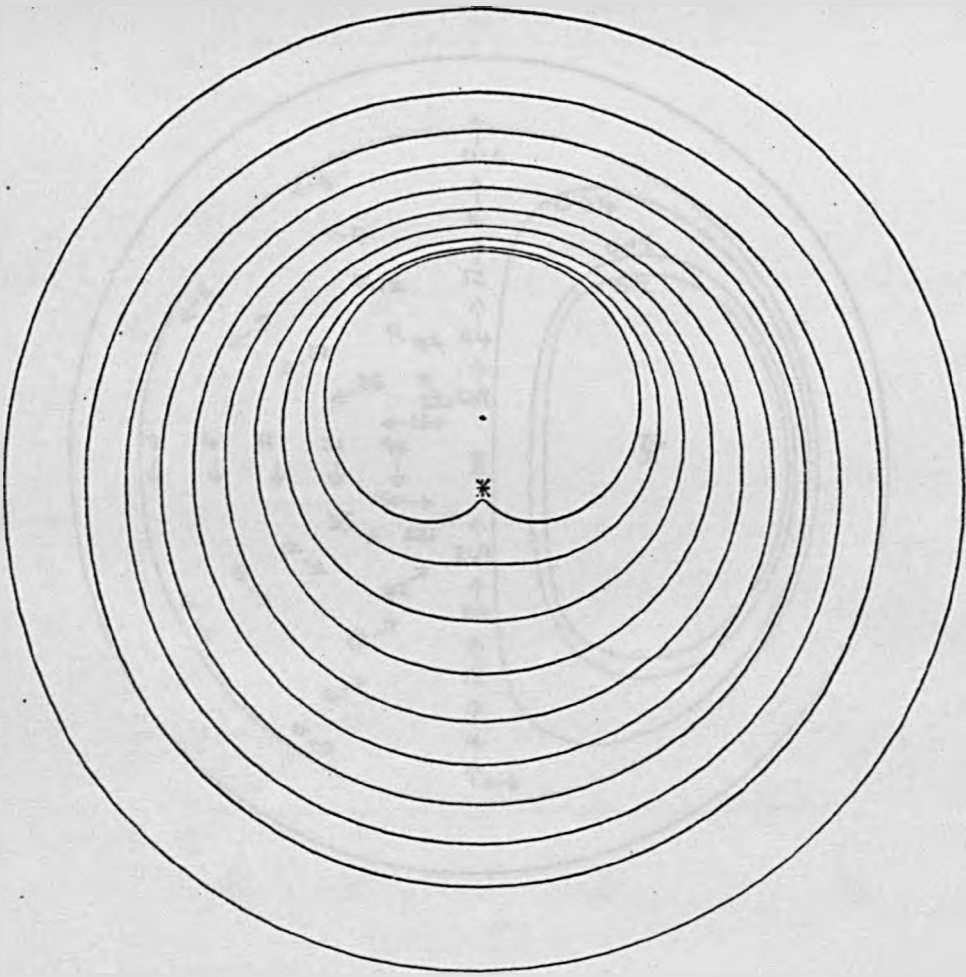

Figure 14. Interfacial Positions for the Sphere

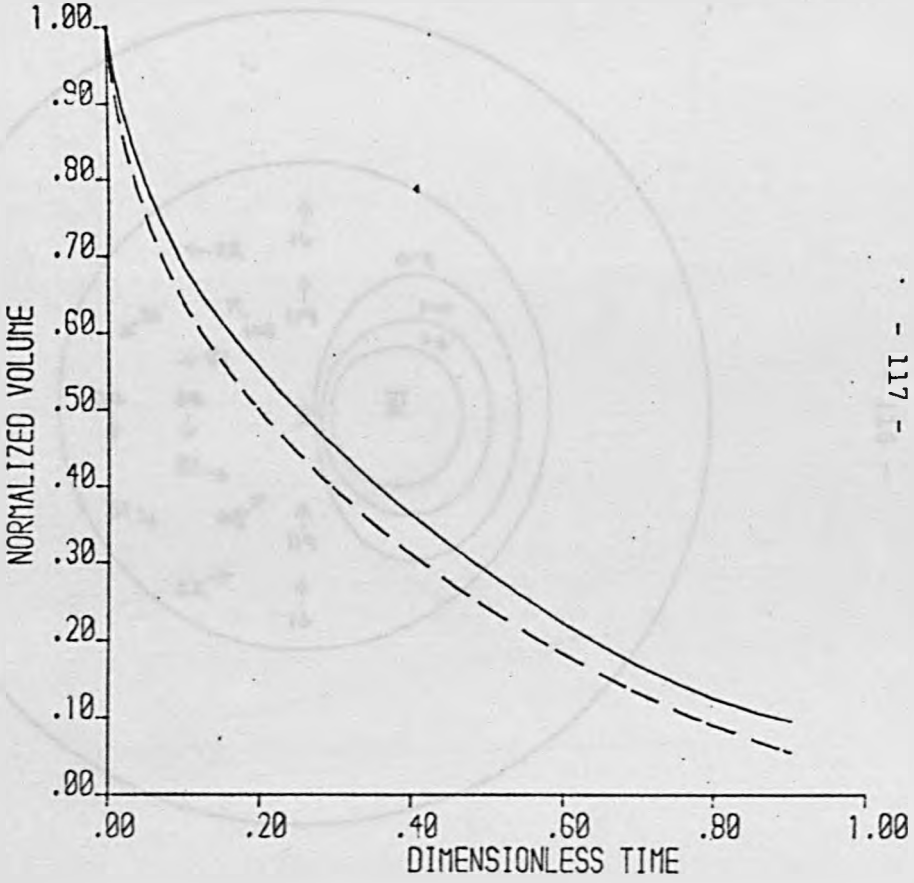

Figure 15. Volume of Liquid remaining in the Sphere

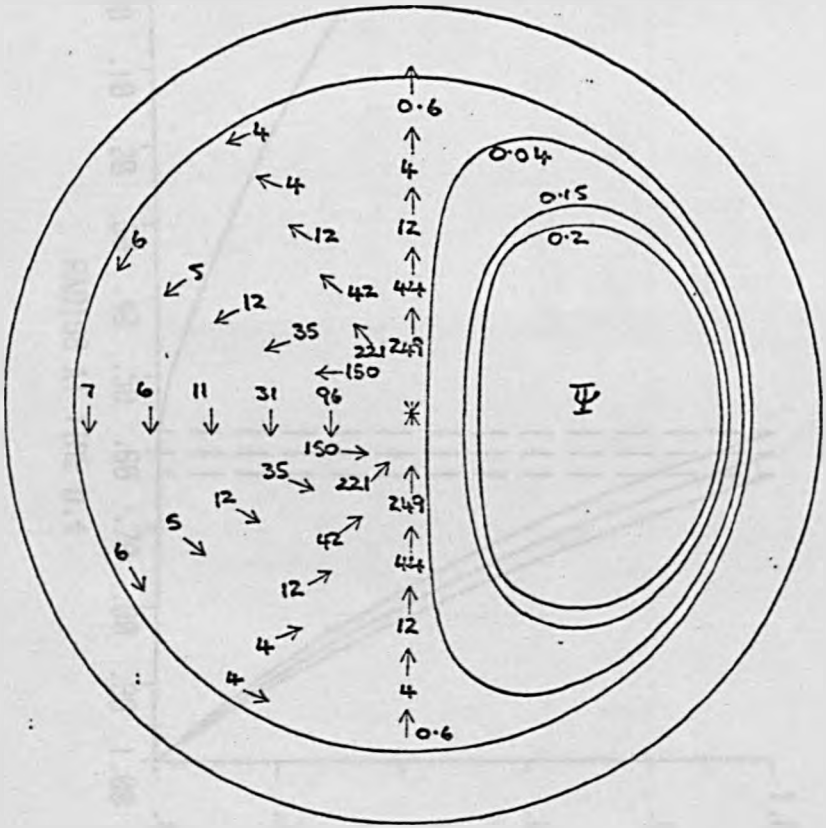

Figure 16. Streamlines and Velocities (10^{-3} m/s) for the Sphere at t = 1.78 sec.

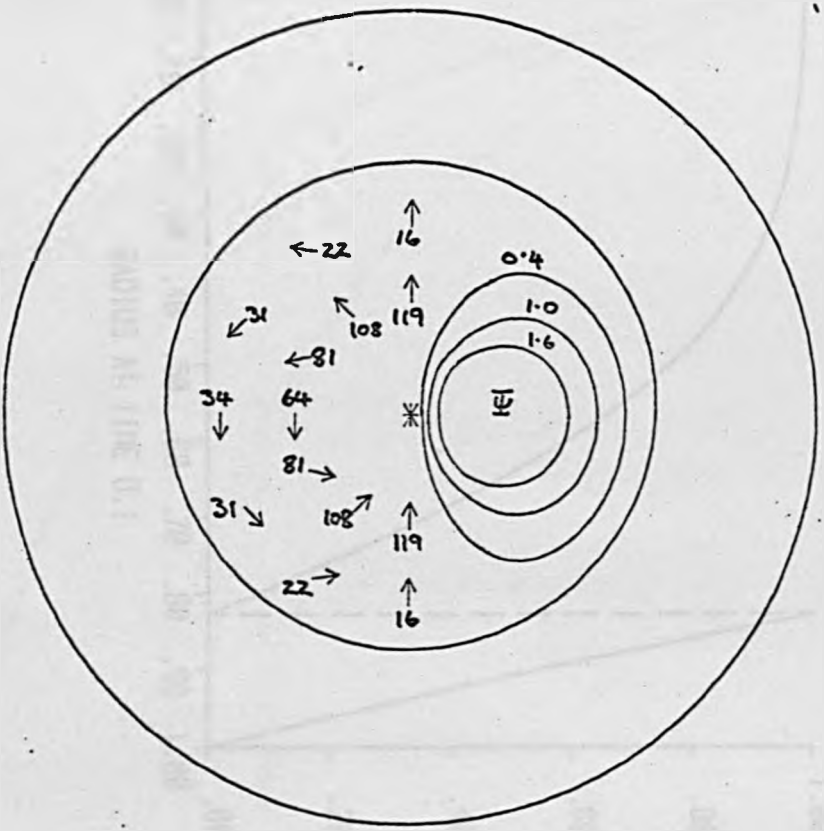

Figure 17. Streamlines and Velocities (10^{-3} m/s) for the Sphere at t = 7.12 sec.

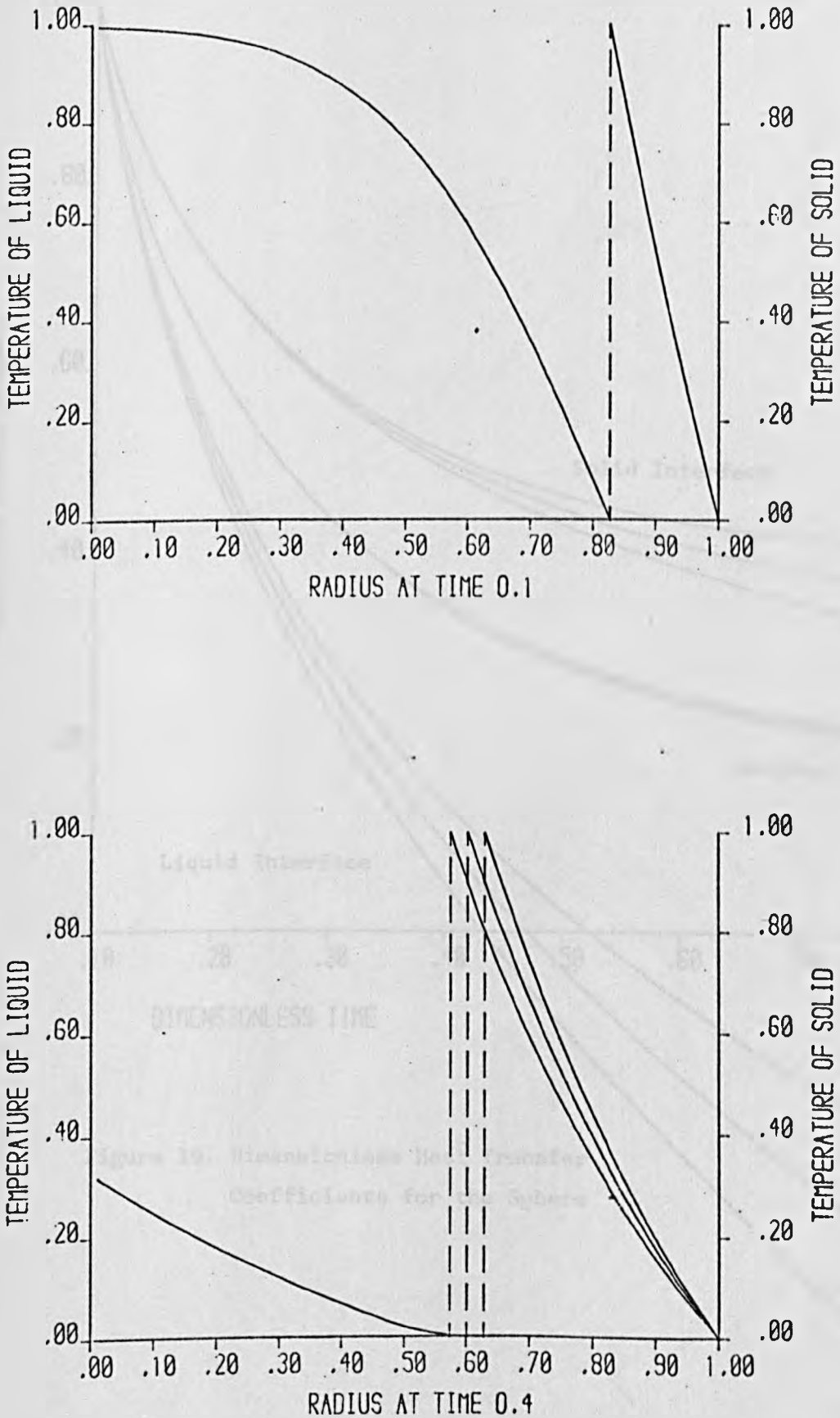

Figure 18. Temperature Distributions for the Sphere

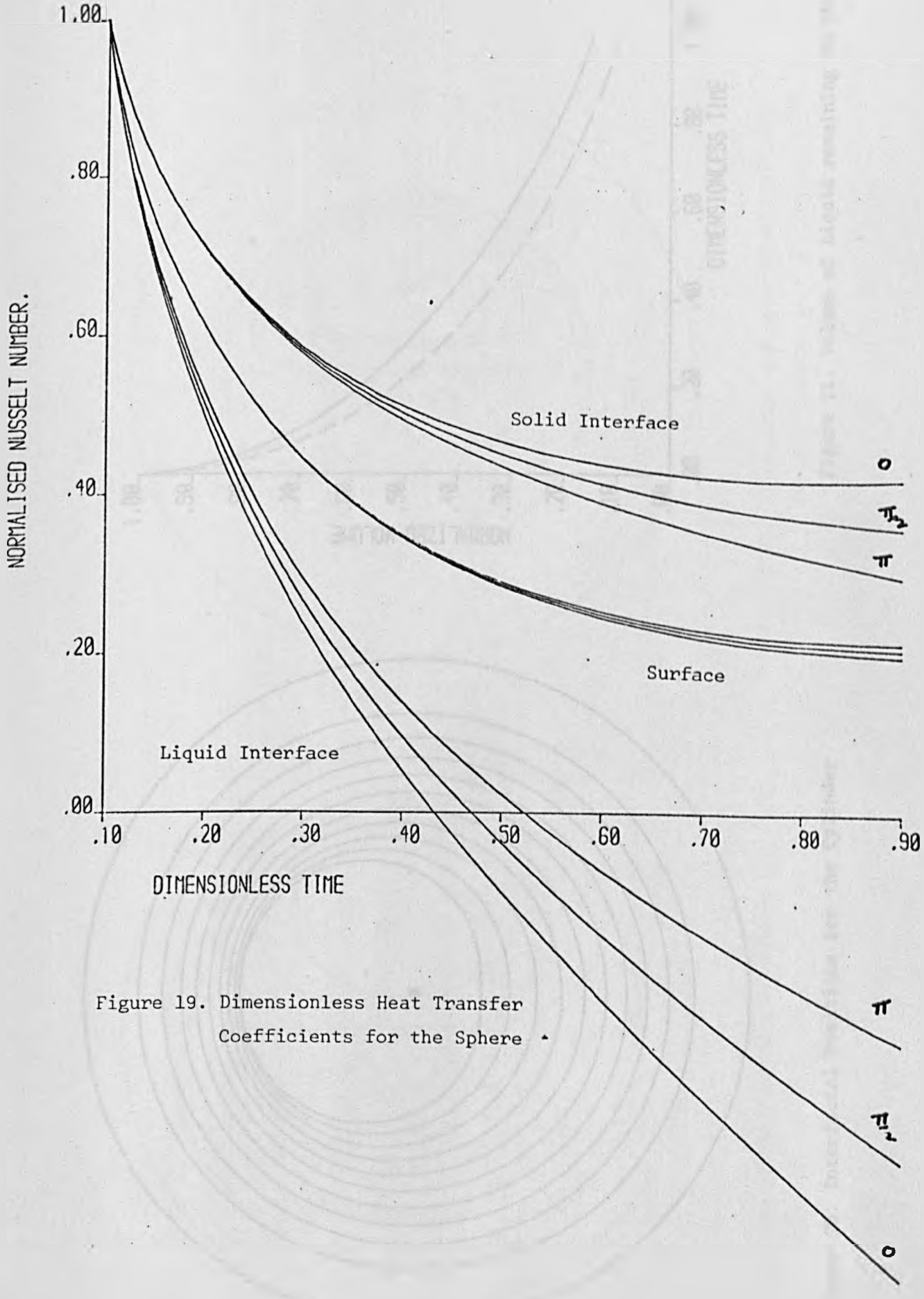

Figure 19. Dimensionless Heat Transfer Coefficients for the Sphere

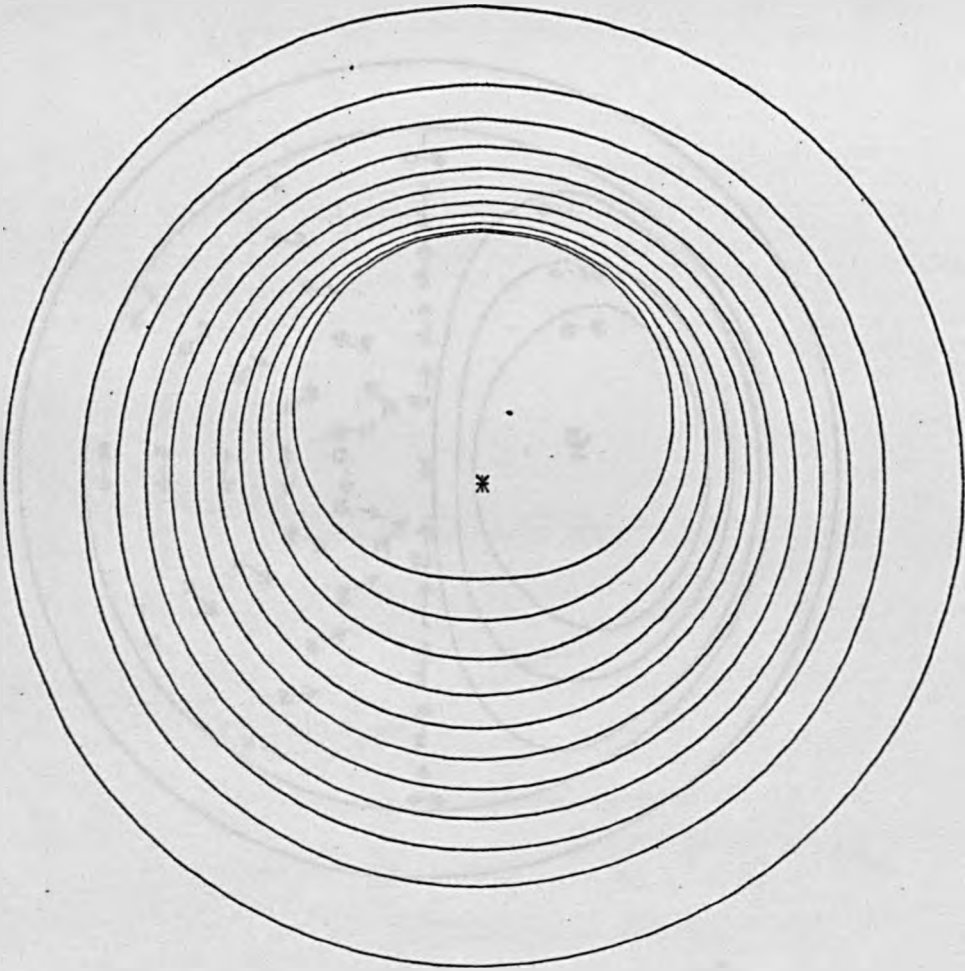

Figure 20. Interfacial Positions for the Cylinder

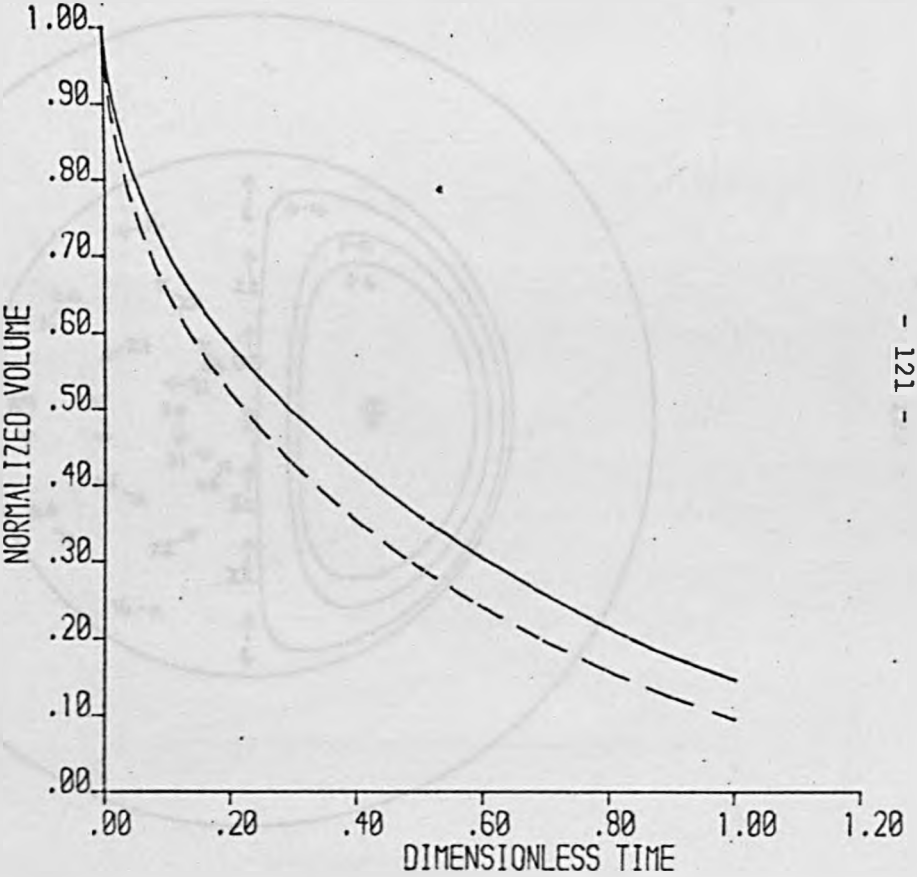

Figure 21. Volume of Liquid remaining in the Cylinder

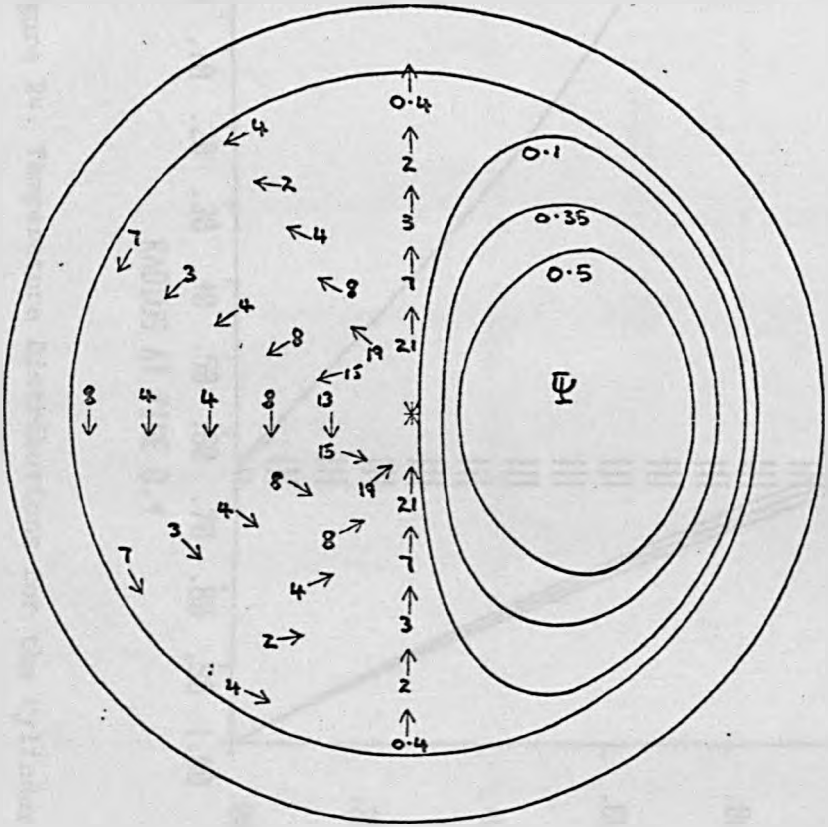

Figure 22. Streamlines and Velocities (10^{-3} m/s)
for the Cylinder at t = 1.78 sec.

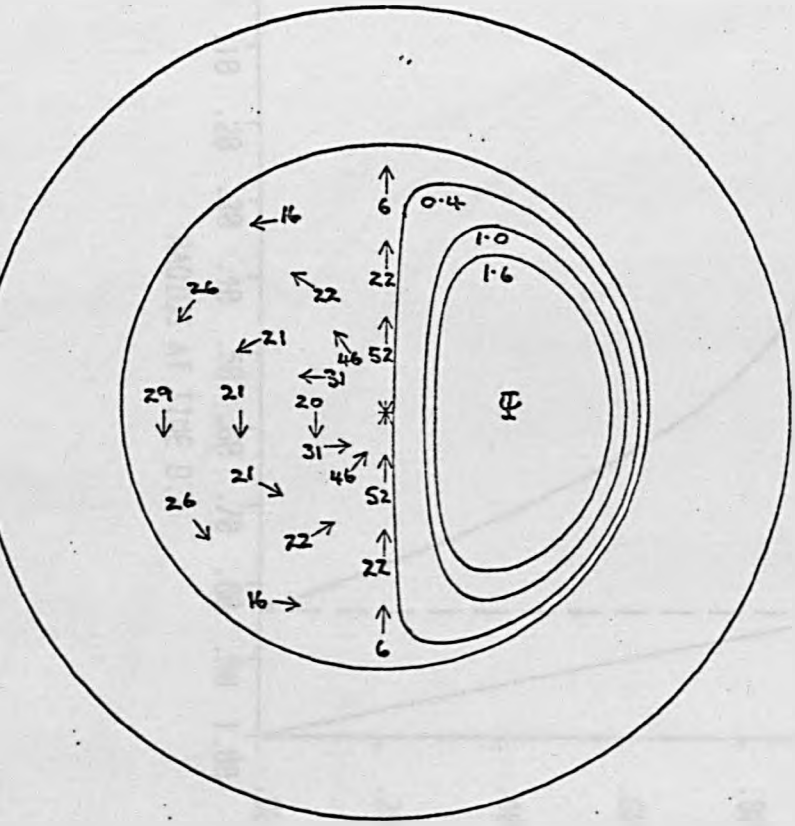

Figure 23. Streamlines and Velocities (10^{-3} m/s) for the Cylinder at t = 7.12 sec.

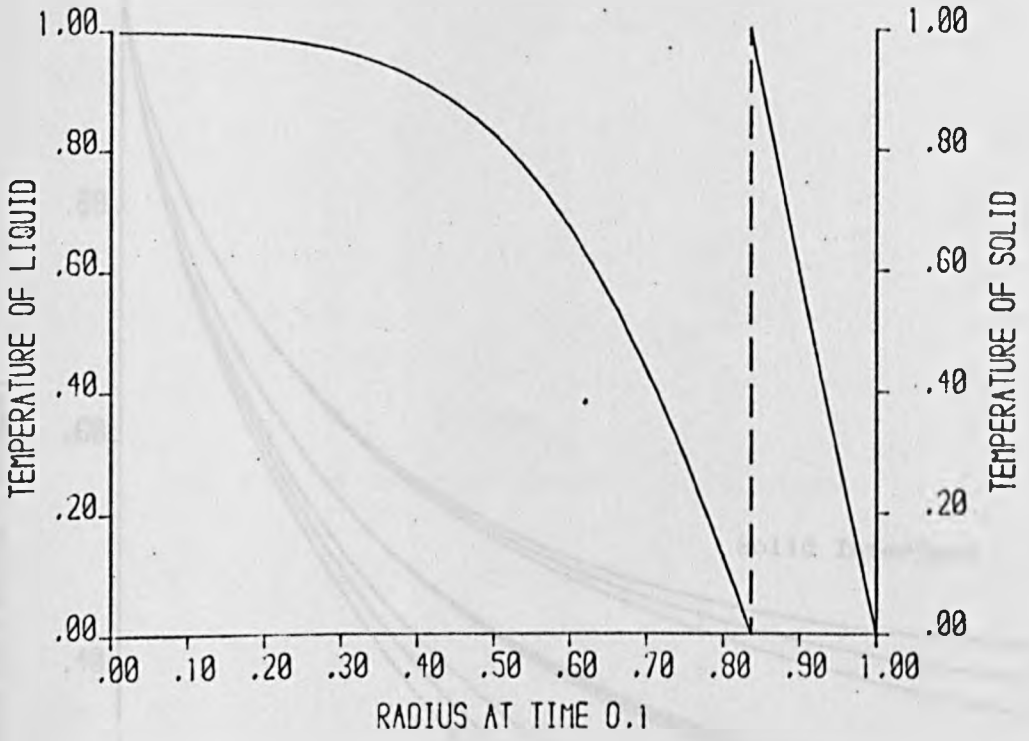

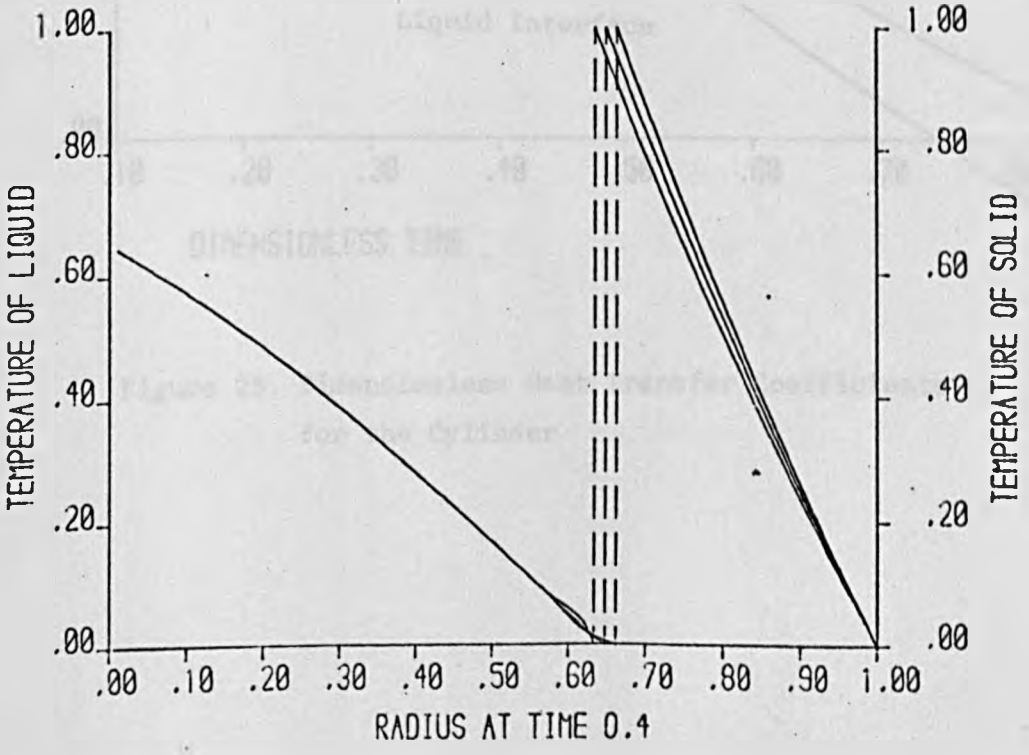

Figure 24. Temperature Distributions for the Cylinder

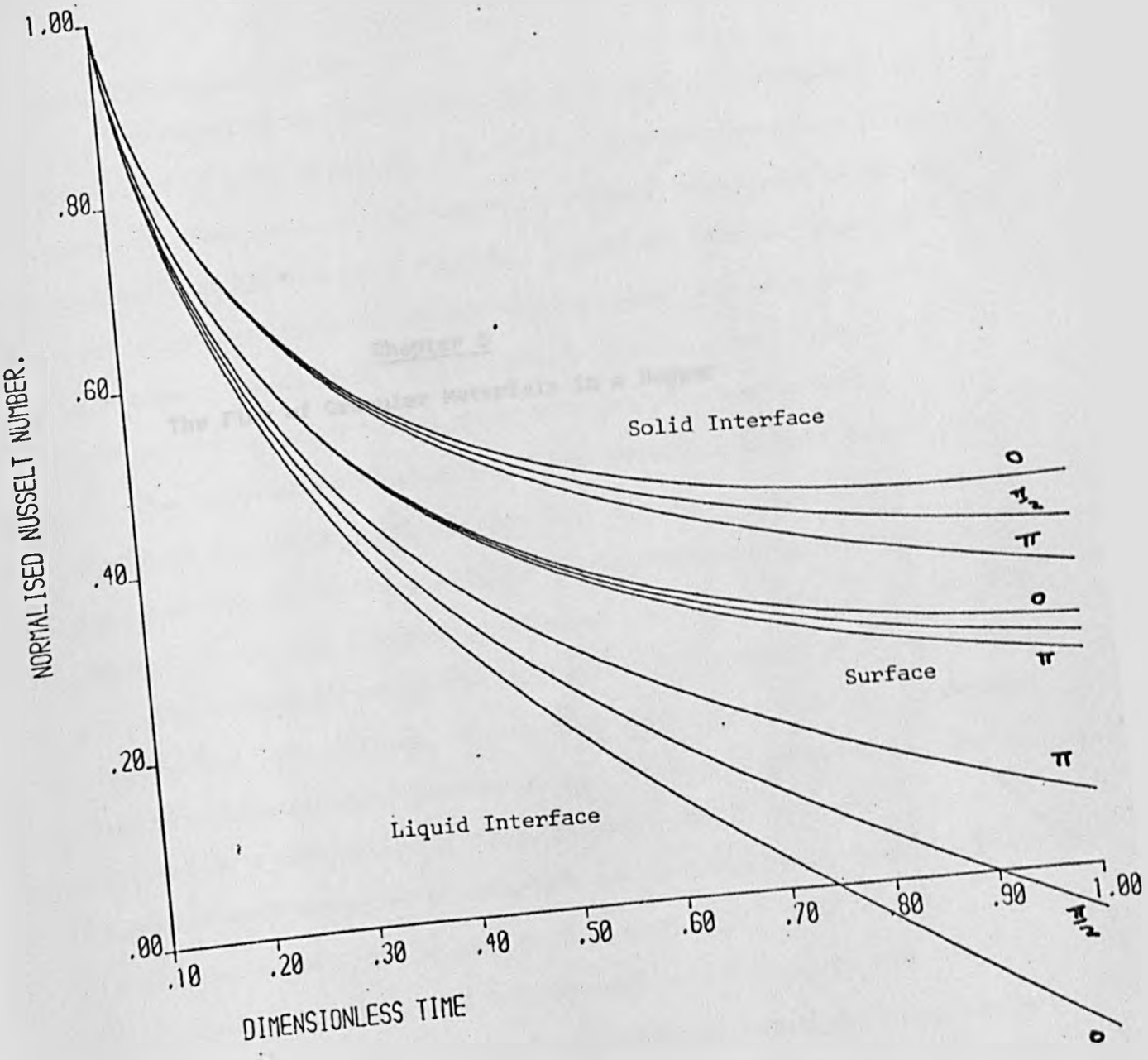

Figure 25. Dimensionless Heat Transfer Coefficients for the Cylinder

Chapter 5

The Flow of Granular Materials in a Hopper

5.1 General Introduction

Understanding the flow of a granular material, particularly in a hopper, is of great practical importance. Each day several million tonnes of grain, coal, ores, chemicals and many other bulk solids are processed and handled using hoppers. Due to the complex nature of these granular materials, the mathematical modelling of this problem is extremely complicated and the (steady and transient) flow of the material through a hopper has never been solved satisfactorily.

The complexities which arise in the modelling of this flow will be discussed in a later section. Firstly, in order to fully understand the importance played by the granular flow of a material in industry, it is instructive to give a practical example.

The example chosen is the problem which has motivated this investigation and is as follows. The British Steel Corporation at Scunthorpe has four furnaces which produce steel. To fire these furnaces coke or sinter, or a combination of both, is used. The device used to fill the furnaces with the granular materials and the iron ore is called a bell-top, a diagram of which can be seen in figure 26.

The material is loaded (or charged) into the top of this bell arrangement. The bell is then lowered and the material (charge) slides out to fall directly, or be deflected by a strategically placed shield, onto the layers of original burden materials below; the surface of these layers is called the stockline.

It is the composition of the burden material layers which is of great importance to BSC. Varying this composition can reduce or increase both the quality and quantity of the end product. Also the life cycle of the interior of the furnace can be reduced, or increased, by the

distribution of the charging constituents. The proportions of the charging mixture also depend on the type of ore used and the quality of iron required.

Since the chemical reactions inside a blast furnace are very complex and not fully understood, BSC were posed with the following problems: where was the charge finally located on the stockline, and what was the distribution made by the various charging materials ?

At BSC a one twelfth scale model of a blast furnace was built. However, it soon became apparent that, unlike a fluid, a granular material cannot be scaled down. This provided difficulties for the experimental modeller. One difficulty is due to the inability to scale successfully the individual granules, their size, shape and density. And so, it was realised that a mathematical model would have to be constructed. At least such a model could be used to determine length and time scales of the motion.

An aim of this thesis is to model the flow of the granular material in the earlier part of this problem. That is, to find a theoretical description of the motion of the material from when the bell is initially charged until it is nearly empty. In particular, the velocity with which the material leaves the bell is required since it is fundamental in determining the flight of the charge and hence its subsequent distribution across the stockline.

Certain assumptions have been made to help simplify the mathematical model. Referring to figure 27, it is assumed that the bell is in the open position and the part of the bell which is denoted by the broken line is ignored since it can be included at a later stage. Consequently, the problem is now essentially one of two-dimensional granular flow in a wedge shaped hopper. Of course, the original bell is three-dimensional

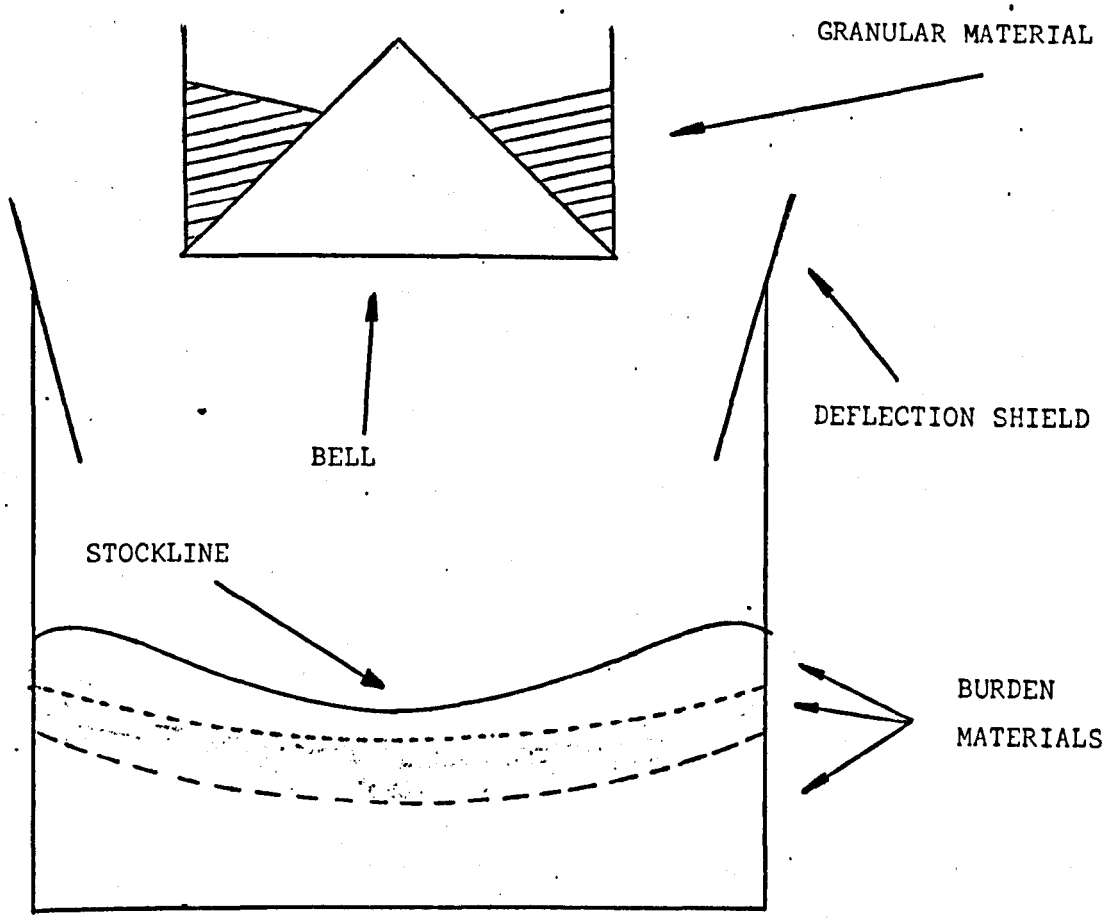

Figure 26
The Blast Furnace

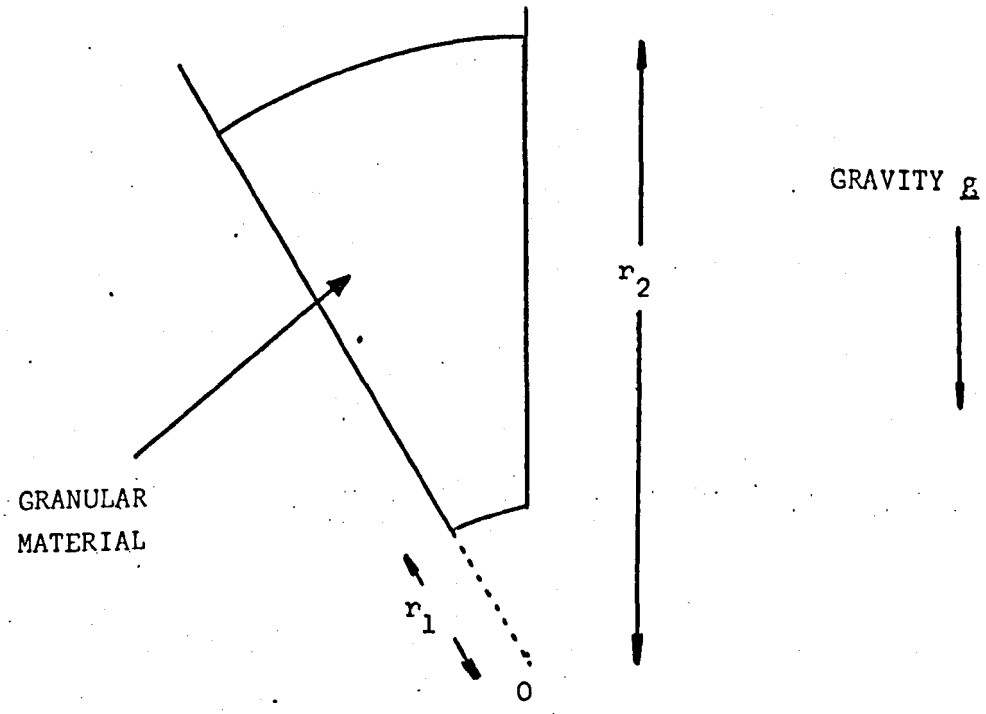

Figure 27
The Two-Dimensional Hopper

but due to its axial symmetry and its size, it can be considered two-dimensional.

Initially the hopper is fully charged and the top of the charge is taken, for example, at a radial distance r_2 from the origin O. The outlet of the hopper is at a radial distance r_1 and the angle between the sloping wall and the vertical wall is θ_w.

Before this investigation proceeds a review of the literature currently available on this subject is made.

5.2 Review of Literature on Granular Flow

In reviewing this literature it becomes immediately apparent that little or no studies have been made on transient flow. Instead it has been assumed that the flow is steady and so, in theory, the hopper never empties since the material is replenished at the top and thus the boundary at $r = r_2$ is constant. In the present model being constructed, this is just not so. There is,in fact, a transient flow as opposed to a steady flow resulting in the boundary at $r = r_2$ moving towards the orifice $r = r_1$.

It is also noticeable that the main criterion for these other studies is the determination of the stress field. This knowledge enables designers to construct hoppers and bunkers which can safely contain granular materials and, at the same time, prevent the material from becoming too densely packed.

In nearly all of the reviewed papers, as with the present theory, the granular material being considered is assumed to be coarse-grained. Thus the material is said to be cohesionless. Whilst the problem to be considered is one of transient flow, it is felt that a study of the steady flow is of interest.

Using the assumption of steady flow, the analysis can be immediately simplified on two counts.

(1) the density of the material may be considered as constant;

(2) the case when r_2 is near r_1 does not have to be considered since the flow through the orifice is found to be virtually independent of the head (the volume of material above the orifice).

In 1961 Brown [31] applied the minimum energy theorem to a small elementary volume of material in a hopper. He postulated that since energy was dissipated on the surface of the element by collisions, rotations and frictional forces then the sum of the kinetic and potential energies decreased along a streamline. This sum reached a minimum at the free-fall arch which is said to form above the orifice. Although the calculated flow rates were found to be of the correct order, this theory seems to take no account of the frictional properties of the material or of the wall.

The first attempt to find the rate of flow using the equation of motion appears to have been made by Savage [32]. Basically these equations are those of soil mechanics with the inertial terms added. Once again the frictional forces at the wall were ignored and Savage introduced the Mohr-Coulomb Yield criterion. This criterion was shown, by a shear-test procedure proposed by Jenike [34], to be

$$\sigma_\theta = \frac{(1 + \sin\phi')}{(1 - \sin\phi')}\,\sigma_r \qquad (5.2.1)$$

where σ_r and σ_θ are the principal stresses in the r and θ directions and ϕ' is the effective angle of friction. However, Jenike found that for a cohesionless material the angle ϕ' coincided with the internal angle of friction ϕ. The dimensionless velocity u found by Savage at

the orifice $r = r_1$ was given by,

$$u^2 = \frac{(k+1)}{(k-2)} \left[\frac{1 - \left(\frac{r_2}{r_1}\right)^{2-k}}{1 - \left(\frac{r_2}{r_1}\right)^{-(1+k)}} \right] \qquad (5.2.2)$$

where k is related to the angle of internal friction by

$$k = \frac{1 + \sin\varphi}{1 - \sin\varphi} \qquad (5.2.3)$$

The expression (5.2.2) was found to give flow rates which were greater than those measured by experiment. This is most probably due to the neglect of the wall friction and hence over-simplification of the analysis. In fact, Savage reported in a later paper [33] that this analysis could, in some circumstances, over-estimate the flow rate by as much as 40% - 100%.

Jenike [34] and Johanson [35] have both contributed a great deal to our understanding of stress fields in hoppers and bunkers. However, whilst studying steady flow in a hopper, they treated the bulk material as a rigid solid and used a quasi-steady equilibrium equation. That is, they assumed that the inertial terms were negligible and thus reduced the problem back to one of static soil mechanics.

In his paper of 1967 Savage [36] set about improving his earlier work by introducing the wall friction into his analysis. He developed a perturbation procedure for small ε, where $\varepsilon = (\tan\delta)^{\frac{1}{2}}$ and δ is the angle of friction between the wall and the material, and considered the limit process $\frac{\tan\delta}{\theta_w} \to 0$ as $\theta_w \to 0$. Savage found that his solution (to two terms) showed that the friction could reduce the flow rates by the correct order. Yet he later realised that due to his poor choice of perturbation parameter, the solution did not converge well for small θ_w.

Also using a perturbation series, Brennen and Pearce [37] investigated the flow (not necessarily radial) of a granular material in a two-dimensional hopper $-\Theta_w \leq \Theta \leq \Theta_w$. Assuming the stress and flow fields to be symmetrical about $\Theta = 0$, the average discharge velocity for the first two terms was

$$u^2 = \frac{(k+1)}{(k-2)}\left[\frac{1-\left(\frac{r_2}{r_1}\right)^{2-k}}{1-\left(\frac{r_2}{r_1}\right)^{-(1+k)}}\right]\left[1+\Theta_w\gamma_w(16\sin\varphi-8)+\Theta_w^2(9\sin\varphi-3)\right] \frac{}{12(1+\sin\varphi)} \qquad (5.2.4)$$

where γ_w is given by

$$\tan\gamma_w = \frac{-\sin\varphi\cos\delta \pm \sqrt{(\sin^2\varphi-\sin^2\delta}}{\sin\delta(\sin\varphi-1)} \qquad (5.2.5)$$

Brennen and Pearce claim that this flow rate agreed reasonably well with experiment for flows of glass beads and sand in two-dimensional hoppers. However, Savage and Sayed [33] believed this to be fortuitous and that the analysis over-estimated the effect of wall friction on the flow rate by as much as 20%. Surprisingly experiments with sand by Sullivan showed that wall roughness can even increase the flow rate for large Θ_w.

Savage and Sayed in considering the gravity flow of granular materials in wedge-shaped hoppers used the method of integral relations, averaging momentum balances across a cross-section of the hopper. The results obtained over-estimated the flow yet again, but it is not clear whether this was due to the approximations introduced in the solution procedures, or some inadequacy in the original equation describing the physical problem.

In the next chapter a model describing the transient flow of a cohesionless granular material in a two-dimensional hopper is constructed.

This method is based on similar assumptions to those made by Savage. It is realised that this original analysis could over-estimate the flow rate but, nevertheless, the present model could indicate the basic structure of the flow profiles.

Chapter 6

The Transient Flow of a Granular Material in a Two-Dimensional Hopper

6.1 Derivation of the Equations and Boundary Conditions

The presentation of a simplified approximate analysis for the transient flow of a granular material in a hopper is now given. The method follows closely that of Savage [32]. The assumptions on which this model is based and which help to simplify the analysis are taken as follows:

(a) the bulk density of the material is constant throughout;

(b) the walls of the hopper are frictionless;

(c) the angle of inclination Θ_w is small;

(d) there is a radial velocity field;

(e) the granules are of a uniform size.

The physical situation of this problem is given in figure 27. The material which is cohesionless initially fills the hopper and the upper surface $\bar{r} = r_2$ is a free boundary. The orifice of the hopper is at $\bar{r} = r_1$ and the flow starts instantaneously at $\bar{t} = 0$. Since (c) assumes that the angle of inclination of the sloping wall is small, then $\cos\Theta_w$ can be approximated to unity. However this restriction could be removed by subsidiary expansions in small Θ_w.

The velocity field of the material is given by $\bar{u}(\bar{r},\bar{t})$ and the stress components in the $\bar{r}$ and Θ directions are represented by $\bar{\sigma}_r$ and $\bar{\sigma}_\Theta$ respectively. The angle of internal friction in the material is Φ and g is the gravitational constant.

And so, the equation of motion is,

$$\bar{\rho}\frac{\partial\bar{u}}{\partial\bar{t}} + \bar{\rho}\bar{u}\frac{\partial\bar{u}}{\partial\bar{r}} = \frac{\partial\bar{\sigma}_r}{\partial\bar{r}} + \frac{(\bar{\sigma}_r - \sigma_\Theta)}{\bar{r}} + \qquad (6.1.1)$$

$$- \bar{\rho}\bar{g}$$

which is subject to the boundary condition,

$$\bar{\sigma}_r(r_1, \bar{t}) = 0 \quad , \quad \bar{t} > 0 \tag{6.1.2}$$

and the initial condition,

$$\bar{\sigma}_r(r_2, 0) = 0 \tag{6.1.3}$$

The equation of continuity is,

$$\frac{\partial(\bar{u}\bar{r})}{\partial \bar{r}} = 0 \tag{6.1.4}$$

subject to the initial condition,

$$\bar{u}(\bar{r}, 0) = 0, \quad r_1 \leq \bar{r} \leq r_2 \tag{6.1.5}$$

By considering appropriate length and time scales, these equations and conditions can be further simplified using the following dimensionless variables:

$$r = \frac{\bar{r}}{r} \quad ; \quad t = \bar{t}\sqrt{\frac{g}{r_1}}$$

and

$$u = \frac{\bar{u}}{\sqrt{g r_1}} \quad ; \quad \sigma_i = \frac{\bar{\sigma}_i}{\bar{\rho} g r_1} \quad , \; i = r, \theta \tag{6.1.6}$$

Before these equations are rewritten in the new variables, the Mohr-Coulomb Yield criterion for a cohesionless material is also introduced. This criterion is defined as

$$\sigma_\theta = \frac{(1 + \sin\phi)}{(1 - \sin\phi)} \sigma_r \tag{6.1.7}$$

or

$$\sigma_\theta = k \sigma_r \tag{6.1.8}$$

The relationship between k and Φ is written as,

$$\sin\Phi = \frac{(k-1)}{(k+1)} \tag{6.1.9}$$

Hence the equation of motion now becomes,

$$\frac{\partial\sigma}{\partial r} + (1-k)\frac{\sigma}{r} = 1 + \frac{\partial v}{\partial t} + u\frac{\partial u}{\partial r} \tag{6.1.10}$$

where, for simplification, the r subscript in the stress variable has been dropped. The equation (6.1.10) is subject to the conditions,

$$\sigma\left(\frac{r_2}{r_1}, 0\right) = 0 \tag{6.1.11}$$

and

$$\sigma(1,t) = 0 \quad , t \geq 0 \tag{6.1.12}$$

The continuity equation is now,

$$\frac{\partial(ur)}{\partial r} = 0 \tag{6.1.13}$$

subject to the initial condition

$$u(r,0) = 0, \quad 1 \leq r \leq \left(\frac{r_2}{r_1}\right) \tag{6.1.14}$$

6.2 Analytical Solutions

From (6.1.13) it can be shown that,

$$u(r,t) = \frac{A(t)}{r} \tag{6.2.1}$$

where A is a function of the time t only. Applying the initial condition (6.1.14) gives,

$$A(0) = 0 \tag{6.2.2}$$

Since this investigation is primarily concerned with the velocity of the material at the orifice, the function A(t) must be determined. Substituting (6.2.1) into (6.1.10) gives,

$$\frac{\partial \sigma}{\partial r} + (1-k)\frac{\sigma}{r} = 1 + \frac{1}{r}\frac{dA}{dt} - \frac{A^2}{r^3} \qquad (6.2.3)$$

The solution to this equation is,

$$\sigma = \frac{B}{r^{1-k}} + \frac{r}{(2-k)} + \frac{1}{(1-k)}\frac{dA}{dt} + \frac{A^2}{r^2(1+k)} \qquad (6.2.4)$$

where B is a constant which is determined by the boundary conditions. This solution is valid only if the value of k is not 2, 1, -1. Should k be equal to any of these values then the solution of (6.2.3) is;

for the special case k = 2,

$$\sigma = B^{(2)}r + r\ln r - \frac{dA}{dt} + \frac{A^2}{3r^2} \qquad (6.2.5)$$

for the special case k = 1,

$$\sigma = B^{(1)} + r + \frac{dA}{dt}.\ln r + \frac{A^2}{2r^2} \qquad (6.2.6)$$

and for the special case k = -1,

$$\sigma = \frac{B^{(-1)}}{r^2} + \frac{r}{3} + \frac{1}{2}\frac{dA}{dt} - \frac{\ln r}{r^2}A^2 \qquad (6.2.7)$$

where $B^{(k)}$ is a constant. Examination of (6.1.9) will reveal that only the first case is of any real importance since for most granular material,

$$15^\circ \leq \varphi \leq 60^\circ \qquad (6.2.8)$$

Multiplying (6.2.4) by r^{1-k} and then applying the boundary condition (6.1.11) yields,

$$B + \frac{\left(\frac{r_2}{r_1}\right)^{2-k}}{(2-k)} + \frac{\left(\frac{r_2}{r_1}\right)^{1-k}}{(1-k)} \left.\frac{dA}{dt}\right|_{t=0} = 0 \qquad (6.2.9)$$

where A(0) = 0. The condition (6.1.12) yields,

$$B + \frac{1}{(2-k)} + \frac{1}{(1-k)} \frac{dA}{dt} + \frac{A^2}{(1+k)} = 0 \qquad (6.2.10)$$

By subtracting these equations, a differential equation for A(t) is obtained,

$$\frac{dA}{dt} - \left(\frac{r_2}{r_1}\right)^{1-k} \left.\frac{dA}{dt}\right|_{t=0} + \frac{(1-k)}{(1+k)} A^2 = - \frac{(1-k)}{(2-k)} \left[1 - \left(\frac{r_2}{r_1}\right)^{2-k} \right] \qquad (6.2.11)$$

At time t = 0, (6.2.11) yields,

$$\left.\frac{dA}{dt}\right|_{t=0} = - \frac{(1-k)}{(2-k)} \left[\frac{1 - \left(\frac{r_2}{r_1}\right)^{2-k}}{1 - \left(\frac{r_2}{r_1}\right)^{1-k}} \right] \qquad (6.2.12)$$

Substituting (6.2.12) into the differential equation (6.2.11) gives,

$$\frac{dA}{dt} - \frac{(k-1)}{(k+1)} A^2 = - \frac{(k-1)}{(k-2)} \left[\frac{1 - \left(\frac{r_2}{r_1}\right)^{2-k}}{1 - \left(\frac{r_2}{r_1}\right)^{1-k}} \right] \qquad (6.2.13)$$

This equation, using (6.1.9), can be written more simply as

$$\frac{dA}{dt} - \text{sn}\Omega . A^2 = - M \qquad (6.2.14)$$

where $$M = \frac{(k-1)}{(k-2)}\left[\frac{1-\left(\frac{r_2}{r_1}\right)^{2-k}}{1-\left(\frac{r_2}{r_1}\right)^{1-k}}\right] \qquad (6.2.15)$$

and is subject to the initial condition (6.2.2).

The solution of this differential equation is,

$$A(t) = -\sqrt{\frac{M}{sw_i Q}}\tanh\left[t\sqrt{M s w_i Q}\right] + C \qquad (6.2.16)$$

where C is a constant. By applying (6.2.2) it is readily seen that C = 0.

Hence, substituting (6.2.16) into (6.2.1) yields the velocity function,

$$u(r,t) = -\frac{1}{r}\sqrt{\frac{M}{s w_i Q}}\tanh\left[t\sqrt{M s w_i Q}\right] \qquad (6.2.17)$$

or,

$$u(r,t) = -\frac{1}{r}\left\{\frac{(k+1)}{(k-2)}\left[\frac{1-(r_2/r_1)^{2-k}}{1-(r_2/r_1)^{1-k}}\right]\right\}^{1/2} \times \tanh\left\{t\left[\frac{(k-1)^2}{(k-2)(k+1)}\left(\frac{1-(r_2/r_1)^{2-k}}{1-(r_2/r_1)^{1-k}}\right)\right]^{1/2}\right\} \qquad (6.2.18)$$

The negative sign shows that the velocity is in a direction from the top to the bottom of the hopper.

6.3 Results and Discussion

The function (6.2.18) describes a velocity flow profile which was observed in experiments conducted by BSC. That is, the material is initially stationary in the hopper, but, as time passes, it begins to flow through the orifice. The acceleration rapidly decreases and the material flows through the hopper at a constant rate and hence the system

effectively becomes one of steady state. Comparison of the terminal velocity obtained from (6.2.18) with the velocity of the steady state system obtained by Savage shows similarities.

The terminal velocity u_T of (6.2.18), that is the $\lim_{t\to\infty} u(r,t)$ is found to be,

$$u_T = \left\{ \frac{(k+1)}{r_1^2(k-2)} \left[\frac{1 - (r_2/r_1)^{2-k}}{1 - (r_2/r_1)^{1-k}} \right] \right\}^{\frac{1}{2}} \tag{6.3.1}$$

Savage's analysis shows that the velocity at the orifice for the steady state is, in dimensionless variables,

$$w(r) = \left\{ \frac{(k+1)}{r_1^2(k-2)} \left[\frac{1 - (r_2/r_1)^{2-k}}{1 - (r_2/r_1)^{1-k}} \right] \right\}^{\frac{1}{2}} \tag{6.3.2}$$

Figures 28 to 30 display the velocity of the material at the orifice of the hopper for various initial heights r_2 and values of the internal frictional angle φ. The curves drawn in each figure show the velocity as a function of time as predicted by this present theory; the straight horizontal lines show the steady state velocity as predicted by Savage's theory for the same values of the parameters.

The graph in figure 28 shows the velocity when the ratio of the initial height of the material to the position of the orifice is 3. The angle of internal friction varies between 20° and 60°. For large frictional angles the present transient flow agrees well with the steady flow at large values of time. However, as this angle decreases the agreement diverges resulting in a higher flow rate for the transient case.

Figure 29 shows a similar graph with $\left(\frac{r_2}{r_1}\right) = 2$ and φ taking values between 20° and 60°; figure 30 displays the graph for $\left(\frac{r_2}{r_1}\right) = 4$.

For large values of Q the flow rates are identical to those in figure 28 for smaller values the flow rates are slightly higher.

It is realised that as the material free surface nears the orifice the flow pattern becomes even more complicated and is not fully understood. Nevertheless, the above simple theory is a first attempt to solve a somewhat intractable problem. It is nonlinear and transient and is governed by a system of hyperbolic equations. The numerical solution of this system for flow in a steady state is still under consideration by research workers in this field.

It is the intention that the emptying velocity profiles of the type (6.2.18), namely

$$u(t) = \alpha\beta \tanh(\alpha\gamma t) \tag{6.3.3}$$

can be used to obtain actual profiles in conjunction with experiments. For example, if the height of the free surface at any time t is h, then a relationship between these two variables can be found using the flow rate (6.2.18). That is, in dimensionless variables,

$$h = r_1\left[\frac{2\alpha\beta}{\Theta_w}\, t + \tanh(\alpha\gamma t) + 1\right]^{\frac{1}{2}} \tag{6.3.4}$$

Using the working model at BSC Scunthorpe or, more ideally, the actual blast furnace hopper measurements can be made for h against t for any given material. In (6.3.4) there are three constants which are known theoretically albeit approximately. We could proceed to find these for a particular hopper.

If h_i is known at a specific time t_i then we can find α, β and γ by the method of least squares as described by Milne [38]. We minimise

$$\frac{I(\alpha,\beta,\gamma)}{r_1} = \sum_{i=1}^{n}\left[h_i^{obs} - \left\{\frac{2\alpha\beta t_i}{\Theta_w} + \tanh(\alpha\gamma t_i) + 1\right\}^{\frac{1}{2}}\right]^2 \tag{6.3.5}$$

where h^{obs} is the observed height of the material during the experiment. Hence α, β and γ are obtained on solving the nonlinear simultaneous equations,

$$\frac{\partial I}{\partial \alpha} = \frac{\partial I}{\partial \beta} = \frac{\partial I}{\partial \gamma} = 0 \qquad (6.3.6)$$

In this way we have now the transient flow from a hopper and this can be fed into existing programmes developed at Hull for the shape of the burden surface in a furnace.

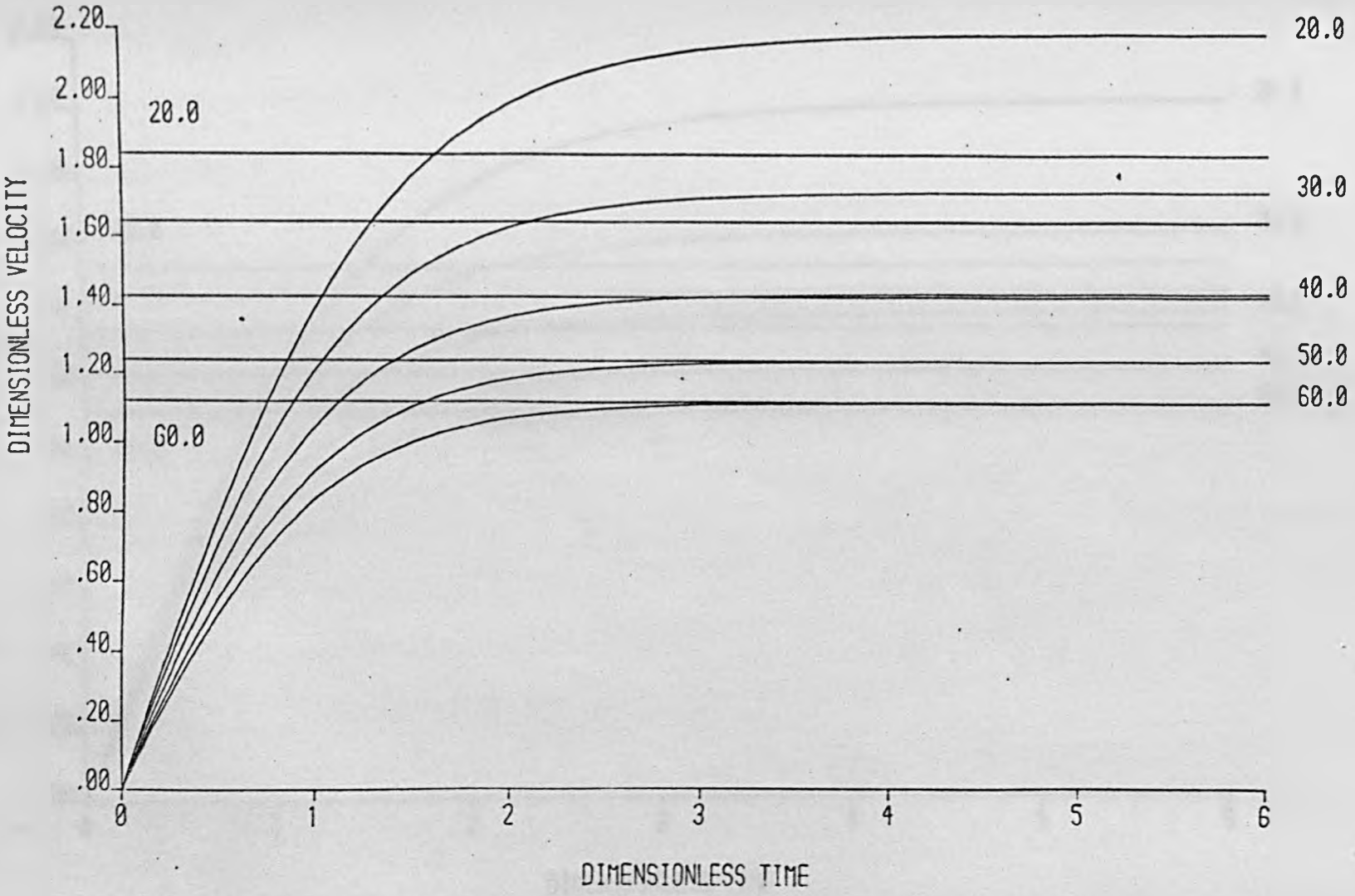

Figure 28. Flow Profiles when $\left(\frac{c_{ij}}{\gamma H}\right) = 3$ and for Various Angles of Internal Friction

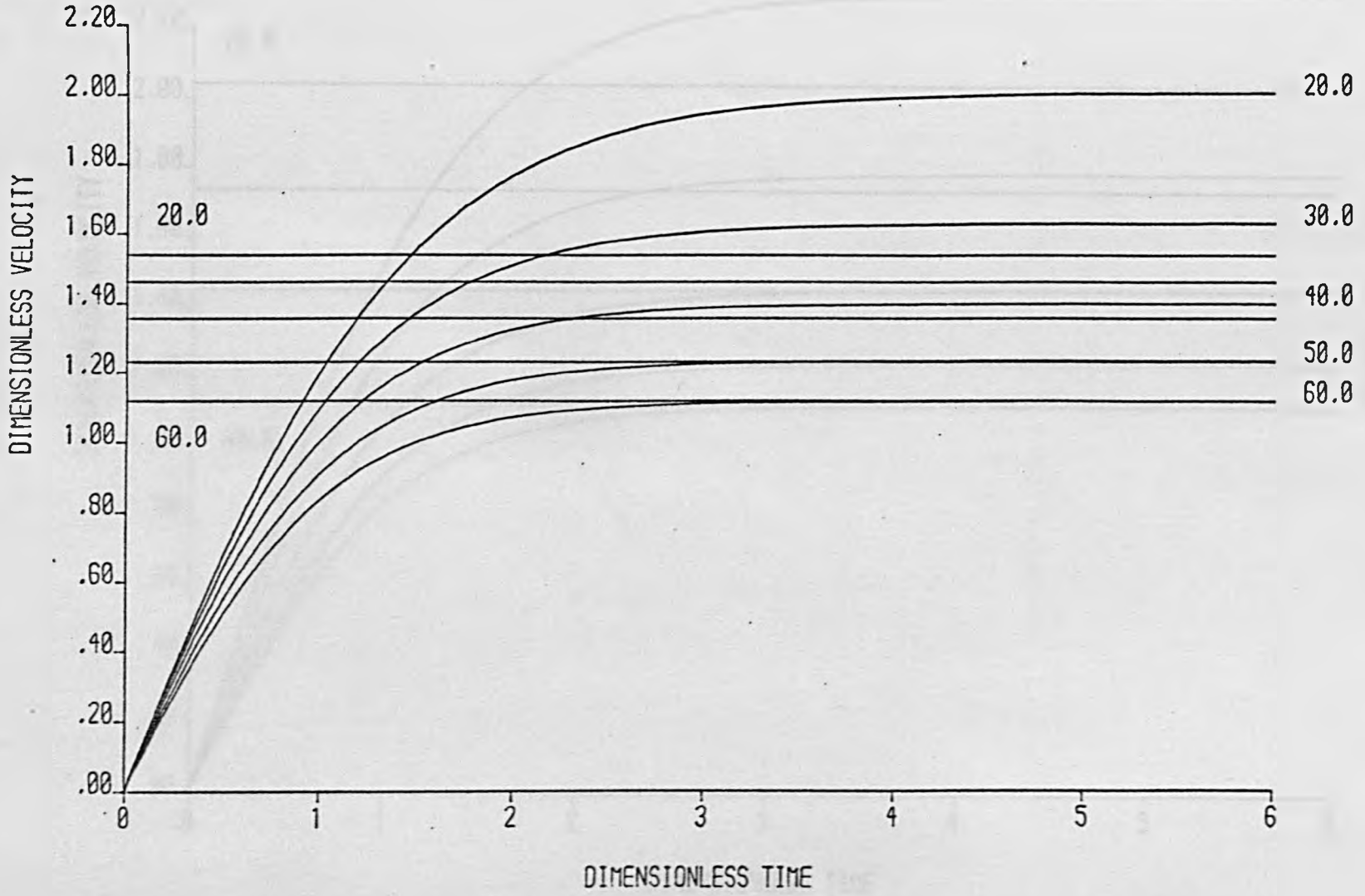

Figure 29. Flow Profiles when $\left(\frac{\gamma_s}{\gamma}\right) = 2$ and for Various Angles of Internal Friction

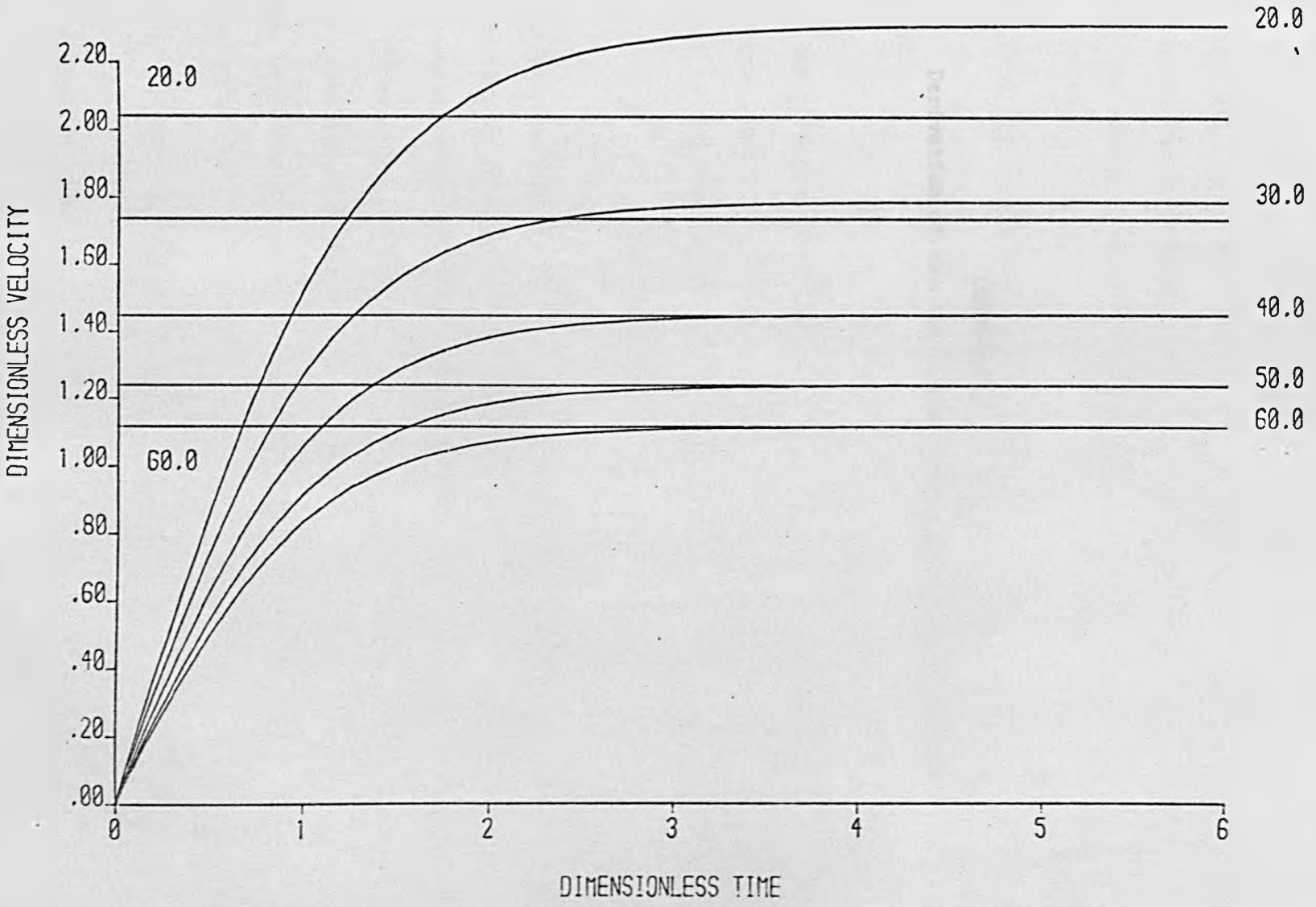

Figure 30. Flow Profiles when $\left(\frac{\tau_w}{\gamma_s}\right) = 4$ and for Various Angles of Internal Friction

Appendix A

Derivation of the Non-Linear Condition at the Interface

In this appendix two methods are given for the general derivation of the non-linear condition at the interface. This is concerned with the liberation and absorption of heat across the moving interface separating the two phases. Before either derivation is given equations which are common to both are established.

A.1 Heat Balance Equation

The equation of the moving interface, or front, is defined by the equation

$$F(\underline{r},t) = 0 \qquad \text{(A.1.1)}$$

Let $\underline{n}$ be the unit normal to the surface F in the solid-liquid direction, and $\underline{v}$ the normal velocity of the interface. Since $\underline{\nabla} F$ is normal to the surface $F(\underline{r},t) = 0$, $\underline{n}$ may be written as,

$$\underline{n} = \frac{\underline{\nabla} F}{|\underline{\nabla} F|} \qquad \text{(A.1.2)}$$

It is assumed that T is the temperature distribution of the phase, K the thermal conductivity, L the latent heat and ρ the density. A superscript * denotes the second phase.

In general, if the front advances a distance δn in a time δt, then since the difference in the heat flux between the two phases is equal to the amount of heat liberated at the front, the heat balance equation is

$$K \underline{\nabla} T . \underline{n} - K^* \underline{\nabla} T^* . \underline{n} = \rho L \underline{v} . \underline{n} \qquad \text{(A.1.3)}$$

Using (A.1.2) gives

$$K \underline{\nabla} T . \frac{\underline{\nabla} F}{|\underline{\nabla} F|} - K^* \underline{\nabla} T^* . \frac{\underline{\nabla} F}{|\underline{\nabla} F|} = \rho L \underline{v} . \frac{\underline{\nabla} F}{|\underline{\nabla} F|} \qquad \text{(A.1.4)}$$

The normal velocity $\underline{v}$ has now to be determined.

A.2 Method 1

Since the total differential of $F(\underline{r},t) = 0$ must be zero,

$$dF = \underline{\nabla} F . d\underline{r} + \frac{\partial F}{\partial t} dt = 0 \qquad (A.2.1)$$

and thus,

$$\underline{\nabla} F . \underline{v} = - \frac{\partial F}{\partial t} \qquad (A.2.2)$$

Straightforward substitution of (A.2.2) into the heat balance equation (A.1.4) gives the required equation

$$K(\underline{\nabla} T . \underline{\nabla} F) - K^*(\underline{\nabla} T^* . \nabla F) = - \rho L \frac{\partial F}{\partial t} \qquad (A.2.3)$$

$$\text{on } F(\underline{r},t) = 0$$

A.3 Method 2

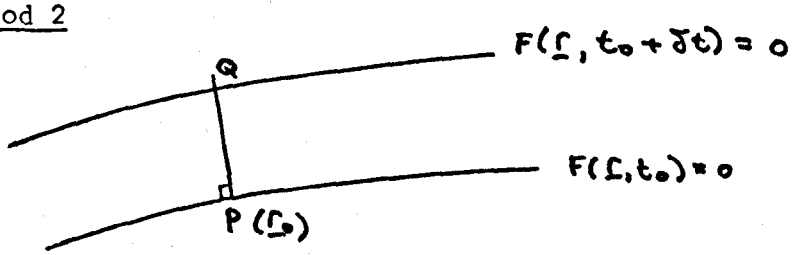

Figure A.1

The normal velocity $\underline{v}$ is now derived explicitly. The point P with position vector $\underline{r}_o$ is now considered on the surface $F(\underline{r},t_o) = 0$. The normal to this surface intersects the neighbouring surface $F(\underline{r},t_o + \delta t) = 0$ at Q. The normal velocity of the surface is

$$\lim_{\delta t \to 0} \frac{\overrightarrow{PQ}}{\delta t} \qquad (A.3.1)$$

The equation of the normal through P is

$$\underline{r} = \underline{r}_o + \lambda \nabla F \tag{A.3.2}$$

and hence

$$\overrightarrow{PQ} = r - r_o = \lambda \nabla F \tag{A.3.3}$$

where λ is a parameter and ∇F is evaluated at $(\underline{r},t_o)$. $\overrightarrow{PQ}$ meets the surface $F(\underline{r},t_o+\delta t) = 0$ at the point Q where the value of λ satisfies

$$F(r_o + \lambda \nabla F, t_o + \delta t) = 0 \tag{A.3.4}$$

Since λ and δt are small and $F(\underline{r}_o,t) = 0$ a linear approximation of the equation gives

$$\nabla F.(\lambda \nabla F) + \frac{\partial F}{\partial t}\,\delta t \simeq 0 \tag{A.3.5}$$

thus,

$$\lambda = -\frac{\frac{\partial F}{\partial t}\,\delta t}{|\nabla F|^2} \tag{A.3.6}$$

Substituting (A.3.6) into (A.3.3) gives,

$$\overrightarrow{PQ} = -\frac{\partial F}{\partial t}\,\frac{\nabla F}{|\nabla F|^2}\,\delta t \tag{A.3.7}$$

and hence the normal velocity of the front, on using (A.3.1), is

$$\underline{v} = -\frac{\partial F}{\partial t}\,\frac{\nabla F}{|\nabla F|^2} \tag{A.3.8}$$

Substitution of (A.3.8) into the heat balance equation (A.1.4) results in (A.2.3) as before.

Appendix B

The Method of Complementary Functions

The method of complementary functions is a general procedure for finding the solution of a set of simultaneous linear differential equations whose boundary conditions are specified at two points. Since an n^{th} order differential equation can be rewritten as a system of n first-order differential equations, then a general system of first-order differential equations in the form of (4.2.4) need only be considered. Let the system be,

$$\frac{dy_i}{dx} + p_{ij} y_j = q_i \qquad i = 1,2,\ldots n \tag{B.1.1}$$

where x is the independent variable and the functions p_{ij} and q_i are dependent on x. The subscript j is summed from 1 to n.

It is assumed that the system of equations is defined over the interval [a,b] and that the boundary conditions are given at the two points

$$y_i(a) = A_i \tag{B.1.2}$$

and

$$y_i(b) = B_i \tag{B.1.3}$$

The method commences by integrating the system of n first-order homogeneous differential equations

$$\frac{du_i}{dx} + p_{ij} u_j = 0 \tag{B.1.4}$$

over the interval using any convenient shooting or initial value procedure subject to the initial conditions,

$$u_i(a) = A_i \tag{B.1.5}$$

and

$$\frac{du_i}{dx}(a) = 0 \quad \text{(say)} \tag{B.1.6}$$

The value of u_i at the point x = b is computed and can be expressed as

$$u_i(b) = \alpha_i \tag{B.1.7}$$

The system of n first-order inhomogeneous differential equations

$$\frac{dv_i}{dx} + p_{ij} v_j = q_i \tag{B.1.8}$$

is now integrated over the interval using the same initial value procedure, but this time subject to the initial conditions

$$v_i(a) = A_i \tag{B.1.9}$$

and

$$\frac{dv_i(a)}{dx} = 1 \tag{B.1.10}$$

The function v_i is evaluated at the point x = b and can be expressed as

$$v_i(b) = \beta_i \tag{B.1.11}$$

The general solution of the system of linear differential equations (B.1.1), subject to the given conditions, may be written as a linear combination of the systems (B.1.4) and (B.1.8) as follows;

$$y_i(x) = c_i u_i(x) + d_i v_i(x) \tag{B.1.12}$$

c_i and d_i are constants which are determined from the boundary conditions.

Finally the original system (B.1.1) is integrated using the initial conditions,

$$y_i(a) = A_i \tag{B.1.13}$$

and

$$\frac{dy_i(a)}{dx} = c_i \frac{du_i(a)}{dx} + d_i \frac{dv_i(a)}{dx} \tag{B.1.14}$$

It is, perhaps, worth noting at this point that the initial conditions (B.1.6) and (B.1.10) specified for the complementary function and the particular integral are not unique, and can be chosen so as to simplify the analysis and subsequent calculations.

References

1. H. S. Carslaw and J. C. Jaeger, Conduction of Heat in Solids, 2nd Edition Oxford, Clarendon Press (1959)

2. G. Poots, On the Application of Integral-Methods to the Solution of Problems Involving the Solidification of Liquids Initially at Fusion Temperature, Int. J. Heat Mass Transfer 5, 525-531, 1962

3. T. R. Goodman, Advances in Heat Transfer 1, 52-120, 1964

4. L. C. Tao, Generalised Numerical Solutions of Freezing a Saturated Liquid in Cylinders and Spheres, A. I. Ch. E. Jl. 13, 165-169, 1967

5. R. I. Pedroso and G. A. Domoto, Perturbation Solutions for Spherical Solidification of Saturated Liquids, J. Heat Transfer 95, 42-46, 1973

6. C.-L. Huang and Y.-P. Shih, A Perturbation Method for Spherical and Cylindrical Solidification, Chem. Eng. Sci. 30, 897-906, 1975

7. D. S. Riley, F. T. Smith and G. Poots, The Inward Solidification of Spheres and Circular Cylinders, Int. J. Heat Mass Transfer 17, 1507-1516, 1974

8. K. Stewartson and R. T. Waechter, On Stefan's Problem for Spheres, Proc. Roy. Soc. Lon. A348, 415-426, 1976

9. A. M. Soward, A Unified Approach to Stefan's Problem for Spheres and Cylinders, Proc. Roy. Soc. Lon. A373, 131-147, 1980

10. J. M. Hill and A. Kucera, Freezing a Saturated Liquid Inside a Sphere, Int. J. Heat Mass Transfer 26, 1631-1637, 1983

11. R. M. Furzeland, A Comparative Study of Numerical Methods for Moving Boundary Problems, J. Inst. Maths Applics 26, 411-429, 1980

12. H. J. Schulze, P. M. Beckett, J. A. Howarth and G. Poots, Analytical and Numerical Solutions to Two-Dimensional Moving Interface Problems with Applications to Solidification of Killed Steel Ingots, Proc. Roy. Soc. A385, 313-343, 1983

13. E. M. Sparrow, S. V. Patanker and S. Ramadhyani, Analysis of Melting in the Presence of Natural Convection in the Melted Region, J. Heat Transfer 99, 520-526, 1977

14. E. M. Sparrow, J. W. Ramsey and R. G. Kemink, Freezing Controlled by Natural Convection, J. Heat Transfer 101, 578-584, 1979

15. N. Ramachandran, J. P. Gupta and Y. Jaluria, Thermal and Fluid Flow Effects During Solidification in a Rectangular Enclosure, Int. J. Heat Mass Transfer 25, 187-194, 1982

16. L. S. Yao and F. F. Chen, Effects of Natural Convection in the Melted Region Around a Heated Horizontal Cylinder, J. Heat Transfer 102, 667-672, 1980

17. D. K. Gartling, Finite Element Analysis of Convective Heat Transfer Problems with Change of Phase, Computer Methods in Fluids, Pentech London (1980)

18. K. Morgan, A Numerical Analysis of Freezing and Melting with Convection, Computer Methods App. Mech. Eng. 28, 275-284, 1981

19. T. Saitoh and K. Hirose, High Rayleigh Number Solutions to Problems of Latent Heat Thermal Energy Storage in a Horizontal Cylindrical Capsule, J. Heat Transfer 104, 545-553, 1982

20. A. Gadgil and D. Gobin, Analysis of Two-Dimensional Melting in Rectangular Enclosures in the Presence of Convection, J. Heat Transfer 106, 20-26, 1984

21. C. J. Ho and R. Viskanta, Heat Transfer During Melting from an Isothermal Wall, J. Heat Transfer 106, 12-19, 1984

22. C. J. Ho and R. Viskanta, Heat Transfer During Inward Melting in a Horizontal Tube, Int. J. Heat Mass Transfer 27, 705-715, 1984

23. R. Viskanta and C. Gau, Inward Solidification of a Superheated Liquid in a Cooled Horizontal Tube, Wärme-und Stoffübertagung 17, 39-46, 1982

24. H. J. Schulze, Analytical and Numerical Solutions to Two-Dimensional Moving Interface Problems with Applications to the Solidification of Killed Steel Ingots, Ph. D. Thesis, The University of Hull, England, 1982

25. L. N. Tao, On Solidification Problems Including the Density Jumps at the Moving Boundary, Q. Jl. Mech. Applied Maths 32, 175-185, 1979

26. F. M. Chiesa and R. I. L. Guthrie, Natural Convective Heat Transfer Rates During the Solidification and Melting of Metals and Alloys, J. Heat Transfer 96, 377-384, 1974

27. M. Van Dyke, Perturbation Methods in Fluid Mechanics, p.13, Parabolic Press Stanford California (1975)

28. A. Watson, The Effect of the Inversion Temperature on the Convection of Water in an Enclosed Rectangular Cavity, Q. Jl. Mech. Applied Maths 25, 423-446, 1972

29. E. M. Sparrow, R. R. Schmidt and J. W. Ramsey, Experiments on the Role of Natural Convection in the Melting of Solids, J. Heat Transfer 100, 11-16, 1978

30. G. Stead, Theoretical Aspects of Moving Interfaces, Ph. D. Thesis, The University of Hull, England, 1976

31. R. L. Brown, Minimum Energy Theorem for Flow of Dry Granules Through Apertures, Nature 191, 458-461, 1961

32. S. B. Savage, The Mass Flow of Granular Materials Derived from Coupled-Velocity Stress Fields, Brit. J. Appl. Phys. 16, 1885-1888, 1965

33. S. B. Savage and M. Sayed, Gravity Flow of Cohesionless Granular Materials in Wedge-Shaped Hoppers, ASME Mechanics Applied to Transport of Materials 31, 1-24, 1979

34. A. W. Jenike, Steady Gravity Flow of Frictional-Cohesive Solids in Converging Channels, J. Appl. Mech. 31, 5-11, 1964

35. J. R. Johanson, Stress and Velocity Fields in the Gravity Flow of Bulk Solids, J. Appl. Mech. 31, 490-506, 1964

36. S. B. Savage, Gravity Flow of a Cohesionless Bulk Solid in a Converging Conical Channel, Int. J. Mech. Sci. 9, 651-659, 1967

37. C. Brennen and J. C. Pearce, Granular Material Flow in Two-Dimensional Hoppers, J. Appl. Mech. 45, 43-50, 1978

38. W. E. Milne, Numerical Calculus, Princeton University Press, (1949)